



UNIVERSITÀ DEGLI STUDI DI SALERNO



UNIVERSITÀ DEGLI STUDI DI SALERNO

Dipartimento di Farmacia

Dottorato di ricerca

in Scienze Farmaceutiche

Ciclo XIV N.S. - Anno di discussione 2016

Coordinatore: Chiar.mo Prof. *Gianluca Sbardella*

***Study of the mechanism of action of
bioactive plant terpenoids***

settore scientifico disciplinare di afferenza: [Chim/09](#)

Dottorando

Dott. *Michele Vasaturo*

Tutore

Chiar.mo Prof. *Fabrizio Dal Piaz*

Lotterò. L'otterrò. Lo terrò.

Index

- Chapter 1 -

Introduction.....	1
1.1 Importance of plant secondary metabolites in drug discovery.....	1
1.2 Terpenes.....	4
1.3 Drug discovery today.....	5
1.4 Proteomic in drug discovery: the state of the art.....	9
1.5 Scope of thesis.....	14
1.5.1 Outline of the thesis.....	15
References.....	16

- Chapter 2 -

Introduction.....	20
2.1 15-ketoatractyligenin methyl ester (SR2017).....	20
2.2 Aims of the project.....	21
Results and discussion.....	23
2.3 Identification of the putative 15-ketoatractyligenin methyl ester targets by chemical proteomics.....	23
2.4 Targets validation by Surface Plasmon Resonance.....	25
2.4.1 Selectivity of 15-ketoatractyligenin methyl ester towards different isoform of PPAR γ	26
2.5 Structural characterization of SR2017/PPAR γ complex.....	27
2.6 15-ketoatractyligenin methyl ester is a bona fide PPAR γ ligand and requires the binding to C285 for its transcriptional activity.....	28
2.7 Molecular docking of SR2017/PPAR γ complex.....	32

2.8 Screening of 15-ketoatractyligenin methyl ester analogous using SPR analysis	36
2.9 Discussion	38
Materials and methods	40
2.10 Chemical proteomics	40
2.11 Surface plasmon resonance (SPR)	42
2.12 PARP γ /LBD peptide mapping	43
2.13 Computational chemistry	43
2.13.1 Protein and Ligand Preparation	43
2.13.2 Docking Simulations	44
2.14 Plasmids and transient transfection experiments	45
References	46

- Chapter 3 -

Introduction	52
3.1 Oridonin: insight its multifunctional effects	52
3.2 Aims of the project	54
Results and discussion	58
3.3 Synthesis and characterization of fluorescent oridonin companion imaging drug	58
3.4 Oridonin uptake in live cells	61
3.5 Optimization of DARTS protocol	62
3.6 Identification of molecular targets for oridonin using DARTS	64
3.6.1 Validation of selectivity of oridonin towards identified molecular targets using DARTS approach	67
3.6.2 Western Blot analysis to validate some of the molecular targets of oridonin	68
3.7 “Complementary” chemical proteomic approach: affinity purification and mass spectrometry analysis of oridonin partners	69
3.8 Characterization of physical interactions between oridonin and nucleolin	73

3.9 Monitoring of nucleolin engagement by oridonin in live cells using CETSA assay	74
3.10 Oridonin/HSP70 interaction validation in cell system using CESTA.....	79
3.11 In vitro imaging of nucleolin colocalization with oridoninBODIPY FL2	80
3.12 Oridonin biological effect on nucleolin into the cell.....	82
3.12.1 Levels and post translational modifications of nucleolin	82
3.12.2 Regulation and influence of target mRNAs of nucleolin by oridonin.....	86
3.12.3 Inhibition of protein synthesis by oridonin	87
3.13 Screening in vitro of new potential nucleolin inhibitors using CETSA approach.....	90
3.14 Discussion	93
Materials and methods	97
3.15 Synthesis and Characterization of Oridonin-BODIPY FL.....	97
3.15.1 Synthesis and characterization of ent-1a,6b-Dihydroxy-7,14-isopropylidene ketal-15-oxo-7,20-epoxy-16-kaurene (compound 1).....	97
3.15.2 Synthesis of compound 2	98
3.15.3 Synthesis of compound 3	98
3.15.4 Synthesis of compound 4	98
3.15.5 Stability assay.....	99
3.16 Biological characterization of oridonin BODIPY FL	99
3.16.1 Cell Viability Assay	99
3.16.2 Covalent binding Oridonin BODIPY FL/ HSP70	100
3.17 Live cell fluorescence microscopy in cell of oridonin BODIPY FL.....	100
3.18 Target identification approaches	101
3.18.1 Optimization of DARTS protocol	101
3.18.2 Evaluation of oridonin interference with subtilisin using DARTS approach	102
3.18.3 DARTS experiment on whole cell lysate.....	102
3.18.4 DARTS experiment on intact cell	103
3.18.5 “Complementary” chemical proteomic	103

3.18.6 Samples preparation for mass spectrometer analysis.....	104
3.19 SPR analysis of nucleolin complexes	105
3.20 CETSA approach	106
3.20.1 Determination of the apparent melting curve of nucleolin by CETSA..	106
3.20.2 Determination of EC ₅₀ of complex nucleolin/oridonin by CETSA	107
3.21 Biological effect of oridonin in cell	108
3.21.1 RNA isolation and quantitative real-time RT-PCR (qRT-PCR).....	108
3.21.2 Protein Synthesis assay	109
3.21.3 Cell viability and cell cycle analysis.....	109
3.22 Synthesis and characterization of oridonin BODIPY FL2.....	110
3.22.1 Synthesis and characterization of compound 1	110
3.22.2 Synthesis and characterization of compound 2.....	110
3.22.3 Immunofluorescence and co localization of oridonin BODIPY FL2	111
3.23 Screening of terpenes using CETSA approach	111
3.24 Western blotting analysis.....	111
3.25 Statistical analysis.....	112
References	113

- Chapter 4 -

Introduction	119
4.1 Background and aims of the projects.....	119
4.2 Fluorescence polarization applied to invitral microscopy analysis.....	120
4.3 A new method based on CESTA approach.....	124
Materials and methods	129
4.4 Live cell fluorecence microscopy in cell of doxorubicin	129
4.5 CETSA approach	129
4.5.1 Determination of the apparent melting curve of Btk by CETSA.....	129
4.5.2 Determination of EC ₅₀ of Btk/IbrutinibSirCOOH complex by CETSA ..	131
4.6 Western Blot analysis	131

4.7 Statistical analysis	132
References.....	133

Abstract

Natural products are small-molecule secondary metabolites displaying considerable structural complexity and “privileged scaffolds”. They are able to bind several endogenous targets eliciting biological effects as chemical weapons or to convey information from one organism to another.

Nowadays, medicinal plant drug discovery continues to provide new and important leads against various pharmacological targets. Therefore, the primary purpose of this PhD thesis has been a comprehensive characterization of the interactome profile and then the molecular mechanism of action of bioactive natural molecules. Achieving this in an effective, unbiased and efficient manner subsists as a significant challenge for the new era in drug discovery and optimization. Indeed, the full understanding of the mechanism of action of natural molecules could lead to a number of advantages: first of all, exploit their full therapeutic potential, the identification of side effects or toxicity, or the ability to set up target-based assays and to allow structure activity relationships studies to guide medicinal chemistry efforts towards lead optimization.

In my research project, the attention was paid on ent-kaurane diterpenes, a class of natural terpenoids with a great structural variability and a wide spectrum of biological activities. Firstly, I focused on the determination of the interactome of a semi synthetic compound 15-ketoatractyligenin methyl ester. This compound has been previously reported to possess high antiproliferative activity against several solid tumor-derived cell lines. In this regard, I decided to investigate the mechanism of action of this atractyligenin derivative researching first of all its molecular targets, responsible for the biological activity. In order to achieve this goal, I used a chemical proteomic approach first. This study led to the identification of PPAR γ as the main cellular partner

of this compound; achieved results were supported and validated through different biological assays.

Subsequently, I studied another diterpene: oridonin. This molecule has been shown to have multiple biological activities. Among them, the anticancer activity has been repeatedly reported by many research groups. With the aim of expanding and validate our knowledge about this molecule, also seen the limitations of the fishing for partners method, I decided to use two orthogonal compound-centric proteomics approaches to define the possible protein target(s) of oridonin. Using this strategy HSP70 and nucleolin were identified. Therefore, several *in vitro* and in cell tests have been performed to validate the interaction of oridonin with these proteins, and to evaluate its effect on their activity. Some of these tests were developed and optimized during my period of research abroad at the Massachusset General Hospital- Center for System Biology -Harvard Medical School; in that twelve months period I expanded my knowledge into the techniques useful for the study of the mechanism of action of a small molecule, also applying experimental methods complementary to proteomics and focusing on the use of high-resolution intravital microscopy imaging for drug pharmacology.

- Chapter 1 -

Introduction

1.1 Importance of plant secondary metabolites in drug discovery

The use of natural substances, particularly plant small molecules, to control human diseases is a centuries old practice that has led to the discovery of more than half of all “modern” pharmaceuticals (Katz L. & Baltz R.H. 2016). Thus, there is increasing interest in the clues from traditional uses of plant extracts to guide new drug discovery; to have an idea of the significance of ethnobotanic use of plant drugs it is sufficient just to consider the wide consumption of medicinal plants in the traditional Chinese medicine to cure and prevent diseases. Besides, more than half of humanity does not have access to modern medicine they rely on traditional treatments (Cordell & Colvard, 2012).

Actually, natural products play a significant role in the drug discovery and development process and this is particularly evident in the areas of cancer and infectious diseases, where over 60% and 75% of therapeutic agents have to be considered of natural origin. This contribution seems impressive, but it can be easily explained in the light of the chemical and evolutionistic properties shown by natural products. First of all, they exhibit a wide range of pharmacophores and a high degree of stereochemistry. Therefore, they have been - and they are still - an invaluable source of inspiration for organic chemist to synthesize novel drug candidates (Beghyn T. *et al.* 2008; Hunter P. 2008; Koehn Koehn F.E. & Carter G.T. 2005), since they provide a new starting point for new synthetic compound with diverse structures and often with multiple stereocenters that can be challenging synthetically (Clardy J. & Walsh C. 2004; Nicolaou K.C. & Snyder S.A. 2004; Peterson E.A. & Overman L.E. 2004). Indeed, many structural features common to natural products (e.g., chiral center, aromatic rings, complex ring system, degree of molecule saturation and number and ratio of heteroatoms) are expected to contribute to their ability to provide hits even against the more difficult

screening targets, such as protein-protein interactions (Balunas M.J. & Kinghorn A.D. 2005). Moreover natural products may have the additional advantage of being natural metabolites: compounds that are efficient as drugs have been suggested to have the propriety of ‘metabolite-likeness’ (Herty J. *et al.* 2009). Then, natural compounds are a good starting point for the setting up of libraries to test for drug discovery, not only for their complex and diversified chemical space but also for their ability to interact with biomolecules.

Although natural products have not been developed to bind to human proteins, they can do it very well. There are two main theories to explain this phenomenon: the first, widely accepted, is that it is the result of long-term co-evolution within biological communities; interacting organism, that evolved in close proximity to one another, developed compounds that could influence the biological process of neighboring species (Ji H.F. *et al.* 2009). The second theory, advanced by Konrad T. *et al.* and called xenohormesis, (Figure 1) is based on the hypothesis that there have been common ancestors of plants and animals able to synthesize a large number of stress- induced secondary metabolites; animals and fungi, that feed on plants, gradually lost the capacity to synthesize these low-weight molecular compounds, but retained the ability to sense these chemical cues in plants, possibly in order to detect when plants were stressed and gain an early warning of changing environmental condition (Konrad T.H. & David A.S. 2008).

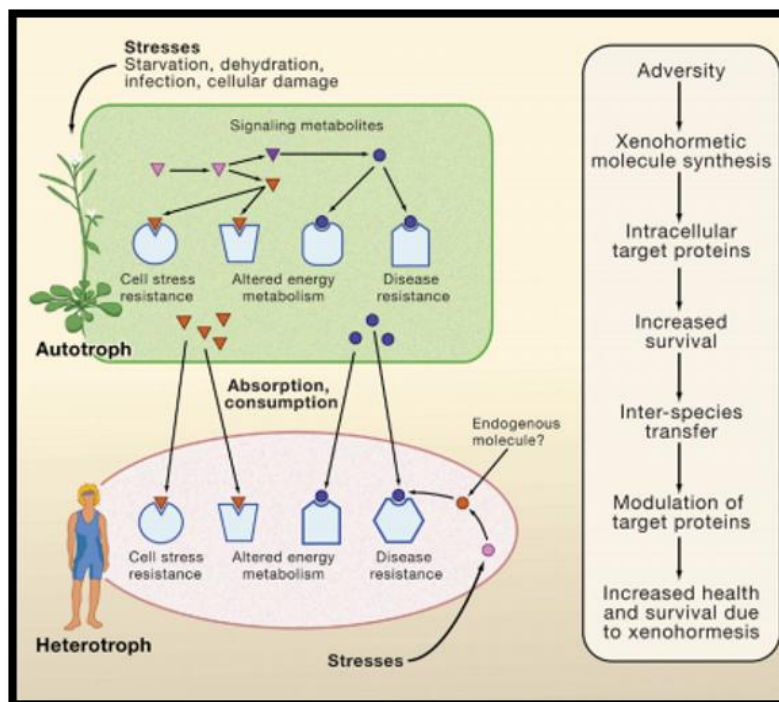


Fig.1: The Xenohormesis hypothesis.

Adopted from Konrad T.H. & David A.S. 2008

In fact, natural products are evolutionary preselected thus representing structural requirements for the binding to proteins. Their structural scaffolds represent the biologically relevant and prevalidated fractions of chemical structure space explored by nature so far (Koch M.A. *et al.* 2005). Moreover, recently Stuart Schreiber, Paul Clemons and their colleagues at the Broad Institute in Boston performed a bioinformatics analysis of natural product targets, thus demonstrating that natural molecules statically tend to target proteins with a high number of protein– protein interactions that are particularly essential to an organism (Dancík V. *et al.* 2010). This observation is consistent with the common role played by natural products as chemical weapons against predators or competitors.

Despite the success of plant molecules as drugs and the large number of benefits they show, they are losing favor among drug developers. One reason is the perceived “dirtiness” of plant molecules: a molecule is considered “dirty” if it interacts with numerous endogenous proteins. Such compounds presumably are more likely to have negative “off target” effects than a molecule that specifically targets a single protein. Flying in the face of this dogma, there are examples of plant molecules that, despite interacting with multiple human enzymes and receptors are surprisingly safe (Prasad S. & Tyagi A.K. 2015). Take for example salicylic acid or curcumin, are surprisingly powerful and nontoxic although they are two multitarget molecules. In fact, having multi-target molecules could be a winning strategy to face various diseases. It has been increasingly recognized that, in several pathologies, there are a large number of mutated genes and/or modified proteins that disrupt multiple pathways, which normally exhibit extensive biological cross-talk and redundancy. Therefore, the development of ‘magic bullet’ drugs that bind selectively to single protein targets also appears less clinically useful, since, interfering with a single target and/or pathway may not abrogate the disease. Moreover, a promising strategy for mitigating an acquired drug resistance or suppress disease, is to simultaneously inhibit multiple molecular pathways, either by using several agents in combination or by using a single agent that concurrently blocks multiple targets or pathways.

1.2 Terpenes

The terpenes are an important class of plant secondary metabolites which constitute a vast family of natural substances structurally different from each other, whose starting elements for the biosynthesis are the isoprene units.

They are produced by diverse organisms to perform an assortment of biological functions in varying ecological contexts. They are derived biosynthetically from units of isoprene, which has the molecular formula

C₅H₈. Isoprene itself does not undergo the building process, but rather activated forms, isopentenyl pyrophosphate (IPP or also isopentenyl diphosphate) and dimethylallyl pyrophosphate (DMAPP or also dimethylallyl diphosphate), are the actual components in the biosynthetic pathway.

Although all terpenoids are synthesized from two five-carbon building blocks, the structures and functions vary widely. Many terpenes have shown several biological activities. Isoprenoids and derivatives play a critical role in all living systems: the cell structure, systems of electron transport in cell-cell signals (steroids, abscisic acid, gibberellic acid, phytol ecc.), in the structure of organisms and interactions between them. Some isoprenoids play a role in plant defense systems against attack by micro-organisms and insects, act as allelopathic compounds in plant-insect and plant-environment (Lange B.M. *et al.*, 2000). Furthermore, they are used for the treatment of human diseases. In fact, there is a wide spectrum of biological and pharmacological activities for these types of substances such as antibacterial, antifungal, antiparasitic, anti-inflammatory, cytotoxic and antitumoral (Coll J. *et al.* 2007, Evans F.J. & Taylor S.E. 1983). Although they shown all of these activities, approximately 35,000 terpenes have been identified and the majority of possible functions of these molecules are unknown. Then, it would be interesting to study this class of natural molecules to find out its potential biological effects and uses in therapy.

1.3 Drug discovery today

Drug discovery is an inherently complex process with an industrial base, through which potential new medicines are identified and it involves a wide range of scientific disciplines, including biology, chemistry and pharmacology. When chemistry had reached a degree of maturity that allowed its principles and methods to be applied to problems outside of chemistry itself and when pharmacology had become a well-defined scientific discipline in its

own right, drug discovery as we know it today began its career; in fact, this discipline is not much older than a century. Drug research has contributed more to the progress of medicine during the past century than any other scientific factor. During the first half of last century, drug research was shaped and enriched by several new technologies, all of which left their imprint on drug discovery and on therapy. Genomic era and then rapid DNA sequencing, combinatorial chemistry, cell-based assays, and automated highthroughput screening (HTS) has led to a “new” concept of drug discovery. Therefore, in the last decade dramatic changes in the approaches to biomedical discovery occurred, also due to the advent of massively parallel sequencing technologies to sequence genomes, the ability to characterize the transcriptome and an improved ability to evaluate the proteome (Roti G. & Stegmaier K. 2012).

The development of a new drug can generally be divided into phases (Figure 2). The first is the preclinical phase, which usually takes 3 to 4 years. If successful, this phase is followed by an application to national or international drug agencies (DA) as an investigational new drug (IND). After an IND is approved, the next steps are clinical phases 1, 2 and 3, which require approximately 1, 2, and 3 years, respectively, for completion. Importantly, throughout this process the DA and investigators leading the trials communicate with each other, so that such issues as safety are monitored. The manufacturer then files a new drug application (NDA) with the DA for approval. This application can either be approved or rejected, or the DA might request further study before making a decision. Following acceptance, the DA can also request that the manufacturer conduct additional post-marketing studies. Overall, this entire process, on average, takes between 8 to 13 years.

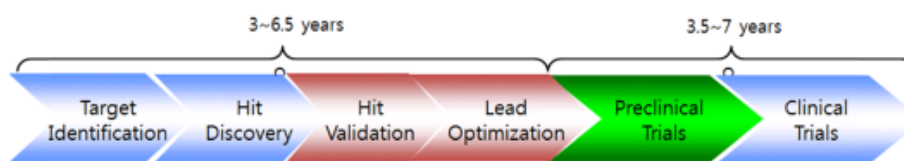


Fig.2: Overview of drug discovery process.

Adopted from: Beom-Su Jang 2013

Generally, drug development often fails at late stages, after significant cost and time investments (Paul S.M. *et al.* 2010). It's enough to consider a current price tag of over US \$1 billion per drug and an average of 13 years of investment (Pawletz C.P. *et al.* 2011; Kola I. & Landis J. 2004; Collins I. & Workman P. 2006). Furthermore, only three out of ten approved drugs manage to recover their respective development costs. Therefore, the large upfront time and monetary expenditures limit the number of drugs that can be moved from the bench to the clinic. Actually, drugs fail in the clinic for two main reasons; the first is that they do not work and the second is that they are not safe. To accelerate drug development, and subsequently reduce exorbitant costs and high failure rates, the pharmaceutical industry needs to increase its overall R&D efficiency, not just productivity (Paul S.M. *et al.* 2010). In order to solve this problem, participation of academic centers in aspects of drug discovery and development beyond target identification and clinical trials is always been significant contributors to the discovery of new drugs in therapies (Shamas-Din A. & Schimmer A.D. 2015).

In the typical drug development process, small-molecule ligands are identified by screening compound libraries against purified targets, using suitable biochemical assays. Hits derived from such screens are then further improved in an iterative medicinal chemistry process that includes profiling and validation in cell-based in vitro assays. This approach relies heavily on high-

throughput screening methods, empirical and experimental compound selection and optimization, and the development of relevant animal models of disease. Additionally, computational techniques, including drug docking simulations and quantitative SAR (QSAR), are increasingly employed to improve the efficiency in lead compound optimization (Vinegoni C. *et al.* 2015). In this regard, academic institutions developed several techniques and skills to evaluate the best candidate in the drug discovery process: they have established high-throughput screening platforms, formed medicinal chemistry teams, and built capabilities in pharmacokinetic studies with the aim of developing small-molecule drugs. Thus, the aim of these institutions is to identify and validate new therapeutic targets through biological studies and testing new drugs developed by the pharmaceutical industry in clinical trials. That's why drug discovery in academic centers represent a unique opportunity for the industry. Therefore, since they do not consider necessarily issues related to market share and profitability, investigators can pursue drug candidates for targets of scientific interest. In addition, chemical probes that do not reach the stage of clinical trials are important experimental tools, since the probes can be used to reveal new biological insights. Finally, academic investigators can make important contributions to the rationale for development of new therapeutic agents, even if the intellectual property rights of the drug are held by others.

However, advancing drugs from academic institutions into clinical trials remains challenging, and these institutions face common obstacles. In fact, heavy investment in money and time is the major obstacle to be overcome. One solution to this problem is for academic groups to replace "old" drug allowing the rapid evaluation of them into the clinical trial phase. The repositioning of thalidomide for myeloma, for example, is a dramatic success but there will likely be few examples of this strategy that show similar impact (Shamas-Din A. & Schimmer A.D. 2015).

An important challenge now is how to best exploit these new capabilities for therapeutic benefit. Thus, it is very important to know not only pharmacokinetic and pharmacodynamic parameters of a drug but above all its mechanism of action. Target identification and confirmation for small molecules is often the rate limiting step in drug discovery. Although drugs can be approved without a clear knowledge of their target and/or mode of action, the full characterization of the protein binding profile of a small molecule is an important prerequisite for a complete picture of the biology behind it. In fact, complete comprehension of a drug leads many advantages in terms of improvement and potential of the molecule itself and in terms of versatility of the same, also allowing its possible use against more pathologies. In this regard proteomic approaches fits very well in the macro complex of drug discovery. Proteomics is an essential and crucial method to discover and explain drugs, not only because of the knowledge of the effects of drug candidates on their protein targets, but also to shed light on the cellular mechanisms behind the observed phenotype (Guo S. *et al.* 2013).

1.4 Proteomic in drug discovery: the state of the art

The publication of the full human genome sequence in 2003 by the International Human Genome Sequencing Consortium is a crucial milestone in the history of genetic research (Yan S.K. *et al.* 2015). The completion of human genome has created much excitement from the impact that this wealth of information is likely to have on the process of drug discovery and development (Reiss T. 2001; Lander E.S. *et al.*, 2001). It has been postulated that scientists could use genomic information to identify and validate a host of new drug targets and tailor specific drugs based on an individual's detailed genetic makeup (Cockett M. *et al.*, 2000). Although this new field of genomics holds many promises, it is clear that analysis of DNA and/or RNA content alone is not sufficient to understand cell biology and disease. However,

analysis of the information produced by genomics, when measured against comparable information regarding protein expression, has led to the conclusion that message abundance fails to correlate with protein quantity (Nutall M.E. 2001). Further, post-translational processes such as protein modifications or protein degradation remain unaccounted for in genomic analysis (Anderson L & Seilhamer J 1997; Mann M. 1999). Since both cell function and its biochemical regulation depend on protein activity, and the correlation between message level and protein activity is low, the mere measurement of expression has proven to be inadequate. Consequently, the development of drug-discovery technologies has begun to shift from genomics to proteomics (Simpson R.J. & Dorow D.S. 2001).

Proteomics, as a scientific field, is defined as the study of the protein products of the genome, and their interactions and functions. Hence, the proteins expressed at a given time in a given environment constitute a proteome (Dove A. 1999). From a technology viewpoint, traditional proteomics involves separation of proteins in a proteome, coupled to a means of identification. This science is very challenging since protein levels vary widely with both cell type and environment (Bichsel V.E. *et al.*, 2001). Second, unlike genomics, which can amplify benefits from the amplification of single genes using the polymerase chain reaction (PCR), protein science has no comparable amplification method (Blackstock W.P. & Weir M.P. 1999). Third, proteomics is complicated by the fact that the absolute quantity of protein is of limited interest to drug discovery, because protein activities are highly regulated post-translationally (Srinivas P.R. *et al.* 2001). Therefore, proteins can be abundant, yet possess little activity. Finally, because proteins interact functionally *in vivo*, protein–protein and protein–small molecule interactions need to be evaluated in processes of interest (Cravatt B.F. & Sorensen E.J. 2001).

The metabolism of a cell or of an entire organism is mainly regulated by proteins, acting individually and, more frequently, in pathways. In particular,

the function of a protein can be defined on the basis of its interactions, and pathways are cascades of specific protein interactions that are necessary to activate distinct cellular functions. Genetic mutations or environmental factors deregulate these pathways, leading to disease conditions. A detailed knowledge of the pathways active inside the cell and of how they are deranged in a particular pathology is fundamental for drug discovery as it allows the identification of new drug targets. Since the pharmacologic effects of a drug can only be appreciated when its interactions with cellular components are clearly delineated, an integrated deconvolution of drug target interactions for each drug is necessary. The wide use of proteomic in drug target identification has enhanced our confidence in improving our understanding of the molecular mechanisms of these drugs. In fact, with the development of related high-throughput analytical technologies and mass spectrometry, proteomics has been rapidly developed in various research fields. Thus, an unprecedented number of biological targets have been tested, and various technologies emerging today provide us with a superior platform to further investigate drug targets.

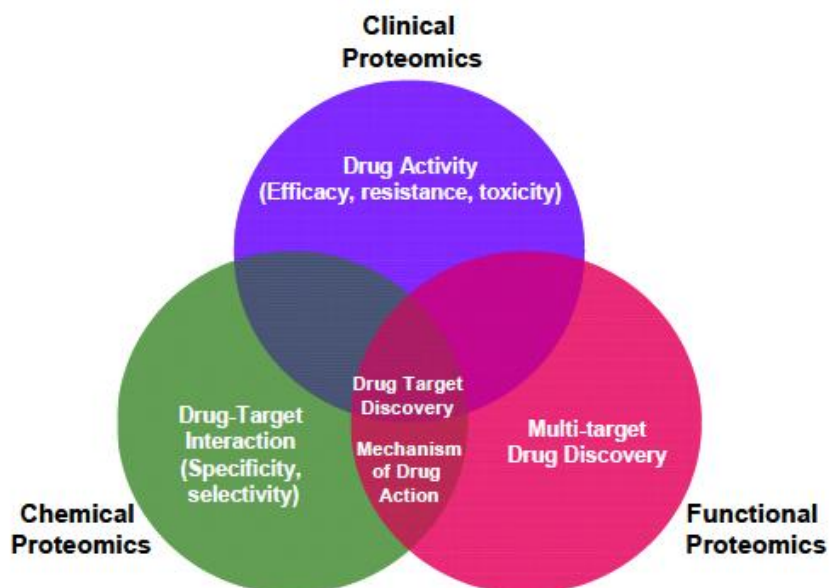


Fig.3: Main applications of functional, chemical and clinical proteomics in drug discovery.

Adopted from Savino R. *et al.* 2012

As mentioned before, proteomic is spread in different fields, namely functional, chemical and clinical proteomics, all going to somehow impact on biomarker and drug discovery processes (Figure3).

The proteome records the flow of information that starting within the cells, through the intercellular protein network, goes beyond the extracellular microenvironment up to come to the blood microenvironment (Matta A. *et al.*, 2010). Accordingly, the proteome may reflect immediate and characteristic changes in response to disease processes and external stimulation. By the means of proteomic tools such as mass spectrometry (MS), it is possible to qualitatively and quantitatively reveal molecular profiles contained in healthy or clinical samples. Consequently, MS technologies offer the opportunity to screen and discovery simultaneously multiple biomarkers, which consist of a pattern of up- or down-regulated molecules (proteins, peptides, metabolites, organic molecules) representative of a given (healthy/disease) condition.

Basically, clinical proteomics covers all MS-based preclinical and basic science studies aimed at discovering and understanding the role of proteins in pathological processes in order to facilitate the early diagnosis of disease, the prognosis prediction, the identification of new therapeutic targets and the evaluation of treatment response (Beretta L. 2007; Matt P. *et al.* 2008).

Another emerging research area in the proteomic is functional proteomics, aimed to monitor and analyze the spatial and temporal properties of the molecular networks and fluxes involved in living cells (Godovac-Zimmermann J. & Brown L.R. 2001). It is focused on the generation of information about proteins, such as expression levels, interacting partners, post-translational modifications (PTMs) and activity, which all contribute to elucidate pathways active inside the cells and, ultimately, to a functional understanding of biological systems.. In recent years, functional proteomics has been used to analyze not only the formation of specific protein-protein interactions, but also to understand how these interactions lead to the assembly of macromolecular protein complexes that are regulated by PTMs and which affect pathway functions. In particular, these approaches are addressed towards two major targets: the elucidation of biological functions of unknown proteins and the definition of cellular mechanisms at the molecular level. In the cells, many proteins display their biological functions through the rapid and transient association within large protein complexes. Understanding protein functions as well as unraveling molecular mechanisms within the cell then depend on the identification of the interacting protein partners. The association of an unknown protein with partners belonging to a specific protein complex involved in a particular mechanism would be strongly suggestive of its biological function (Gavin A.C. *et al.* 2002; Ho Y. *et al.* 2002). Furthermore, a detailed description of the cellular signaling pathways might greatly benefit from the elucidation of protein-protein interactions in vivo (Lewis T.S. *et al.*, 2000).

Finally a powerful weapon to profile previously uncharacterized proteins via identifying drug target interactions is chemical proteomics: a multidisciplinary research area integrating biochemistry and cell biology with organic synthesis and MS. Chemical proteomics comes in two different flavors: (i) activity based probe profiling (ABPP), which focuses on the enzymatic activity of a particular protein family, and (ii) a compound-centric approach, which focuses on characterizing the molecular mechanism of action of an individual bioactive small molecule (Rix U. & Superti-Furga G. 2009). Thus, they also serve different purposes. ABPP detects members of a defined class of enzymes that are active under certain conditions—for example, in a disease. This method can lead to the identification of new proteins with the respective biochemical activity, or it can be applied to determine the selectivity profile of drugs targeting an enzyme family via pretreatment of the lysate with the drug of interest and subsequent labeling and identification of the remaining enzymes using appropriate reactive probes. Compound centric chemical proteomics consists of classical drug affinity chromatography that is similar to the method used for decades but that is now performed in combination with modern high-resolution MS analysis and statistics or bioinformatics for subsequent identification of binding proteins (Savino R. *et al.*, 2012).

Finally, understanding protein function and unraveling cellular mechanisms at the molecular level constitute a major need in modern biology. Therefore, chemical proteomics is an initial technology that is useful in clinical testing and drug development.

1.5 Scope of thesis

Naturally occurring secondary metabolites are small molecules displaying considerable structural complexity and “privileged scaffolds”. They are able to bind several endogenous targets, eliciting biological effects as chemical weapons or as information vectors from one organism to another. Concerning

the human use, medicinal plant drug discovery continues to provide new and important leads against various diseases including cancer, HIV/AIDS, Alzheimer's, malaria, and pain. Therefore, the overall aim of this Ph.D. study was to set-up, optimize, develop, and apply proteomics methods to elucidate the molecular mechanisms of action of bioactive natural molecules. It is indeed evident that the full understanding of these mechanisms could lead to a number of advantages: first of all, exploit the full therapeutic potential of promising compounds, the identification of their side effects or toxicity, or the ability to set up target-based assays. Moreover, it would allow performing structure activity relationships studies to guide medicinal chemistry efforts towards lead optimization. Achieving this in an effective, unbiased and efficient manner subsists as a significant challenge for the new era in drug discovery and optimization. Therefore, protein sample preparation, fractionation, high-throughput LC-MS/MS, data analysis, and, in particular, label free and chemical proteomic approaches were used.

1.5.1 Outline of the thesis

This research paid attention on diterpenes, a class of natural terpenoids with a wide structural variability and known spectrum of biological activities. Firstly, (**Chapter 2**) the determination of the interactome of a semi synthetic compound 15-ketoatractyligenin methyl ester is described. This compound has been previously reported to possess high antiproliferative and cytotoxicity activities against several solid tumor-derived cell lines. Therefore, we select it to investigate its mechanism of action, through the identification of the molecular targets responsible for its biological activity. In order to achieve this goal, a chemical proteomic approach was used; the emerged results were subsequently validated by biophysics, biological and bioinformatic assays.

In the **Chapter 3** the chemical-biological study of oridonin is discussed. This diterpene has been shown to have multiple biological activities. Among them,

the anticancer activity has been repeatedly reported by many research groups. With the aim of expanding and validate our knowledge about this molecule, we decided to use several approaches for the identification of its possible targets in cell. More in details, two orthogonal compound-centric proteomics approaches were used. Moreover, to validate the interaction of oridonin with these proteins, and to evaluate its effect on their activity several *in vitro* and in cell tests have been performed.

Finally, to expand my knowledge into the techniques useful for the study of the mechanism of action of a small molecule, methods complementary to proteomics have been applied. In particular, in **Chapter 4** new orthogonal techniques useful for the study of the mechanism of action of drugs and the use of high-resolution intravital microscopy imaging for drug pharmacology were discussed.

References

- Anderson L. & Seilhamer J., (1997), A comparison of selected mRNA and protein abundances in human liver., *Electrophoresis.*, 18:533-537.
- Balunas M.J. & Kinghorn A.D., (2005), Drug discovery from medicinal plants., *Life Sci.*,22;78(5):431-41.
- Beghyn T, Deprez-Poulain R, Willand N, Folleas B, Deprez B, (2008), Natural compounds: leads or ideas? Bioinspired molecules for drug discovery, *Chem Biol Drug Des*, 72(1):3-15.
- Beretta L., (2007), Proteomics from the clinical perspective: Many hopes and much debate. *Nat. Methods.*, 4(10):785-6.
- Bichsel V.E., Liotta L.A., Petricoin E.F., (2001), Cancer proteomics: from biomarker discovery to signal pathway profiling., *Cancer J.*,7:69-78.
- Blackstock W.P. & Weir M.P., (1999), Proteomics: quantitative and physical mapping of cellular proteins., *Trends Biotechnol.*, 17:121-127.
- Clardy J. & Walsh C., (2004), Lessons from natural molecules., *Nature.*,432(7019):829-37.

- Cockett M., Dracopoli N., Sigal E., (2000), Applied genomics: integration of the technology within pharmaceutical research and development., *Curr Opin Biotechnol.*, 11(6):602-9.
- Coll J., Tandrón Y.A., Zeng X., (2007), New phytoecdysteroids from cultured plants of *Ajuga nipponensis* Makino., *72(3):270-7.*
- Collins I.& Workman P., (2006), New approaches to molecular cancer therapeutics., *Nat. Chem. Biol.*, 2, 689–700.
- Cordell G.A. & Colvard M.D., (2012), Natural products and traditional medicine: turning on a paradigm. *J Nat Prod.*,23;75(3):514-25.
- Cravatt B.F. & Sorensen E.J., (2000), Chemical strategies for the global analysis of protein function., *Curr Opin Chem Biol* .,4:663-668.
- Dancík V., Seiler K.P., Young,D.W., Schreiber, S.L., Clemons,P.A., (2010), Distinct biological network properties between the targets of natural products and disease genes., *J. Am.Chem.Soc.*, 132(27):9259-61.
- Dove A., (1999), Proteomics: translating genomics into products?., *Nat Biotechnol.*, 17:233-236.
- Evans F.J. & Taylor S.E., (1983), Pro-inflammatory, tumour-promoting and anti-tumour diterpenes of the plant families Euphorbiaceae and Thymelaeaceae., *Fortschr Chem Org Naturst.*,44:1-99.
- Gavin A.C., Bösch M., Krause R., Grandi P., Marzioch M., Bauer A., Schultz J., Rick J.M., Michon A.M., Cruciat C.M., Remor M., Höfert C., Schelder M., et al., (2002), Functional organization of the yeast proteome by systematic analysis of protein complexes., *Nature.*, ;415(6868):141-7.
- Godovac-Zimmermann J. & Brown L.R., (2001), Perspectives for mass spectrometry and functional proteomics., *Mass Spectrom Rev.*20(1):1– 57.
- Guo S. Zou J., Wang G. (2013), Advances in the proteomic discovery of novel therapeutic targets in cancer, *Drug. Des. Ther.* 24;7:1259-71.
- Hert J., Irwin J.J., Laggner C., Keiser M.J., Shoichet B.K., (2009), Quantifying biogenic bias in screening libraries.,*Nat Chem Biol.*, 5(7):479-83.
- Ho Y., Gruhler A., Heilbut A., Bader G.D., Moore L., Adams S.L., Millar A., Taylor P., Bennett K., Boutilier K., Yang L., Wolting C., Donaldson I., Schandorff S., Shewnarane J., Vo M., et al .,(2002), Systematic identification of protein complexes in *Saccharomyces cerevisiae* by mass spectrometry., *Nature.*, 415(6868):180-3.
- Howitz K.T. & Sinclair D.A., (2008), Xenohormesis: sensing the chemical cues of other species., *Cell.*, 133(3):387-91.
- Hunter P., (2008), Harnessing Nature's wisdom. Turning to Nature for inspiration and avoiding her follies, *EMBO Rep*, 9(9):838-4.

- Ji H.F., Li X.J., Zhang H.Y. (2009), Natural products and drug discovery. Can thousands of years of ancient medical knowledge lead us to new and powerful drug combinations in the fight against cancer and dementia? *EMBO RepMar*; 10(3): 194–200.
- Ji H.F., Li X.J., Zhang H.Y., (2009), Natural products and drug discovery. Can thousands of years of ancient medical knowledge lead us to new and powerful drug combinations in the fight against cancer and dementia?., *EMBO RepMar*; 10(3): 194–200.
- Katz L & Baltz R.H., (2016), 76 Natural product discovery: past, present, and future., *J Ind Microbiol Biotechnol.*;43(2-3):155-59.
- Koch M.A., Schuffenhauer A., Scheck M., Wetzel S., Casaulta M., Odermatt A., Ertl P., Waldmann H., (2005), Charting biologically relevant chemical space: a structural classification of natural products (SCONP)., *Proc Natl Acad Sci U S A*. 2005 Nov 29;102(48).
- Koehn F.E. & Carter G.T., (2005), Rediscovering natural products as a source of new drugs. *Discov Med.*, 5(26):159-64.
- Kola I. & Landis J., (2004), Can the pharmaceutical industry reduce attrition rates?., *Nat Rev Drug Discov.*, 3(8):711-5.
- Konrad T.H. & David A. S., (2008), Xenohormesis: Sensing the Chemical Cues of Other Species *Cell*. 2; 133(3): 387–391.
- Lander E.S., Linton L.M., Birren B., Nusbaum C., Zody M.C., Baldwin J., Devon K., Dewar K., Doyle M., FitzHugh W., Funke R., Gage D., Harris K., Heaford A., Howland J., Kann L., et al., (2001), Initial sequencing and analysis of the human genome., *Nature.*, 15;409(6822):860-921.
- Lange B.M., Rujan T., Martin W., Croteau R., (2000), Isoprenoid biosynthesis: the evolution of two ancient and distinct pathways across genomes., *Proc Natl Acad Sci U S A*;97(24):13172-7.
- Lewis T.S., Hunt J.B., Aveline L.D., Jonscher K.R., Louie D.F., Yeh J.M., Nahreini T.S., Resing K.A., Ahn N.G., (2000), Identification of novel MAP kinase pathway signaling targets by functional proteomics and mass spectrometry, *Mol Cell*, 6:1343–54.
- Mann M., (1999), Quantitative proteomics?., *Nat Biotechnol*,17:954-955.
- Matt P., Fu Z., Fu Q., van Eyk J.E., (2008), Biomarker discovery: Proteome fractionation and separation in biological samples.,*Physiol., Genomics.*,14, 33,(1) 12–17.
- Matta A., Ralhan R., DeSouza L.V., Siu K.W., (2010), Mass spectrometry-based clinical proteomics: Head-and-neck cancer biomarkers and drug-targets discovery. *Mass Spectrom. Rev.*, 29(6)945–961.
- Nicolaou K.C. & Snyder S.A., (2004), The essence of total synthesis., *Proc Natl Acad Sci U S A.*, 17,101(33):11929-36.

- Nuttall M.E., (2001), Drug discovery and target validation., *Cells Tissues Organ.*, 169:265-271.
- Paul S.M, Mytelka D.S., Dunwiddie C.T., Persinger C.C., Munos B.H., Lindborg S.R., Schacht A.L., (2010), How to improve R&D productivity: the pharmaceutical industry's grand challenge., *Nat Rev Drug Discov.*, 9(3):203-14.
- Paweletz C.P., Andersen J.N., Pollock R., Nagashima K., Hayashi M.L., Yu S.U., Guo H., Bobkova E.V., Xu Z., Northrup A., Blume-Jensen P., Hendrickson R.C., Chi A., (2011), Identification of direct target engagement biomarkers for kinase-targeted therapeutics., *PLoS One.*, 6(10):e26459.
- Peterson E.A. & Overman L.E., (2004), Contiguous stereogenic quaternary carbons: a daunting challenge in natural products synthesis., *Proc Natl Acad Sci U S A.*, 101(33):11943-8.
- Prasad S. & Tyagi A.K., (2015), Curcumin and its analogues: a potential natural compound against HIV infection and AIDS. *Food Funct.*6(11):3412-9.
- Reiss T., (2001), Drug discovery of the future: the implications of the human genome project., *Trends Biotechnol.*, 19(12):496-9.
- Rix U. & Superti-Furga G., (2009), Target profiling of small molecules by chemical proteomics, *Nature Chemical Biology* ,5, 616 – 624.
- Savino R, Paduano S, Preianò M, Terracciano R, (2012), The Proteomics Big Challenge for Biomarkers and New Drug-Targets Discovery, *Int. J. Mol. Sci.*, 13(11):13926-48.
- Shamas-Din A. & Schimmer A.D., (2015), Drug discovery in academia., *Exp Hematol.*, 43(8):713-7.
- Simpson R.J. & Dorow D.S., (2001), Cancer proteomics: from signaling networks to tumor markers., *Trends Biotechnol.*, 19:S40-S48.
- Srinivas P.R., Srivastava S., Hanash S., Wright G.L., (2001), Proteomics in early detection of cancer., *Jr. Clin Chem.*, 47:1901-1911.
- Vinegoni C., Dubach J.M., Thurber G.M., Miller M.A., Mazitschek R., Weissleder R., (2015), Advances in measuring single-cell pharmacology in vivo., *Drug Discov Today.*, 20(9):1087-92.
- Yan S.K., Liu R.H., Jin H.Z., Liu X.R., Ye J., Shan L., Zhang W.D., Chin J., (2015), "Omics" in pharmaceutical research: overview, applications, challenges, and future perspectives., *Nat Med.* 13(1):3-21.

- Chapter 2 -

Introduction

2.1 15-ketoatractyligenin methyl ester (SR2017)

Ent kaurenes represent one of the most important classes of diterpenoids and they are constituted by a perhydrophenantrene unit fused with a cyclopentane unit forming a bridge between carbons C-8 and C-13 (Hanson J.R. 2009). These diterpenes have been shown to possess several biological activities and they are present in different plant species belonging to several families such as Asteraceae, Euphorbiaceae, Apiaceae, Lamiaceae and other families. Thus, they can be used as drug or lead compounds (Sun H.D. *et al.* 2006; García P.A. *et al.* 2007; Wang L. *et al.* 2011).

Atractyligenin, the nor-ent-kaurane diterpene aglycon of the glycoside atractyloside originally extracted from the roots of *Atractylis gummifera* L. (Popat A. *et al.* 2001), exerts a weak inhibition of oxidative phosphorylation in the mitochondria of hepatocytes and some anti-proliferative effects towards several cancer cell lines, but it also shows a significant toxicity for normal cells. Therefore, atractyligenin is considered an unsafe compound, and its high toxicity of this compound is due to its strychnine-like action, producing convulsions of a hypoglycemic type 2 (Santi R. & Luciani, S.1978; Klingenberg, M. 1989). Atractyligenin and other related compounds are quite common in nature (Piozzi F. *et al.* 1967). They are present in different species: *Wedelia glauca* (Schteingart C.D. & Pomilio A.B. 1984), *Iphinona aucheri* (Roeder E. *et al.* 1994), *Drymaria arenariodes* (Vargas D. *et al.* 1988) and were implicated in the death of cattle, camels, and other livestock that accidentally ingested these plants. Moreover, they are present in *Coffea* beans (arabica and to a lesser extent robustica). It has been suggested that atractylosides may possibly be responsible for the statistical link between coffee drinking and pancreatic cancer.

In order to overcome the high toxicity of atractylgenin, several semisynthetic analogues were synthesized. Among these the 15- ketoatractyligenin methyl ester, here named SR2017 (Figure 1), showed the higher potency as anticancer drug, having anti-proliferative and pro-apoptotic activity towards different cancer cell lines with IC_{50} in the order of nano molar (Rosselli S. *et al.* 2007). Studies performed *in vitro* and *in vivo*, revealed that treatment of cancer cells with SR2017 affects Akt activation inhibiting the PI3K pathway (Cotugno R. *et al.* 2014). Even if in literature there are several papers regarding biopharmacological and toxicological effects of this molecule, few data are available concerning the identification of the SR2017 molecular target(s). Therefore, the molecular mechanism of action of this drug is still not clear.

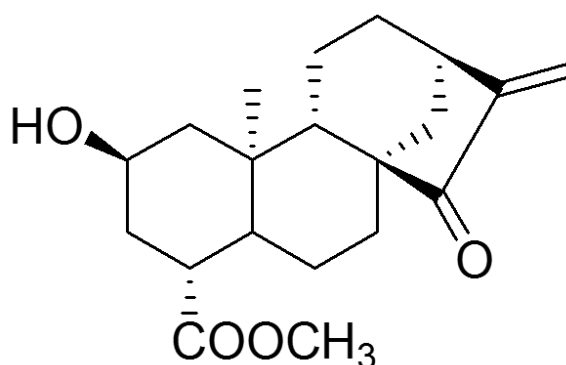


Fig.1: Chemical structure of SR2017

2.2 Aims of the project

In the attempt to discover and develop new drugs, the full understanding of the mechanism of action at a molecular level of bioactive compounds is an essential step. Actually, the mere observation of the effects of chemical entities on cells, tissues or organisms is not enough to consider them for further uses or optimizations. Therefore, unbiased approaches aimed to the identification of the molecular target(s) of action of promising molecules are emerging as a required starting point for many pharmaceutical and

biochemical researches. In that field, proteomic-based studies play a central role, potentially allowing to describe all the possible interactors of a selected compound (Rix U. & Superti-Furga G. 2008). In this regard in the present study, to define the possible protein target(s) of the semi synthetic diterpene SR2017 we used a chemical proteomic approach. This study allowed us to identify a list of possible targets, that were confirmed and validate using orthogonal experimental approaches. Moreover, the effects of SR2017 on the biological activity of its target(s) were investigated, as well as the binding mode of this diterpene to its protein partner(s). The achieved results would permit to further optimize the compound for a possible therapeutic use.

Results and discussion

2.3 Identification of the putative 15-ketoatractyligenin methyl ester targets by chemical proteomics

To attempt the identification of the molecular target(s) of 15-ketoatractyligenin methyl ester (SR2017), responsible for its activity, a chemical proteomics approach was used. This is one of the most versatile methods to profile cellular targets of selected drug candidates, and it is based on compound-immobilized affinity chromatography (Katayama H. & Oda Y. 2007; Dal Piaz F. *et al.* 2013). The chemical immobilization of a small molecule ligand is usually achieved through suitable functional group. For the immobilization of SR2017, the hydroxyl group at position C-2 of the diterpene, not fundamental to its biological activity (Rosselli S. *et al.* 2007), was modified by an epoxy-activated sepharose resin. Reaction conditions were selected in order to prevent the modification of the α,β -unsaturated carbonyl group, essential for the activity of this class of diterpenes (Lee I.S. *et al.* 1996; Wijeratne E.M. *et al.* 2012). All the modification steps were monitored by HPLC; the whole procedure led to 80% of immobilization of SR2017 on the solid support used.

The obtained drug-linked beads were incubated with protein extracts from Jurkat cells (Human T cell lymphoblast-like cell line), selected for their previously demonstrated susceptibility to SR2017 (Cotugno R. *et al.* 2014). After 30 minutes of incubation, the beads were extensively washed to remove any non-specifically interacting protein. Negative control experiments were simultaneously performed, using the same resin capped with ethanolamine to distinguish between specifically bound components and background contaminants (Figure 2).

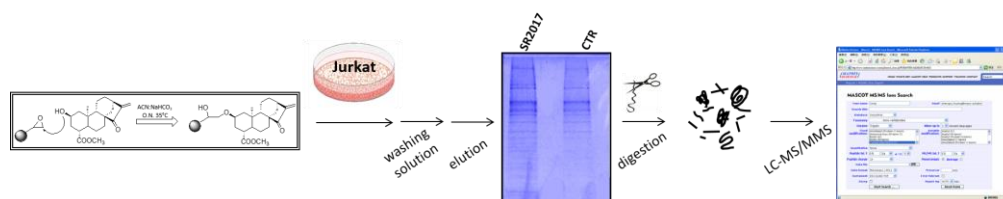


Fig.2: Workflow of chemical proteomic approach used for SR2017

The proteins tightly bound to each resin were eluted and resolved by SDS-PAGE; the gel lanes containing the proteins eluted from the beads modified with SR2017 and the control ones were cut in 10 pieces, digested with trypsin, and analyzed by high resolution nanoLC MS/MS. Resulting MS and MS/MS data were analyzed by Mascot Search Engine software. Chemical proteomic experiments were performed in triplicate and only proteins identified in all the experiments were taken into account; moreover, proteins identified from both SR2017-modified and control beads were excluded. Using this strategy, it was possible to identify the molecular chaperone heat shock protein 60 (Hsp60), and the nuclear receptor peroxisome proliferator-activated receptor gamma (PPAR γ) as putative protein targets of our diterpene (Figure 3).

Swiss-Prot code	Identified protein	Mr	Sequence coverage*	Matches unique*	Mascot score*
PPARG_HUMAN	Peroxisome proliferator-activated receptor gamma	57620	31%	11	581
CH60_HUMAN	60 kDa heat shock protein	61055	15%	5	136

* Values reported represent the mean of three independent experiments

Fig.3: Proteins identified by chemical proteomic experiments as putative SR2017 molecular targets

2.4 Targets validation by Surface Plasmon Resonance

The ability of SR2017 to interact with each of the proteins identified in the chemical proteomics experiments was assayed by surface plasmon resonance (SPR). SPR is an optical technique, based on the evanescent wave phenomenon, able to measure changes in refractive index onto a sensor surface, and it is suitable for characterizing macromolecular interactions. The binding between a compound in solution and its ligand immobilized on the sensor surface results in a change of the refractive index, that could be monitored in real time allowing the measurement of association and dissociation rates; therefore, different concentration of the diterpene were injected on each of the putative protein target, singularly immobilized on sensor chips (Dal Piaz F. *et al.* 2009). Obtained sensorgrams (Figure 4A) clearly showed a significant interaction of SR2017 with PPAR γ (Festa C. *et al.* 2012); a software aided elaboration of SPR results allowed measuring an equilibrium dissociation constants (K_D) of 89.3 ± 5.5 nM for the SR2017/PPAR γ complex. Conversely, no affinity of the diterpene towards Hsp60 was observed (Figure 4B).

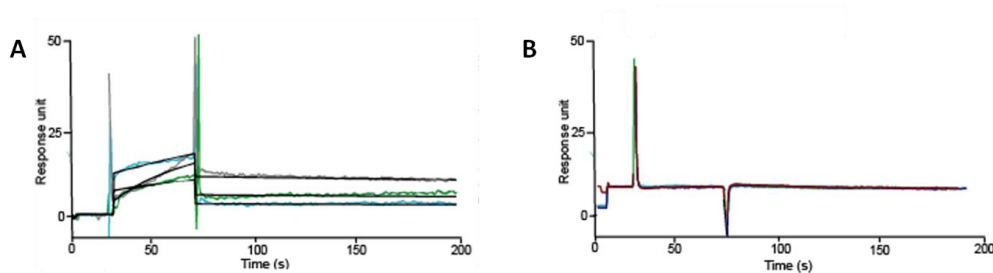


Fig.4: A) Sensorgrams obtained from the binding of SR2017 to PPAR γ ; B) Sensorgrams obtained from the binding of SR2017 to Hsp60.

Therefore, considering all these data we decided to perform an in-depth investigation on the biological role of SR2017 in the interaction with this protein. PPAR γ is a member of the PPARs subfamily (peroxisome

proliferator-activated receptors) of the nuclear receptor of ligand-inducible transcription factors (Laudet V. *et al.* 1992). It probably is the main regulator of adipocytes differentiation in human, but also plays a key role in lipid and glucose metabolism equilibrium, thus controlling cell proliferation (Tontonoz P. & Spiegelman B.M. 2008). Therefore, this protein is considered a pharmacologic target for metabolic dysfunctions (Choi J.H. *et al.* 2010), and for cancer (Reka A.K. *et al.* 2010). Several thiazolidinediones have been identified as PPAR γ agonists, and some of them have been approved for type 2 diabetes therapy (Meggs D.G. *et al.* 1998; Kumar S. *et al.* 1998); however, some problems concerning the cardiovascular safety and possible hepatotoxicity of these drugs were observed (Watkins P.B. & Whitcomb R.W. 1998; Nissen S.E. & Wolski K. 2010). Therefore, there is still a significant requirement of new types of PPAR γ ligands, possibly acting by a mechanism different from that of thiazolidinediones. Recently, some bioactive compounds derived from plants have been described as promising activators of PPAR γ (Wang L. *et al.* 2014). On these basis, the identification of PPAR γ as a possible molecular target of SR2017 was interesting, since modulation of PPAR γ activity could account for many of the cellular effects previously described for this compound (Cotugno R. *et al.* 2014). Indeed, a pro-apoptotic activity mediated by inhibition of the PI3K/Akt system was reported for several PPAR γ activators (Moon L. *et al.* 2011; Kulkarni A.A. *et al.* 2011; Honda A. *et al.* 2009). Therefore, we performed different experiment in order to get more details.

2.4.1 Selectivity of 15-ketoatractyligenin methyl ester towards different isoform of PPAR γ

PPAR nuclear receptor is a big family including three different isoforms, PPAR γ , PPAR α and PPAR δ encoded by different genes. Therefore, to evaluate the selectivity of SR2017 towards PPAR γ , this compound was also

subjected to SPR analyses on PPAR α and PPAR δ , two proteins structurally and functionally related to PPAR γ (Fruchart J.C. 2009; Reilly S.M. & Lee C.H. 2008). All the SPR experiments were performed using the full length proteins.

PPAR δ and PPAR α were immobilized on a sensor chip and increasing concentration of our diterpene were injected. No binding occurred between SR2017 and PPAR δ ; conversely, some interaction of this compound with PPAR α was observed, but the K_D measured ($1.32 \pm 0.08 \mu\text{M}$) was about 50 time higher than that measured for the PPAR γ /SR2017 complex. A comparison between the sensorgrams acquired for the interaction of SR2017 with PPAR α and PPAR γ reveals that the binding phases are similar, but there are clearly different kinetics of dissociation: PPAR α /SR2017 complex was completely dissociated after less than 50 s, whereas PPAR γ /SR2017 complex dissociation required long times and remains uncompleted.

2.5 Structural characterization of SR2017/PPAR γ complex

The SR2017/PPAR γ complex appeared to be very stable, as inferred by the measured low k_{off} ; (see Table 1) moreover, SPR sensorgrams showed that the dissociation of this complex required long times and remains uncompleted. This data, and the presence in the PPAR γ amino acidic sequence of a cysteine residue (Cys285), highly reactive towards nucleophile groups such as α,β -unsaturated ketones (Shiraki T. *et al.* 2005), prompted us to investigate the possible formation of a covalent bond between our diterpene and the nuclear receptor. Such bond could indeed be almost partially responsible for the high stability of the complex. In that aim, we performed a classic MS-based peptide mapping on the SR2017/PPAR γ complex using trypsin as proteolytic agent, to investigate the presence of covalently modified peptides. This analysis allowed us covering most of the protein sequence. Besides, a doubly charged ion at m/z 659,8481 was observed suggesting the presence of the peptide 281-

288 covalently bound to SR2017; this hypothesis was confirmed by MS/MS analysis of this ion, thus revealing the modification occurring to Cys285 via Micheal addition (Figure 5).

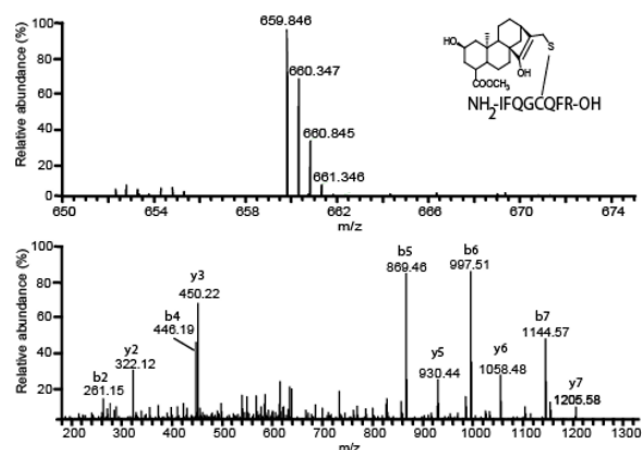


Fig.5: High resolution mass spectrum and MS/MS data of peptide 281-288 covalently bound to SR2017

2.6 15-ketoatractyligenin methyl ester is a bona fide PPAR γ ligand and requires the binding to C285 for its transcriptional activity

To verify if SR2017 is a *bona fide* PPAR γ ligand able to activate PPAR γ -mediated transcription, we transiently transfected a PPRE-TK-luciferase-reporter plasmid in HEK293 cells (Human Embryonic Kidney 293) that stably express an exogenous PPAR γ (in addition to the endogenous protein). In collaboration with Prof. Vittorio Colantuoni from the University of Sannio, it was possible to evaluate the biological relevance of SR2017 *in vitro*. More in details, HEK293 cells were selected as they express a fixed and known amount of PPAR γ , so that the differences in luciferase activity are due to the different ligand used.

First, we tested the antiproliferative effect of SR2017 on HT-29 colon-cancer derived cells and compared the achieved results with those observed for rosiglitazone, a fully characterized PPAR γ agonist (Hong G. *et al.* 2003). Cells

were cultured for 24 and 48 hs in the presence of increasing amounts of SR2017 or rosiglitazone, and counted (Figure 6). 15-Ketoatractyligenin methyl ester displayed a dosage-dependent inhibition of cell growth that was more pronounced than that produced by rosiglitazone. This stronger effect suggests that it likely activates specific antiproliferative and/or proapoptotic pathways.

Once established the cytotoxic effect of SR2017 also on this cell model, transfected HEK 293 cells were treated with increasing concentrations of rosiglitazone or SR2017 for 24 h and harvested for luciferase activity 48 h later. Rosiglitazone induced luciferase activity in a dose-dependent manner reaching a peak at 0.8 μ M and declining at higher concentrations as illustrated in Figure 7. Therefore, it was possible to validate the interaction of SR2017 with PPAR γ . The obtained results displayed a transactivation activity of SR2017 that was about 40% lower than the full agonist rosiglitazone, with a peak at 1 μ M. These results demonstrate that SR2017 can be considered a PPAR γ partial agonist compared to the full agonist.

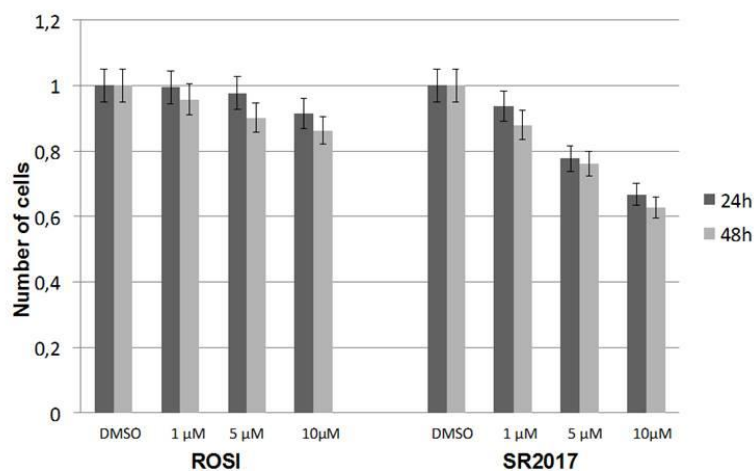


Fig.6: To assess the effect of SR2017 on exponentially growing HEK293 cells, cells were treated with increasing doses of SR2017 or rosiglitazone (1,5 and 10 μM). Cells were collected and counted after 24 and 48h.

Finally, we asked whether the binding of SR2017 to Cys285 in the ligand-binding pocket is required for the PPAR γ transcriptional activity. In fact, previous results (see 2.5) shown the covalent interaction of SR2017 with this cysteine and its implication on the stabilization of the complex. To this goal we transiently transfected basal HEK293T cells with the PPRE-TK-luciferase-reporter plasmid along with the expression vectors for the wild-type PPAR γ 1 or a mutant version carrying the Cys285Ala substitution (Waku T. *et al.* 2009).

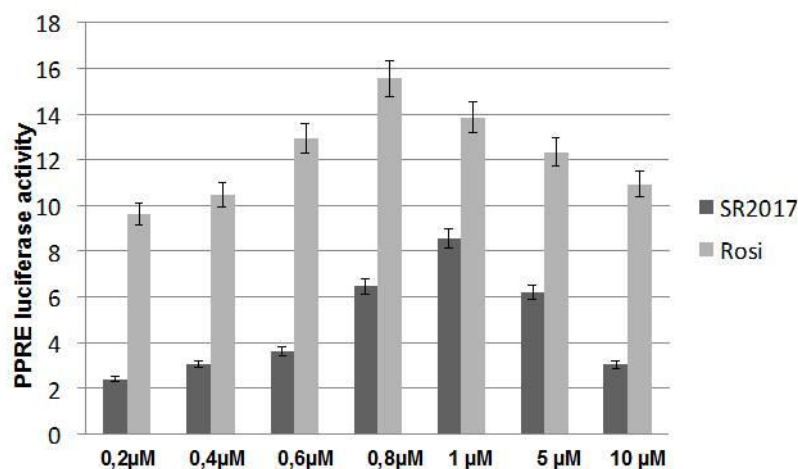


Fig.7: Transient transfection assay of the PPRE-luciferase reporter gene in human HEK293T cells stably expressing an exogenous Flag-tagged wild type PPAR γ 1. After transfection, cells were treated for 24 h with rosiglitazone or SR2017 respectively, at the indicated doses. Luciferase activity is reported as fold induction after normalization to β -galactosidase activity used as transfection control.

Cells were exposed for 24 h either to the vehicle alone or two concentrations of rosiglitazone and SR2017 shown to produce the highest induction; luciferase activity was measured in the cell extracts 48 h later. Rosiglitazone was able to bind both the wild type and mutant receptor with similar affinity and stimulate equivalent luciferase activity. SR2017 interacted with wild type PPAR γ and stimulated 40 % less luciferase activity than rosiglitazone, in line with being a partial agonist, as reported above. Strikingly, the interaction of SR2017 with the C285A mutant resulted in an even lower luciferase activity (Figure 8). These results show that the C285A mutation does not influence rosiglitazone-induced PPAR γ transcriptional activity, while it impairs the induction elicited by SR2017, clearly demonstrating that the binding to this amino-acid residue is absolutely required for stimulating PPAR γ transcriptional activity.

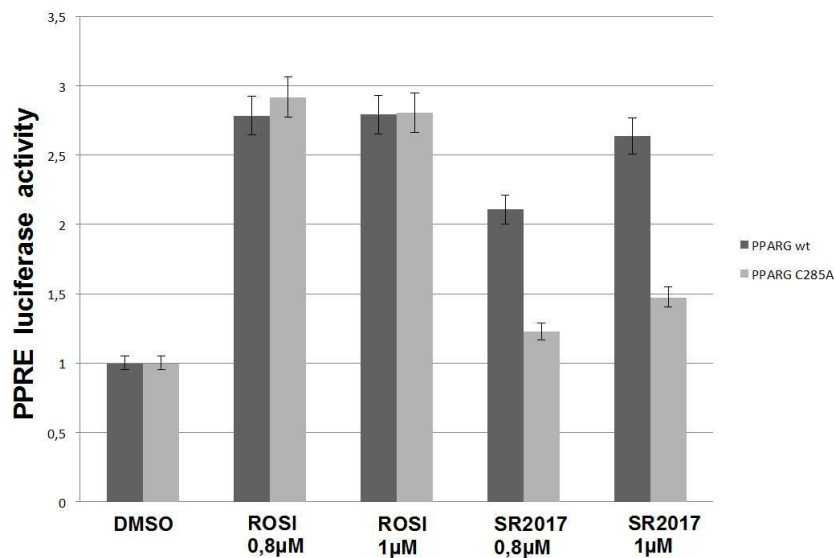


Fig.8: Human HEK293T cells were cotransfected with the PPRE-luciferase reporter gene along with wild-type PPAR γ 1 or its (Cys285Ala) mutant version. After transfection, cells were treated for 24 h with rosiglitazone or SR2017 at the indicated concentrations. Luciferase activity is reported as fold induction after normalization to β -galactosidase activity used as transfection control.

2.7 Molecular docking of SR2017/PPAR γ complex

SR2017 is determined to be a partial agonist covalently bound to PPAR γ in the current work (Figure 5). The covalent coupling of the ligand to Cys285 of PPAR γ is the result of a Michael addition (conjugate addition) for which the organic reaction is well established and illustrated in Figure 9. The Michael acceptor contains an electron withdrawing group conjugated to an activated carbon that is then subject to attack by the nucleophilic Cys285.

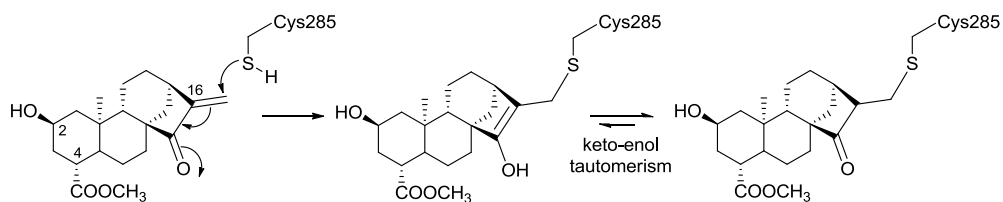


Fig.9: Mechanism of covalent coupling of SR2017 to Cys285 of PPAR γ

Thus, in collaboration with Prof. Antonio La Vecchia from the University of Naples Federico II, we chose to employ the covalent docking protocol CovDock (Zhu, K. *et al.* 2014; Toledo-Warshaviak D. *et al.* 2014.) implemented in the in the Schrödinger Suite (Schrödinger, LLC, New York, NY, 2015) in order to visualize possible conformational states of the Cys285 thioether resulting from a reaction with compound SR2017, assuming that its chemical reactivity (*vide supra*) is relevant in the context of the protein. CovDock uses different tools of the Schrödinger Suite to mimic distinct stages of covalent inhibitor binding. The first step is a classical noncovalent docking with an alanine mutation of the nucleophilic side chain followed by an automated bond formation and a second docking step with the covalent bond in place. The basic concept of the software is that a covalently bound ligand has to adopt an energetically favorable unbound pose before bond formation occurs and that these unbound poses do not change dramatically during the reaction pathway, because conformational sampling is done solely prior the noncovalent docking step. Docking was carried out employing the publicly available X-ray crystal structure of PPAR γ in complex with the partial agonist LT175 (PDB code: 3B3K) (Montanari R. *et al.* 2008).

A low-energy pose of SR2017 covalently bound to Cys285 was predicted by CovDock, and this conformation, which adopts a *R* configuration at position 16 of the Michael acceptor, is stabilized by several H-bonds with the key residues in the β -sheet subpocket.

Unlike rosiglitazone, which takes a U-shape conformation in the ligand-binding pocket and wrap around H3 to directly contact the AF-2 helix (H12), SR2017 occupies the region of PPAR γ delimited by the H3 and the β -sheet (β -sheet sub-pocket) and makes no contact with H12 or residues involved in co-activator recruitment (Figure 10a,c), as already observed in other structures of complexes with partial agonists, such as the complexes with BVT.13, MRL-24, and nTZDpa (Bruning, J. B. *et al.* 2007). In contrast, the full agonist rosiglitazone occupies roughly 40% of the ligand-binding site of PPAR γ in a U-shaped conformation and consists of a polar head and hydrophobic tail. The polar head makes a net of the H-bonds with Ser289, His323, His449, and Tyr473 PPAR γ side chains, while forming a hydrophobic region with Phe363, Gln286, Phe282, and Leu469. Despite the fact that SR2017 binds in a different mode than rosiglitazone, occupying the β -sheet sub-pocket, the *ent*-kaurane skeleton of SR2017 overlaps with the hydrophobic region of rosiglitazone when the two structures are superposed (Figure 10b).

The carbonyl and the ethereal oxygens of the ester group at position 4 of the ligand form two H-bonds, one with the NH backbone of Ser342 (located at the β -sheet) and one with both NH₂ and N^ε of Arg288 side chain on H3. The hydroxyl group at position 2 establishes a H-bond with the C=O backbone of Ile281 ($d_{\text{OH-O}} = 2.8 \text{ \AA}$) as well as a very weak H-bond ($d_{\text{OH-N}} = 4.1 \text{ \AA}$) with the side chain of His266, located at the Ω loop that links H2 to H3. Non-polar contacts are observed along the full extension of the SR2017 molecule. These contacts start at the Ω -loop of the protein, and extend all the way through the ligand binding pocket. Residues involved in these interactions include Phe264 (part of the Ω -loop), Ile281, Gly284, and Phe287 on H3, Val339, Ile341 and Met348 on the β -sheet, Leu330 (H5), and Met364 (H7).

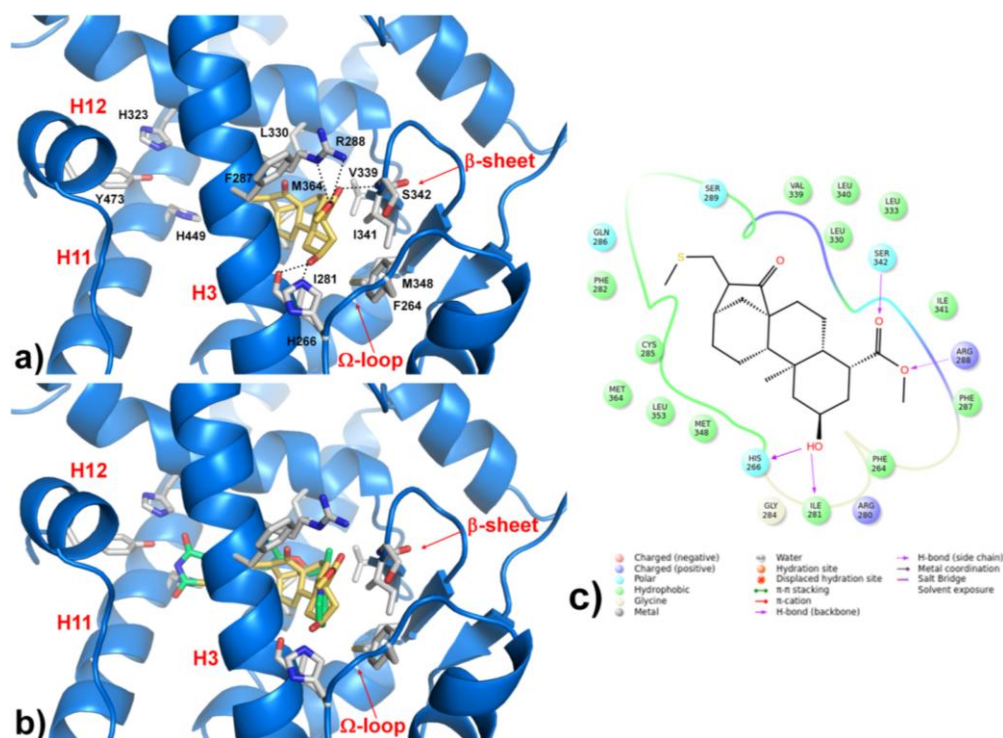


Fig.10: a) and c) Binding mode of SR2017 (yellow sticks) into the PPAR γ binding site represented as a blue ribbon model. b) C α superposition of the complexes of PPAR γ with SR2017 and rosiglitazone (green sticks, PDB code 2PRG). Only amino acids located within 4 Å of the bound ligand are displayed (white sticks) and labeled. The Ω -loop, a flexible loop region between H2' and H3, and the β sheet region of the LBD, are displayed. H-bonds discussed in the text are depicted as dashed black lines.

Recent experimental evidences showed that PPAR γ partial agonists, that is ligands that lack direct contact with H12 but can still activate PPAR γ to a lesser extent, use alternative mechanisms not involving the stabilization of H12, but rather the stabilization of H3 and the β -sheets (Bruning, J.B *et al.* 2007) and/or modifications in the structure and dynamics of the flexible region known as Ω -loop, a flexible loop region comprising ~15 residues between H20 and H3 spanning D260-K275 (Waku T *et al.* 2009b; Waku T. *et al.* 2009; Puhl A.C. *et al.* 2012; Hughes T.S *et al.* 2014). Structural comparison of SR2017 with the previously published partial PPAR γ agonists BVT.13, MRL-24, and nTZDpa reveals closely related interactions with PPAR γ . All of these ligands

occupy the same binding site and interact similarly with H3 and the β -sheet. Their carboxyl or ester groups interact directly with Ser342 of the β -sheet. H3 is always stabilized by a ligand carboxyl or hydroxyl group forming a direct or a water-mediated H-bond. Ligand binding to PPAR γ seems to induce a cooperative folding transition between the H3 and β -sheet regions because the stability of these structural elements appears to be strongly correlated. Because the cyclin-dependent kinase 5 (Cdk5) recognition site extends into the first β -strand of PPAR γ , structural stabilization of the β -sheet region, elicited by SR2017 and other ligands, presumably renders Ser273 inaccessible to the kinase, protecting the receptor from phosphorylation, as originally proposed by Choi J.H. *et al.* 2010.

2.8 Screening of 15-ketoatractyligenin methyl ester analogous using SPR analysis

In order to identify the structural feature playing a pivotal role in the SR2017/PPAR γ interaction, we investigated the affinity of some SR2017 analogous (compounds **2-9**, Figure 3) towards this protein using SPR analyses. In particular, diterpenes with different functional groups and stereochemistry were tested. As a positive control, rosiglitazone was also assayed.

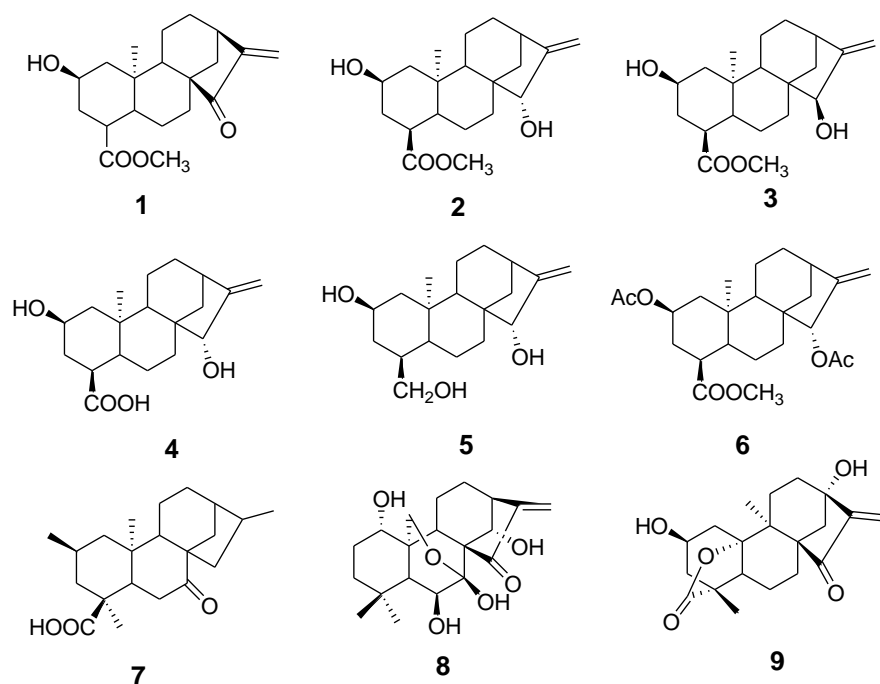


Fig.11: Structure of compounds **1-9**. Compound **1** is SR2017

All these compounds displayed an affinity towards the PPAR γ ligand binding domain (PPAR γ LBD) lower than that of SR2017 (Table 1). In particular, compounds whose bi-cyclic portion was clearly different from that of **1** (SR2017), did not interact with the protein, regardless of the presence of the α - β unsaturated keto-group (see compounds **8** and **9**); on the other hand, elimination of the α - β unsaturated keto-group from SR2017 structure significantly affected interaction with PPAR γ LBD, strongly increasing both thermodynamic (K_D) and kinetic (k_{off}) dissociation constants (compounds **2** and **3**). Finally, the presence of a free acidic function prevented interaction of the diterpenes with PPAR γ LBD (compounds **4** and **7**).

Table 1: Thermodynamic and kinetic constants measured by SPR for compounds 1-9 and rosiglitazone injected on immobilized PPAR γ .

Compound	K _D (nM)	k _{off} (s ⁻¹)
1 (SR2017)	89.3	0.0015
2	1856	0.051
3	4587	0.096
4	no binding	
5	no binding	
6	no binding	
7	no binding	
8	no binding	
9	no binding	
Rosiglitazone	320.5	0.0286

2.9 Discussion

Natural compounds represent an incomparable source of bioactive chemical entities. However, their use is largely limited by the poor knowledge of their molecular mechanism and of their actual targets. In particular, plant metabolites carrying reactive groups are often considered unspecific and, therefore, poorly interesting; however, recent studies – also performed using proteomic based approaches- suggested that this is not always true. In the present study, we demonstrated that 15-ketoatractyligenin methyl ester (SR2017) selectively interacts with a specific protein (PPAR γ), even if in its structure is present a α,β -unsaturated ketone reactive towards thiol groups. However, the formation of the covalent bond involving Cys285 is both required for the PPAR γ /SR2017 complex stabilization and for the protein activation. The binding mode of SR2017 to the protein, with the ligand occupying the PPAR γ β -sheet sub-pocket, suggested that SR2017 is a PPAR γ partial agonist. This hypothesis was confirmed by studies on PPAR γ activation by SR2017, in comparison with that achieved using the full agonist rosiglitazone. Recent findings revealed that some partial agonists show high

insulin sensitivity and significant activity, but side effects lower than PPAR γ full agonist; therefore, SR2017 could be a promising lead for the development of new therapeutic and/or biochemical tool.

Materials and methods

Materials

Solvents and water (HPLC grade) were purchased from Romil (ROMIL Ltd, Cambridge, UK). Recombinant human PPAR γ ligand binding domain (PPAR γ LBD) consisting of the region 195-477 of PPAR γ , was purchased from Bertin-Pharma (Bertin-Pharma, Montigny le Bretonneux, France); recombinant human Hsp60 was acquired from Tebu-Bio (Tebu-Bio, Megenta, Italy). Proteomic grade trypsin was from Promega (Promega, Milano, Italy), Compounds 1-7 were synthesized as reported elsewhere (Rosselli S. *et al.*, 2007); compounds 8 and 9 were selected from those present in the natural compound library of the Department of Pharmacy of the University of Salerno. Purification and structural characterization of these compounds were previously published (Dal Piaz F. *et al.* 2007; Dal Piaz F. *et al.* 2013).

2.10 Chemical proteomics

In order to perform chemical proteomic experiments, SR2017 (1.1 mg) was incubated at 30 °C with 8.5 mg of an epoxy-activated sepharose resin 6B (Sigma-Aldrich) in 500 μ l of 30 mM NaHCO₃, 40% (v/v) CH₃CN (pH 8), to achieve compound immobilization. The reaction was monitored by LC/MS using a LC-Q Advantage instrument coupled with a Accela HPLC system (Thermo Fisher Scientific). Reaction was completed after 4 h, leading to a SR2017 concentration of about 10 mmol for 1 ml of resin. Un-reacted resin epoxy groups were deactivated by adding 50 μ l of 1 M ethanolamine. Control resin was prepared directly incubating 8.5 mg of a epoxy-activated sepharose resin 6B with 1 M ethanolamine.

Jurkat (human leukemia, T cell lines) obtained from American Type Cell Culture (ATCC, Sesto San Giovanni, Italy), were maintained in RPMI 1640 medium supplemented with 10 % (v/v) Fetal Bovine Serum (FBS), 2 mM l-

glutamine and antibiotics at 37 °C in humidified 5 % CO₂ atmosphere. To ensure logarithmic growth, cells were sub-cultured every 2 days. All experiments were performed using cells at 2x10⁵ cells/ml density. Under given experimental conditions, untreated cells were able to double in number in less than 24 hr. For protein extracts, control or treated cells were harvested by using a solution of trypsin-EDTA and washed three times with phosphate buffer saline (PBS). Cells were collected by centrifugation for 10 min at 400 g and lysed for 30 min on ice in PBS containing 0.1 % Igepal (lysis buffer) and a protease and phosphatase inhibitor cocktail (P8340, Sigma-Aldrich, St. Louis, MO, USA). Samples were clarified by centrifugation for 15 min at 15000 g at 4 °C. Protein concentration was determined by Bio-Rad DC Protein Assay (Bio-Rad, Hercules, CA, USA) using bovine serum albumin as a standard.

Jurkat cell lysates (500 µg) were incubated with SR2017 loaded or with control resin. The beads were washed three times with lysis buffer and then three times with PBS. Interacting proteins were eluted by 50 µl of Laemmli buffer (60 mM Tris HCl pH 6.8, 2 % sodium dodecylsulfate, 10 % glycerol, 0.01 % blue bromophenol, 5 % β-mercaptoethanol). Eluted proteins were separated on a mono-dimensional 12 % SDS-PAGE and stained with Brilliant Blue G-Colloidal (Sigma-Aldrich). Each gel line was cut in 10 pieces, reduced by DTT, alkylated using iodoacetamide, and digested by trypsin. The resulting fragments were extracted and analyzed by LC/MS/MS using a LTQ Orbitrap XL ESI-mass spectrometer (Thermo Fisher Scientific) equipped with a nano-ESI source, coupled with a nano-Aquity capillary UPLC (Waters): peptides separation was performed on a capillary BEH C18 column (0.075 mm × 100 mm, 1.7 µm, Waters) using aqueous 0.1% formic acid (A) and CH₃CN containing 0.1% formic acid (B) as mobile phases. Peptides were eluted by means of a linear gradient from 10 % to 40% of B in 45 min and a 300 nl•min⁻¹ flow rate. Peptide fragmentation was achieved using helium as collision gas and a collision cell energy of 30 eV. Mass spectra were acquired

in a m/z range from 400 to 1800, and MS/MS spectra in a m/z range from 25-2000. MS and MS/MS data were used by Mascot (Matrix Science) to interrogate the Swiss Prot non-redundant protein database. Settings were as follows: mass accuracy window for parent ion, 10 ppm; mass accuracy window for fragment ions, 50 millimass units; fixed modification, carbamidomethylation of cysteines; variable modifications, oxidation of methionine. Proteins with scores > 65 and identified by at least 2 significant sequences, were considered as reliable proteins.

2.11 Surface plasmon resonance (SPR)

SPR analyses were carried out on a BIACORE 3000 instrument (GE-Healthcare) according to our previously published procedures (Dal Piaz F. *et al.* 2009; Dal Piaz F. *et al.* 2010). Briefly, PARP γ and HSP60 surfaces were prepared on a research-grade CM5 sensor chips (GE Healthcare). Proteins (100 $\mu\text{g}\cdot\text{ml}^{-1}$ in 10 mM CH_3COONa , pH 5.0) were immobilized using a standard amine-coupling protocol, to obtain densities of 3–5 kRU (1000 RU corresponds to the binding of ~ 1 ng per square mm of protein on the dextran surface). Testing compounds were dissolved in 100 % DMSO to obtain 4 mM solutions, and then diluted in PBS (10 mM NaH_2PO_4 , 137 mM NaCl , 2.7 mM KCl pH 7.4) containing variable amounts of DMSO, in order to achieve a final DMSO concentration of 0.1 %. For each molecule a six-point concentration series spanning 0.025–1 μM was set up. SPR experiments were carried out at 25 °C, with a 50 $\mu\text{l}\cdot\text{min}^{-1}$ flow rate. Association and dissociation times were set at 60 s and 300 s, respectively. Simple interactions were adequately fit to a single-site bimolecular interaction model to yield K_D . BIAevaluation software (GE Healthcare) was used for sensorgrams elaboration. Same procedure was utilized for PPAR α and PPAR δ

2.12 PARP γ /LBD peptide mapping

PARP γ was incubated with a 2:1 molar excess of SR2017 under stirring for 15 min in PBS at 37 °C. To eliminate the un-reacted diterpene, reaction mixtures were loaded on a GELoader micropipette tips (Eppendorf, Milano, Italy) packed with Poros R2 (Perseptive Biosystems, Firingam, MA, USA) reversed phase materials. Eluted proteins were loaded on a mono-dimensional 12% SDS-PAGE, stained with Brilliant Blue G-Colloidal, reduced, and digested by trypsin. The resulting fragments were extracted and analyzed by LC/MS/MS as described above.

2.13 Computational chemistry

Molecular modeling and graphics manipulations were performed using Maestro (Maestro, version 10.1, Schrödinger, LLC, New York, NY, 2015) and UCSF-Chimera 1.8.1 software packages (Huang C.C. *et al.* 1996) running on a E4 Computer Engineering E1080 workstation provided of a Intel Core i7-930 Quad-Core processor. CovDock algorithm (Zhu K. *et al.* 2014) of the Schrodinger Small Molecule Drug Discovery Suite was used for all docking calculations. Figures were generated using Pymol 1.0 (Warren L. DeLano "The PyMOL Molecular Graphics System." DeLano Scientific LLC, San Carlos, CA, USA. <http://www.pymol.org/>).

2.13.1 Protein and Ligand Preparation

The crystal structure of PPAR γ in complex with ligand LT175 (PDB code: 3B3K) (Montanari R. *et al.* 2008) was download from the PDB Bank (Berman H.M. *et al.* 2002) and employed for the automated docking studies. The protein was processed through the Protein Preparation Wizard in Maestro (Sastry G.M. *et al.* 2013). The right bond orders as well as charges and atom types were assigned and the hydrogen atoms were added to protein. Arginine and lysine side chains were considered as cationic at the guanidine and

ammonium groups, and the aspartic and glutamic residues were considered as anionic at the carboxylate groups. All crystallographic water molecules were deleted. Imidazole rings of H449 and H323 into PPAR γ were set in their N τ -H (N tau-H) tautomeric state. Moreover, an exhaustive sampling of the orientations of groups, whose H-bonding network needs to be optimized, was performed. Finally, the protein structures were refined with a restrained minimization with the OPLS2005 force field (Song Z. *et al.* 2000) by imposing a 0.3 Å root-mean-square deviation (rmsd) limit as the constraint.

The core structure of SR2017 was retrieved from the Cambridge Structural Database (CSD) (Allen F.H. 2002) (CSD refcode: YALXIU) and modified with the fragment dictionary of Maestro. The ligand was then preprocessed with LigPrep 3.3 (LigPrep, version 3.3, Schrödinger, LLC, New York, NY, 2015) and optimized by MacroModel 10.7 (MacroModel, version 10.7, Schrödinger, LLC, New York, NY, 2015) using the MMFFs force field with the steepest descent (1000 steps) followed by truncated Newton conjugate gradient (500 steps) methods. Partial atomic charges were computed using the OPLS-AA force field.

2.13.2 Docking Simulations

Docking of SR2017 to PPAR γ was performed with the CovDock algorithm, which comprises three main stages: first, conventional noncovalent docking of the prereactive species into the alanine mutated form of the receptor, on the basis of the rapid sampling provided by Glide (Friesner R.A. *et al.* 2004; Halgren T.A. *et al.*, 2004; Friesner R.A. *et al.* 2006). Then, the residue is mutated back to its original chemical structure and its side chain conformation is sampled with a rotamer library, in order to find a state consistent with covalent bond formation. The covalent bond parameters are taken from the OPLS force field, such that any nonphysical bond distances, angles, or torsions will be appropriately penalized. Finally, refinement of the covalently

bound protein–ligand complex, followed by selection of optimal structures with program Prime (Jacobson M.P. *et al.* 2004; Jacobson M.P. *et al.* 2002). The resultant protein-ligand geometries are ranked based on VSGB 2.0, an all-atom energy function based on OPLS force field and Generalized Born solvation model (Li J. *et al.* 2011). As input, we specified Michael’s addition as the type of reaction by which the ligand binds to the receptor. The reaction is predefined to recognize the ligand reactive group with the encoded SMARTS pattern (in this case the α,β -unsaturated carbonyl moiety present in SR2017), and to perform the postreaction changes in hybridization of the ligand. In the receptor section, the sulfhydryl group Cys285 side chain of PPAR γ was selected as the reactive residue. 5 output poses were generated. The top one pose, based on its Prime energy property, was selected and is presented in Figure 10. The reaction generated a chiral center at position 16 in the (R)-configuration.

2.14 Plasmids and transient transfection experiments

The recipient cells used for transfection experiments were HEK293T cells that stably express an exogenous Flag-tagged PPAR γ from a transfected PCDNA-3 vector carrying a complete PPAR γ cDNA. The PPRE-Luc plasmid contains a luciferase reporter gene under the transcriptional control of three copies of the PPRE (Peroxisome Proliferator Response Element) derived from Acyl-CoA oxidase gene fused upstream to the herpes simplex thymidine kinase (TK) promoter. The RSV-Gal plasmid, expressing -galactosidase gene driven by the strong Rous Sarcoma Virus (RSV) promoter/cassette was used as an internal control for transfection efficiency. The day before transfection, the Flag-PPAR γ -HEK293 cells were plated in 12-well plates to reach 70% confluence. After 24 hr, the growth medium was replaced with OPTI-MEMI without serum and antibiotics and cells transfected with the luciferase reporter gene (PPRE-Luc) using lipofectamine 2000 reagent according to manufacturer’s

instructions. Ten-twelve hours after transfection, cells were washed and treated with different concentrations of rosiglitazone and SR2017. The wild-type and mutant PPAR γ 1 containing expression vectors were kindly provided by Dott. Takuma Shiraki. The mutant receptor carries an Alanine that replaces a Cysteine residue at position 285 (C285A). The experiments were carried out as above into basal HEK293T cells and also in these cases the RSV--Gal plasmid was used as control for transfection efficiency. At least three independent experiments were performed for each transfection carried out in duplicate. Luciferase activity was normalized to β -galactosidase activity and reported as fold induction.

References

- Allen F.H., (2002). The Cambridge Structural Database: a quarter of a million crystal structures and rising. *Acta Crystallogr. B.* 58, 380–388.
- Berman H.M., Battistuz T., Bhat T.N., Bluhm W.F., Bourne P.E., Burkhardt K., Feng Z., Gilliland G.L., Iype L., Jain S., Fagan P., Marvin J., Padilla D., Ravichandran V., Schneider B., Thanki N., Weissig H., Westbrook J.D., Zardecki, C., (2002)., The protein data bank. *Acta Crystallogr. D.* 58, 899-907.
- Bruning J.B., Chalmers M.J., Prasad S., Busby S.A., Kamenecka T.M., He Y., Nettles K.W., Griffin, P.R., (2007). Partial agonists activate PPAR γ using a helix 12 independent mechanism. *Structure.* 15, 1258–1271.
- Choi J.H., Banks A.S., Estall J.L., Kajimura S., Boström P., Laznik, D., Ruas J.L., Chalmers M.J., Kamenecka T.M., Blüher M., Griffin P.R., Spiegelman B.M., (2010) Anti-diabetic drugs inhibit obesity-linked phosphorylation of PPAR γ by Cdk5. *Nature.* 466, 451-456.
- Cotugno R., Gallotta D., Dal Piaz F., Apicella I., De Falco S., Rosselli S., Bruno M., Belisario M.A. (2014). Powerful tumor cell growth-inhibiting activity of a synthetic derivative of atractyligenin: Involvement of PI3K/Akt pathway and thioredoxin system. *Biochim. Biophys. Acta.* 1840, 1135–1144.
- Dal Piaz F., Cotugno R., Lepore L., Vassallo A., Malafrente N., Lauro G., Bifulco G., Belisario M.A., De Tommasi N., (2013). Chemical proteomics reveals HSP70 1A as a target for the anticancer diterpene oridonin in Jurkat cells. *J. Proteom.* 82, 14–26.
- Dal Piaz F., Nigro P., Braca A., De Tommasi N., Belisario M.A. (2007). 13-Hydroxy-15-oxo-zoapatlin, an ent-kauranediterpene, induces apoptosis in human leukemia cells, affecting thiol-mediated redox regulation. *Free Radic. Biol. Med.* 15, 1409-22.

- Dal Piaz F., Tosco A., Eletto D., Piccinelli A.L., Moltedo O., Franceschelli S., Sbardella G., Remondelli P., Rastrelli L., Vesci L., Pisano C., De Tommasi N., (2010). The identification of a novel natural activator of p300 histone acetyltransferase provides new insights into the modulation mechanism of this enzyme. *Chem. Bio. Chem.* *11*, 818–27.
- Dal Piaz F., Vassallo A., Lepore L., Tosco A., Bader A., De Tommasi, N., (2009) Sesterterpenes as TTL Inhibitors. First insight of Structure-Activity relationship and Discovery of New Lead. *J. Med. Chem.* *52*, 3814-3828.
- Festa C., Lauro G., De Marino S., D'Auria M.V., Monti M.C., Casapullo A., D'Amore C., Renga B., Mencarelli A., Petek S., Bifulco G., Fiorucc, S., Zampella A., (2012). Plakilactones from the marine sponge *Plakinastrellamamillaris*. Discovery of a new class of marine ligands of peroxisome proliferator-activated receptor γ . *J. Med. Chem.* *55*, 8303-17.
- Friesner R.A., Banks J.L., Murphy R.B., Halgren T.A., Klicic J.J., Mainz D.T., Repasky M.P., Knoll E.H., Shelley M., Perry J.K., Shaw D.E., Francis P., Shenkin, P.S., (2004). Glide: a New Approach for Rapid, Accurate Docking and Scoring. 1. Method and Assessment of Docking Accuracy. *J. Med. Chem.* *47*, 1739–1749.
- Friesner R.A., Murphy R.B., Repasky M.P., Frye L.L., Greenwood J.R., Halgren T.A., Sanschagrin P.C., Mainz D.T., (2006). Extra Precision Glide: Docking and Scoring Incorporating a Model of Hydrophobic Enclosure for Protein-Ligand Complexes. *J. Med. Chem.* *49*, 6177–6196.
- Fruchart J.C., (2009), Peroxisome proliferator-activated receptor-alpha (PPAR α): At the crossroads of obesity, diabetes and cardiovascular disease, *Atherosclerosis*, *205*(1), 1-8.
- García P.A., de Oliveira A.B., Batista R., (2007), Occurrence, biological activities and synthesis of kaurane diterpenes and their glycosides., *Molecules*, *13*;12(3):455-83.
- Halgren T.A., Murphy R.B., Friesner R.A., Beard H.S., Frye L.L., Pollard W.T., Banks J.L., (2004). Glide: a New Approach for Rapid, Accurate Docking and Scoring. 2. Enrichment Factors in Database Screening. *J. Med. Chem.*, *47*, 1750–1759.
- Hanson J.R., (2009), Diterpenoids., *Nat Prod Rep.*; *26*(9):1156-71.
- Honda A., Matsuura K., Fukushima N., Tsurumi Y., Kasanuki H., Hagiwara N., (2009),. Telmisartan induces proliferation of human endothelial progenitor cells via PPAR γ -dependent PI3K/Akt pathway. *Atherosclerosis*. *205*, 376-384.
- Hong G., Davis B., Khatoun N., Baker S.F., Brown, J., (2003) PPAR γ -dependent anti-inflammatory action of rosiglitazone in human monocytes: suppression of TNF α secretion is not mediated by PTEN regulation. *Biochem. Bioph. Res. Co.* *303*, 782-787.
- Huang C.C., Couch G.S., Pettersen E.F., Ferrin, T.E., (1996), Chimera: an extensible molecular modelling application constructed using standard components. *Pac. Symp. Biocomput.* *1*, 724; <http://www.cgl.ucsf.edu/chimera>.

- Hughes T.S., Giri P.K., De Vera I.M.S., Marciano D.P., Kuruvilla D.S., Shin Y., Blayo, A.L., Kamenecka T.M., Burris T.P., Griffin P.R., Kojetin D. J., (2014). An alternate binding site for PPAR γ ligands. *Nat. commun.* 5, 3571.
- Hyun S., Kim M.S., Song Y.S., Bak, Y., Ham S.Y., Lee D.H., Hong J., Yoon Do, Y. (2015) Peroxisome Proliferator-Activated Receptor-Gamma Agonist 4-O-Methylhonokiol Induces Apoptosis by Triggering the Intrinsic Apoptosis Pathway and Inhibiting the PI3K/Akt Survival Pathway in SiHa Human Cervical Cancer Cells. *J. Microbiol. Biotechnol.* 25, 334–342.
- Jacobson M.P., Friesner R.A., Xiang Z., Honig, B., (2002). On the Role of Crystal Packing Forces in Determining Protein Sidechain Conformations. *J. Mol. Biol.* 320, 597-608.
- Jacobson M.P., Pincus D.L., Rapp C.S., Day T.J.F., Honig B., Shaw D.E., Friesner, R.A., (2004), A Hierarchical Approach to All-Atom Protein Loop Prediction. *Proteins.* 55, 351-367.
- Katayama H. & Oda Y., (2007)., Chemical proteomics for drug discovery based on compound-immobilized affinity chromatography. *J. Chromatography B.* 855, 21–27.
- Klingenberg M., (1989), Survey of carrier methodology: strategy for identification, isolation, and characterization of transport systems. *Methods Enzymol.*; 171:12-23.
- Kulkarni A.A., Thatcher T.H., Olsen K.C., Maggirwar S.B., Phipps R.P., Sime, P.J., (2011). PPAR- γ Ligands Repress TGF β -Induced Myofibroblast Differentiation by Targeting the PI3K/Akt Pathway: Implications for Therapy of Fibrosis. *PlosOne.* 6, e15909.
- Kumar S., Prange A., Schulze J., Lettis S., Barnett, A.H., (1998). Troglitazone, an insulin action enhancer, improves glycaemic control and insulin sensitivity in elderly type 2 diabetic patients. *Diabet. Med.* 15, 772–779.
- Laudet V., Hänni C., Coll J., Catzeflis F., Stéhelin, D., (1992). Evolution of the nuclear receptor gene superfamily. *EMBO J.* 11, 1003-1013.
- Lee I.S., Shamon L.A., Chai H.B., Chagwedera T.E., Besterman J.M., Farnsworth N.R., Cordell G.A., Pezzuto J.M., Kinghorn, A.D. (1996). Cell-cycle specific cytotoxicity mediated by rearranged ent-kauranedieterpenoids isolated from *Parinaricuratellifolia*. *Chem. Biol. Interact.* 99, 193–204.
- Li J., Abel R., Zhu K., Cao Y., Zhao S., Friesner R.A., (2011), The VSGB 2.0 Model: a Next Generation Energy Model for High Resolution Protein Structure Modeling. *Proteins.* 79, 2794–2812.
- Maggs D.G., Buchanan T.A., Burant C.F., Cline G., Gumbiner B., Hsueh W.A., Inzucchi S., Kelley D., Nolan J., Olefsky J.M., Polonsky K.S., Silver D., Valiquett T.R., Shulman G.I., (1998). Metabolic effects of troglitazonemonotherapy in type 2 diabetes mellitus. A randomized, double-blind, placebo-controlled trial. *Ann. Internal. Med.* 128, 176–185.
- Michalik L., Auwerx J., Berger J.P., Chatterjee V.K., Glass C.K., Gonzalez F.J., Grimaldi P.A., Kadowaki T., Lazar M.A, O'Rahilly S., Palmer C.N., Plutzky J, Reddy J.K.,

- Spiegelman B.M., Staels B., Wahli W., (2006), International Union of Pharmacology. LXI. Peroxisome proliferator-activated receptors. *Pharmacol. Rev.* 58, 726–741.
- Montanari R., Saccoccia, F., Scotti E., Crestani M., Godio C., Gilardi F., Loiodice F., Fracchiolla G., Laghezza A., Tortorella P., Lavecchia A., Novellino E., Mazza F., Aschi M., Pochetti, G., (2008). Crystal structure of the peroxisome proliferator-activated receptor gamma (PPAR γ) ligand binding domain complexed with a novel partial agonist: a new region of the hydrophobic pocket could be exploited for drug design. *J Med. Chem.* 51, 7768-76.
- Moon L., Ha Y.M., Jang H.J. Kim H.S., Jun M.S., Kim Y.M., Lee, Y.S., Lee D.H., Son K.H., Kim H.J., Seo H.G., Lee J.H., Kim Y.S, Chang, K.C., (2011). Isoimperatorin, cimicifugoside E and 23-O-acetylshengmanol-3-xyloside from *Cimicifugae* Rhizome inhibit TNF- α -induced VCAM-1 expression in human endothelial cells: Involvement of PPAR- γ upregulation and PI3K, ERK1/2, and PKC signal pathways. *J. Ethnopharmacol.* 133, 336-344.
- Nissen S.E. & Wolski K., (2010). Rosiglitazone revisited: an updated meta-analysis of risk for myocardial infarction and cardiovascular mortality. *Arch. Internal. Med.* 170, 1191–1201.
- Piozzi F., Quilico A., Fuganti C., Ajello, T.; Sprio V., (1967), *Gazz. Chim. Ital.*, 97, 935.
- Popat A., Shear N.H., Malkiewicz I., Stewart M.J., Steenkamp V., Thomson S., Neuman M.G., (2001), The toxicity of *Callilepis lauroleola*, a South African traditional herbal medicine., *Clin Biochem.*;34(3):229-36. Review.
- Puhl A.C., Bernardes A., Silveira R.L., Yuan J., Campos J.L., Saidemberg D.M., Palma, M.S. Cvoro, A., Ayers S.D., Webb P., Reinach P.S., Skaf M.S., Polikarpov I., (2012). Mode of peroxisome proliferator-activated receptor γ activation by luteolin. *Mol. Pharmacol.* 81, 788–799.
- Reilly S.M. & Lee C.H., (2008), PPAR δ as a therapeutic target in metabolic disease *FEBS Letters*, 582(1), 26-31.
- Reka A.K., Kurapati H., Narala V.R., Bommer G., Chen J., Standiford T.J., Keshamouni, V.G., (2010). Peroxisome proliferator-activated receptor-gamma activation inhibits tumor metastasis by antagonizing Smad3-mediated epithelial-mesenchymal transition. *Mol. Cancer Ther.* 9, 3221-32.
- Rix U. & Superti-Furga G., (2008). Target profiling of small molecules by chemical proteomics. *Nat. Chem. Biol.* 5, 616-624.
- Roeder E., Bourauel T., Meier U., Wiedenfeld H., (1994), Diterpene glycosides from *Iphionia aucheri*., *Phytochemistry.*;37(2):353-5.
- Rosselli S., Bruno M., Maggio A., Bellone G., Chen T.H., Bastow KF., Lee K.H., (2007). Cytotoxic activity of some natural and synthetic ent-kauranes. *Nat. Prod.* 70, 347–352
- Santi R. & Luciani, S., (1978), *Atractyloside: Chemistry, Biochemistry and Toxicology*, Eds.; Piccin Medical Books: Padova, Italy

- Sastry G.M., Adzhigirey M., Day T., Annabhimoju R., Sherman W., (2013), Protein and ligand preparation: parameters, protocols, and influence on virtual screening enrichments. *J. Comput. Aid. Mol. Des.*, 27, 221-234.
- Schteingart C.D. & Pomilio A.B., (1984), Atractyloside, toxic compound from *Wedelia glauca*, *J Nat Prod.* ;47(6):1046-7.
- Shiraki T., Kamiya N., Shiki S., Kodama T.S., Kakizuka A., Jingami H., (2005). Alpha,beta-unsaturated ketone is a core moiety of natural ligands for covalent binding to peroxisome proliferator-activated receptor gamma. *J. Biol. Chem.* 280, 14145-53.
- Song Z., Kovacs F.A., Wang J., Denny J.K., Shekar S.C., Quine, J.R., Cross T.A., (2000). Transmembrane domain of M2 protein from influenza A virus studied by solid-state (15N) polarization inversion spin exchange at magic angle NMR. *Biophys. J.* 79, 767-75.
- Sun H.D., Huang S.X., Han Q.B., (2006), Diterpenoids from *Isodon* species and their biological activities., *Nat Prod Rep.*;23(5):673-98.
- Toledo-Warshaviak D., Golan G., Borrelli K.W., Zhu K., Kalid O., (2014), Structure-based virtual screening approach for discovery of covalently bound ligands. *J. Chem. Inf. Model.* 54, 1941–1950.
- Tontonoz P. & Spiegelman B.M., (2008), Fat and beyond: the diverse biology of PPARgamma. *Annu. Rev. Biochem.* 77, 289-312.
- Vargas D., Domingueza X.A., Acuña-Askara K., Gutierrez, M.; Hostettmann, K., (1988), Norditerpenes and norditerpene glycosides from *Drymaria arenarioides*, *Phytochemistry*;27, 1532.
- Waku T., Shiraki T., Oyama T., Fujimoto Y., Maebara K., Kamiya N., Jingami H., Morikawa K., (2009b), Structural insight into PPAR γ activation through covalent modification with endogenous fatty acids. *J. Mol. Biol.* 385, 188–199.
- Waku T., Shiraki T., Oyama T., Morikawa, K., (2009), Atomic structure of mutant PPARgamma LBD complexed with 15d-PGJ2: novel modulation mechanism of PPARgamma/RXRalpha function by covalently bound ligands. *FEBS Letters.* 583, 320–324.
- Waku T., Shiraki T., Oyama T., Maebara K., Nakamori R., Morikawa K., (2010), The nuclear receptor PPARgamma individually responds to serotonin- and fatty acid-metabolites. *Embo J.* 29, 3395–3407.
- Wang L., Li D., Wang C., Zhang Y., Xu J., (2011), Recent progress in the development of natural ent-kaurane diterpenoids with anti-tumor activity., *Mini Rev Med Chem.*;11(10):910-9.
- Wang L., Waltenberger B., Pferschy-Wenzig E.M., Blunder M., Liu X., Malainer C., Blazevic T., Schwaiger S., Rollinger J.M., Heiss E.H., Schuster D., Kopp B., Bauer R., Stuppner H., Dirsch V.M., Atanasov A.G., (2014), Natural product agonists of

peroxisomeproliferator-activated receptor gamma (PPAR γ): a review.
Biochem.Pharmacol. 92, 73-89.

Watkins P.B. & Whitcomb R.W., (1998), Hepatic dysfunction associated with troglitazone.
New England J. Med. 338, 916–917.

Wijeratne E.M., Bashyal B.P., Liu M. X., Rocha D.D., Gunaherath G.M., U'Ren J.M.,
Gunatilaka M.K., Arnold A.E., Whitesell L., Gunatilaka, A.A., (2012), Geopyxins A-
E, ent-KauraneDiterpenoids from Endolichenic Fungal Strains *Geopyxisaff. majalis*
and *Geopyxis* sp. AZ0066: Structure-Activity Relationships of Geopyxins and Their
Analogues. *J. Nat. Prod.* 75, 361-369.

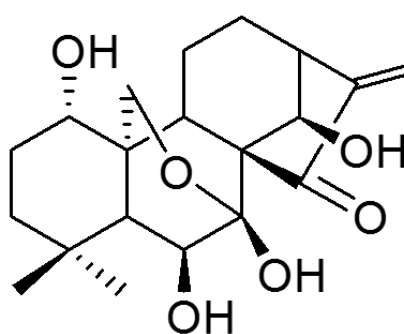
Zhu K., Borrelli K.W., Greenwood J.R., Day T., Abel R., Farid R.S., Harder E., (2014).
Docking Covalent Inhibitors: A Parameter Free Approach To Pose Prediction and
Scoring. *J. Chem. Inf. Model.* 54, 1932–1940.

- Chapter 3 -

Introduction

3.1 Oridonin: insight its multifunctional effects

Oridonin (7,20-epoxy-ent-kauranes), a diterpenoid isolated from the medicinal herb *Rabdosia rubescens* (Hemsl.) H. Hara (Figure 1), was firstly identified in the 1967 (Fujita E. *et al.* 1967) and subsequently synthesized in the 1973 (Fujita T. *et al.* 1973).



Oridonin

Fig.1: Chemical structure of oridonin

This compound has been shown to have multiple biological activity; in fact it has been used in Chinese medicine to treat several diseases. It has aroused high interest especially in cancer researchers due its potential to be developed into tumor chemotherapeutic drug (Sartippour M.R. *et al.* 2005). About its structural requirements for its anticancer activity it is reported that the α -methylene cyclopentanone of the chemical structure of oridonin, is the pharmacophore of this molecule. In fact, changes in this portion of the molecule (e.g., split ring or saturated methylene) significantly affect its anticancer activity (Fujita E. *et al.* 1967). Besides, also the presence of a hydrogen bond between the hydroxyl group at C-6 and the carbonyl group at

C-15 plays an important role for oridonin activity; inducing a partial positive polarization at C-17, thus increasing its susceptibility to nucleophilic attack (Node M. *et al.* 1983).

The ability of oridonin to inhibit tumor cell growth either in *in vitro* or *in vivo* experimental models has indeed been repeatedly confirmed by many research groups. Inhibition of tumor cell growth by oridonin was ascribed to the ability of the drug to affect cell cycle progression and/or to promote cell death by apoptosis and autophagy. Several studies indicated that oridonin inhibits cell cycle progression and then cell growth and proliferation in a variety of human cancer cell lines, including those from the breast, lung, and prostate (Ikezoe T. *et al.* 2003). However, flow cytometric analysis revealed that oridonin elicited a G1/S block in several cell lines, and an S-G2/M arrest in other ones. These blocks are produced by modulating the expression/activity of different cell cycle regulatory proteins. Specifically, it has been shown that oridonin can affect cell cycle progression by regulating a series of essential cell cycle-related proteins such as cdc2, cdc25c, cyclinB, p53 and p21 (Ikezoe T. *et al.*, 2003).

In many cancer cell lines oridonin is also able to induce apoptosis. There are two major pathways of apoptosis: the death-receptor pathway, which is mediated by the activation of death receptors, and the mitochondrial pathway, which is mediated by noxious stimuli that ultimately lead to mitochondrial injury. Again, depending on the cell type and the experimental conditions used, oridonin has been shown to modulate the expression of proteins implicated in either death receptor-mediated (i.e. FAS, FAS ligand) (Liu Y.Q. *et al.* 2006) or mitochondria-dependent apoptotic pathways (i.e. increased BAX/Bcl2 ratio (Zhang C. *et al.* 2004). Therefore, oridonin-induced apoptosis occurs via a variety of mechanisms. Evidences showed that oridonin induces apoptosis through both extrinsic and intrinsic pathways, since a large number

of proteins interfering with these pathways into the cell were modulated by oridonin (Zhang TM. 1982).

In recent years, in addition to the pro-apoptotic ability of oridonin, it was being increasingly highlighted its ability to induce autophagy in some cancer cells. Distinct from apoptosis, autophagy (an evolutionarily conserved, multi-step lysosomal degradation process in which a cell destroys long-lived proteins and damaged organelles) may play crucial regulatory roles in many pathological processes, most notably in cancer. Recent studies showed that oridonin induced HeLa cell autophagy. In fact, oridonin was reported to negatively modulate several pro-survival signaling proteins, such as NF- κ B, MAPKs and PI3K/Akt.

Besides the aforementioned anti-tumor properties *in vitro*, oridonin has been demonstrated to bear remarkable anti-neoplastic activities *in vivo*. It suppressed proliferation of different cell lines in mice (Zhu Y. *et al.* 2007; Gao F.H. *et al.* 2010), induced typical mitochondrial apoptosis in acute myeloid leukemic (AML) cells, and exhibited substantial anti-leukemia activities with negligible side-effects in murine models (Zhou G. B, *et al.* 2007 a,b).

Moreover, oridonin possessed high stability under different conditions: it was observed to be over 99% of the nominal concentrations after storage at $-20\text{ }^{\circ}\text{C}$ for 30 days and $4\text{ }^{\circ}\text{C}$ for 7 days, respectively (Mei Y. *et al.* 2008).

In summary, oridonin may become an effective anti-tumor agent due to its versatile anti-proliferative capabilities including regulating cell cycle, apoptosis and autophagy, but more studies are necessary to elucidate better its mechanism of action.

3.2 Aims of the project

Recently, our research group identified and validated the possible targets of this molecule by chemical proteomic approach (Dal Piaz F. *et al.* 2013). In particular, we provided evidences that oridonin is able to directly bind the

multifunctional, stress-inducible heat shock protein 70 1A (HSP70). Although the identification of HSP70 as a molecular target of this molecule suggested a mechanism of action of oridonin consistent with the multiple biological activities described for this diterpene, a large number of proteins and then pathway are affected by the treatment of cells with this molecule (Zhang T.M. 1982; Ikezoe T. *et al.*, 2003). Then, it's obvious to think that oridonin is able to bind more than one target in cell and give several biological effects.

Moreover, we decided to study this molecule again in order to overcome the limitations of the technique used before. More in details, the study of the possible interactors of a biological small molecule can be carried out with different methods, but affinity chromatography remains the most widely used method. Like any other technology, chemical proteomic has strengths and weakness that require careful consideration up front. The primary limitation of affinity chromatography is the need to derivatize the small molecule of interest. Unfortunately, many small molecules cannot be modified without affecting their bioactivity, and presumably binding. Furthermore, this approaches are performed using cell lysates, but it is important to keep in mind that the lysis method generally used dose not capture all proteins equally well and that it's difficult to evaluate which proteins are missing from the respective lysate preparation (e.g. membrane proteins). On the other hand, some proteins are simply so abundant or prone to interacting generically with either hydrophobic or charged surfaces that they create a high background level (Rix U & Superti-Furga G. 2008). A further problem is the accurate identification of proteins interacting with the molecule covalently immobilized on a solid support. Therefore, affinity chromatography of small molecules is severely limited due to the vast structural diversity and complexity of biologically active small molecules thus resulting a method that cannot be universally applied to the target identification of a studied small molecule.

Given the shortcomings of current target identification methodologies, we decided to use another and orthogonal approach to define the partners of oridonin, called with acronym DARTS (Drug Affinity Responsive Target Stability). Such approach could potentially identify any protein targets of small molecules with no limitations posed by chemistry or mechanism of action. In fact, DARTS is a general methodology for identifying and studying protein-ligand interactions. The idea that a small molecule drug would stabilize its target protein's structure and result in protease resistance offers a possible solution to the problem of target identification, so long as the decreased proteolysis could be readily detected in complex samples. This enhanced stability is postulated to result from a shift in the thermodynamic landscape of the protein to favor the ligand-bound state, which prevents much of the protein's innate flexibility and movement from being realized. It is similar to affinity chromatography in that both are affinity-based methods that start with complex protein samples and selectively enrich the target protein(s) while depleting all non-target proteins. However, whereas affinity chromatography utilizes positive enrichment by selectively pulling out the target proteins and leaving behind non-targets, DARTS uses negative enrichment by digesting away non-target proteins, while leaving behind the target proteins that are rendered protease-resistant. Therefore, DARTS is particularly useful for the initial identification of the protein targets of small molecules, but can also be used to validate potential protein-ligand interactions predicted or identified by other means and to estimate the affinity of interactions. Finally, this approach is simple and advantageous because it can be performed using crude cell lysates and other complex protein mixtures (without requiring purified proteins), and uses native, unmodified small molecules (Figure 2).

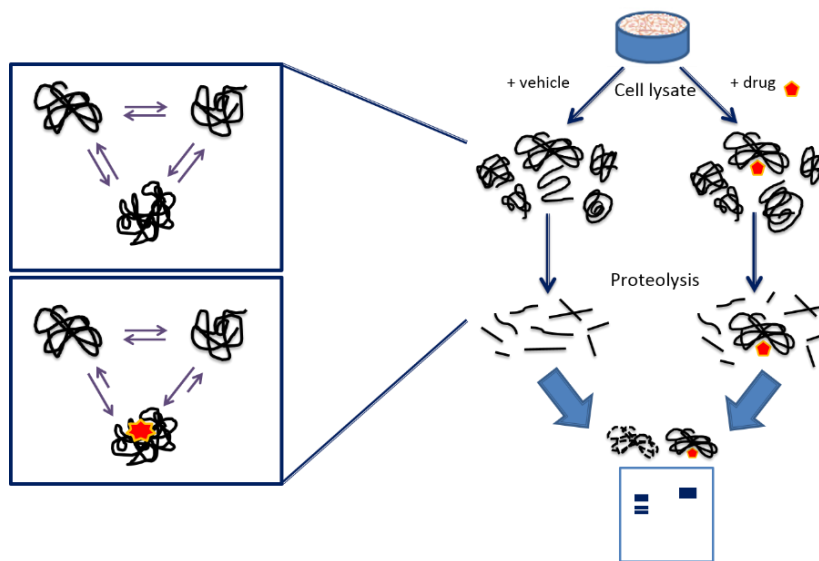


Fig 2: Theoretical model and basic strategy of DARTS.

Adopted from Lomenick B *et al.* 2009

Thus, with the final aim of expanding and validate our knowledge about the mechanism of action of this molecule, also seen the limitations of the used chemical proteomic approach mentioned before, we decided to use this method of identification of possible targets.

Finally, we selected a set of experiments to validate targets and understand the role of oridonin in cell.

Results and discussion

3.3 Synthesis and characterization of fluorescent oridonin companion imaging drug

The knowledge of pharmacokinetics and pharmacodynamics parameters of drugs in live cells could lead to a better understanding of their mechanism of action. Approaches currently used to this aim require tissue/cells lysis or rely on indirect assays and thus often provide an incomplete view of drugs fate and metabolism. In this project, in order to provide more detailed information about the mechanism of action of oridonin inside the cells and to get experimental conditions for the further studies, firstly, we synthesized its fluorescent derivate. Using a fluorescence microscopy based technique, it was possible to measure drug uptake and to get the map drug-target interaction in real time at subcellular resolution. In particular, this approach enabled high-resolution spatial and temporal mapping of drug distribution inside the cancer cell and led us to put the basis for the subsequent experiments.

The fluorescence microscopy is generally applicable to fluorescently labeled drugs; in our experiments BODIPY FL was chosen as fluorescent tool since its chemical features are useful probe for intracellular assays. In particular, (i) BODIPY is relatively non-polar with the chromophore presenting electrical neutrality, therefore minimizing perturbation to the modified drug; (ii) it has a relatively long lifetime (lifetime about 4.0 ns); (iii) it's highly permeant to live cells, easily passing through the plasma membrane, where it accumulates over time (Dubach J.M. & Vinegoni C. 2014).

To develop fluorescent oridonin companion imaging drug (CID), two different final modified versions of the drug were chose. On the basis of literature data showing that the hydroxyl group at position C-1 is not essential for the cytotoxic activity of oridonin (Wenjing Z. *et al.* 2010), this group was selected as point of attachment of the dye. We first synthesized the esterification

version of oridonin, but this derivate resulted not stable in our experimental conditions. Therefore, we produce the carbamate version of oridonin, using the synthetic scheme reported in Figure 3.

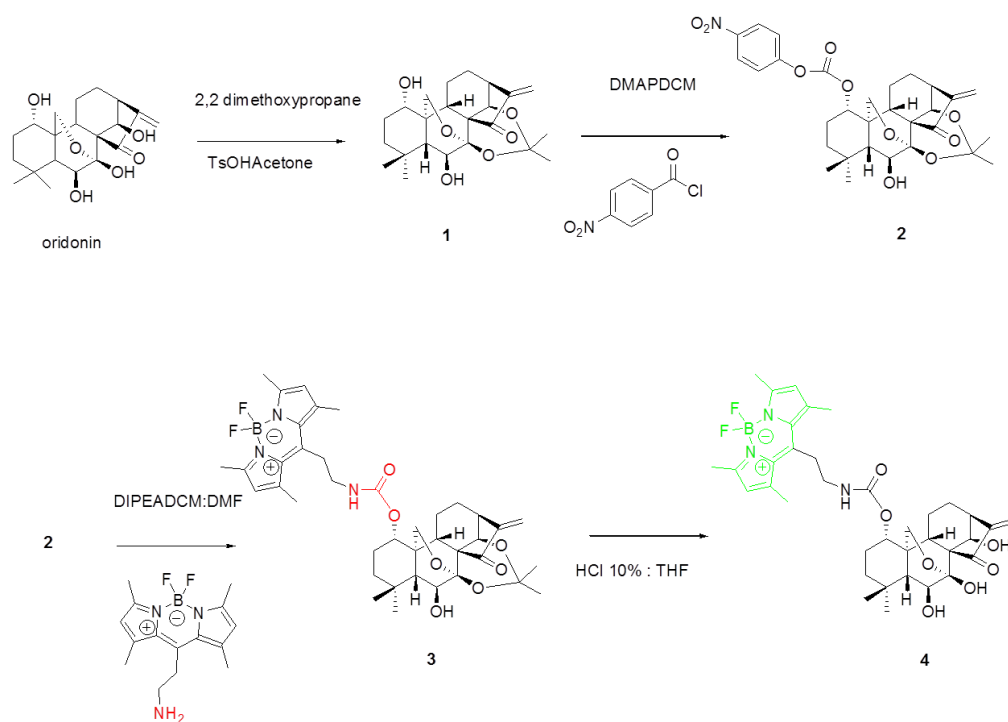


Fig.3: Synthetic route for oridonin-BODIPY FL (compound 4)

Before using the fluorescent version of oridonin for our study, it was mandatory to verify if the chemical modification caused significant effects of its biological activity. To that aim, Jurkat cell proliferation inhibition potential of this CID to that of unmodified oridonin was compared: exponentially growing cultures of Jurkat (T-cell leukemia) cells were exposed to increasing concentrations of both drugs and cell viability was evaluated after 24 h and 48h of treatment. Achieved results (Figure 4) demonstrated that, under our

experimental conditions, the two molecules had similar antiproliferative activities.

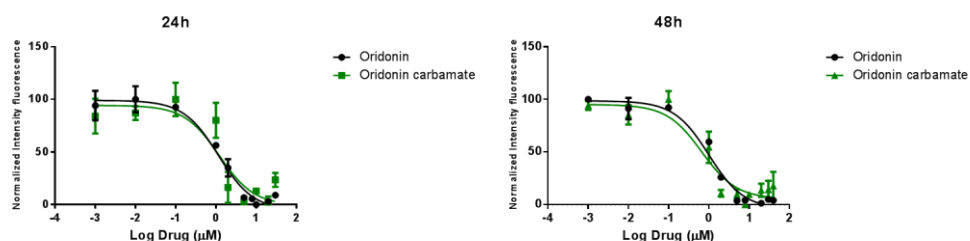


Fig. 4: Comparison of tumor cell growth inhibition activity of modified and unmodified oridonin. Values of IC_{50} for oridonin was $1.25\mu M$ and $1\mu M$ for 24h and 48h; IC_{50} for oridonin BODIPY FL was $1.2\mu M$ and $0.66\mu M$ for 24h and 48h.

Given the known ability of oridonin to covalently interact with HSP70 (Dal Piaz F. *et al.* 2013), we evaluated if also the imaging drug retains this skill. Therefore, we incubated HSP70 with different concentrations of CID for 15 min and samples by SDS-PAGE experiment were resolved. Fluorescence intensity was analyzed and a dose dependent covalent binding of CID to the protein was observed (Figure 5).

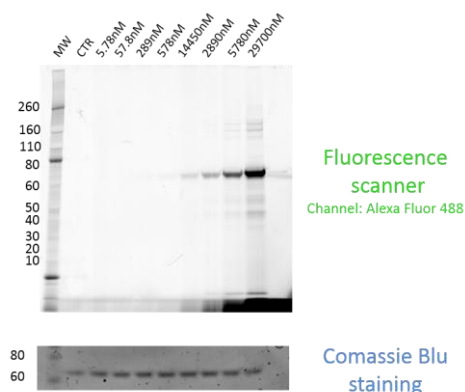


Fig.5: Denaturing gel electrophoresis of increasing concentration of oridonin BODIPY FL incubated with purified HSP70 for 15 min and imaged with a fluorescence gel scanner using 488 nm excitation/512 nm emission. Note the dose dependent covalent binding of oridonin BODIPY FL to HSP70

Finally, the stability of fluorescent oridonin in our experimental conditions was studied. The lifetime of CID at different pH and incubation times was investigated using MS and fluorescence detectors.

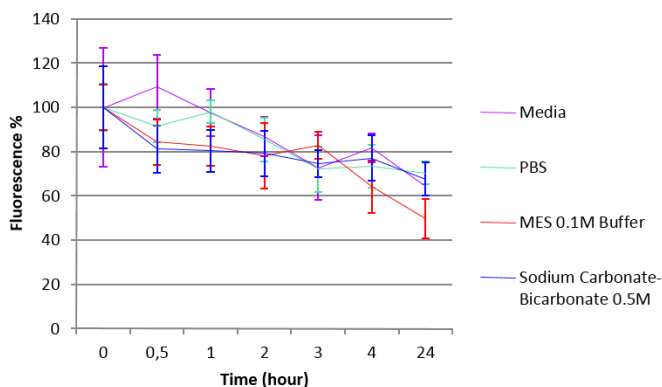


Fig.6: Lifetimes of CID in different buffer solutions for different indicated time points

Achieved results (Figure 6) demonstrated that this molecule was stable for 24h in almost all the tested conditions, unless in 2-(N-morpholino)ethanesulfonic acid (MES) buffer, due to the reactivity of carbamate function in acid conditions.

All together, these data indicated this new CID as a hopeful probe for imaging experiments to investigate the mechanism of action of oridonin.

3.4 Oridonin uptake in live cells

In order to evaluate the kinetic of oridonin penetration into the cells, Jurkat cells were treated with a CID concentration corresponding to its IC_{50} . Real-time *in vitro* measurements (Figure 7) showed that the amount of modified oridonin within the cells increased at 1 h and reached its maximum after 2 h of incubation time and after 3h it started decreasing. The drug accumulated both into the cytosol and in the nucleus of the treated cells was also evaluated.

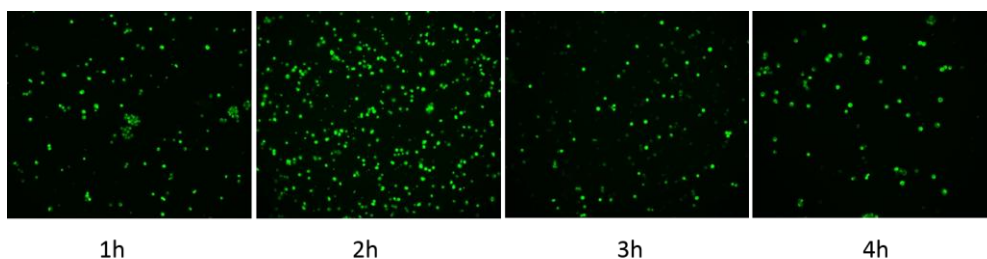


Fig.7: Imaging of Jurkat cells to determinate the uptake of oridonin BODIPY FL in cell. Green signal: oridonin BODIPY FL. Scale bar: 20 μ m.

Moreover, the cellular localization of oridonin in Jurkat cells after a long washing time was investigated. Jurkat cells were first treated with the CID and then washed for different times (from 1h up to 3h). As reported in Figure 8, also after 2h of treatment and 3h of washing, fluorescent oridonin was still within cytoplasm and nuclei. This long persistence of oridonin into the cells could be due to a covalent stabilization of the interaction of oridonin with its protein targets.

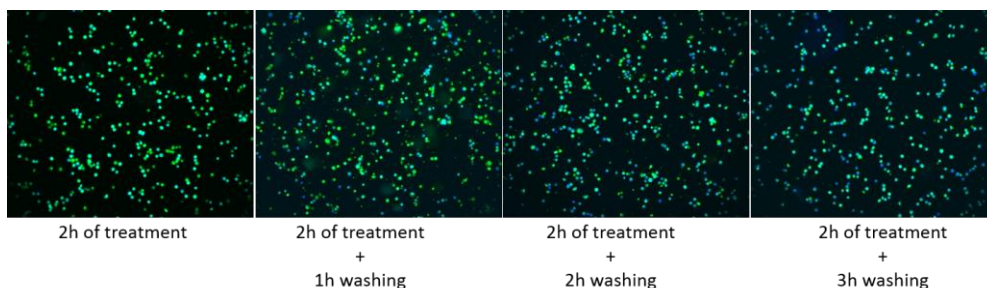


Fig.8: Real time imaging of Jurkat cells following 2h of incubation of oridonin BODIPY FL and different washing times. Green signal: oridonin BODIPY F; Blue signal: Hoechst 33342. Scale bar: 20 μ m

3.5 Optimization of DARTS protocol

Once set the experimental conditions for the cell treatment with oridonin, we moved to proteomic studies in order to identify the putative molecular targets of this diterpene. In particular, we carried out a proteomic-based study, using a

DARTS approach. This method is useful for the identification and to study protein-small molecule interactions.

As first step, we optimized enzymatic digestion conditions, selecting the better proteolytic agent, and the amount of enzyme to be used. There are different proteases that could be used for DARTS, in our experiments subtilisin was selected because we needed a rapid kinetic of hydrolysis and a protease with a broad specificity; in fact, protein lysates are highly heterogeneous mixture of proteins with diverse physiochemical properties, including native and denatured proteins. Thermolysin, another enzyme widely used for this technique, it is not very stable and there is a significant proportion of the proteome that is not highly resistant to its proteolytic activity (Lomenick B. *et al.* 2009).

A wide range of subtilisin concentrations were tested to define the best ratio of proteins/protease, using 30 min as experimental time. The obtained results (Figure 9) shown that ratio of 1:1000 enzyme:lysate (w:w) resulted as the best experimental condition.

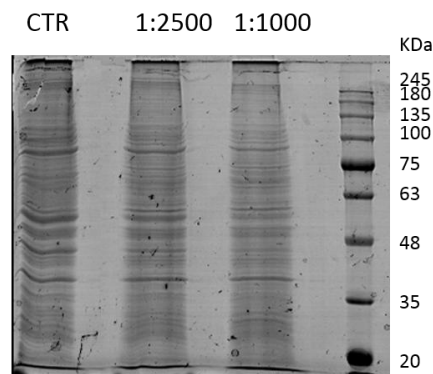


Fig.9: Optimization of DARTS protocol. Lysates from untreated human Jurkat cells were incubated with DMSO for 1h at room temperature. Each sample was then split into seven aliquots that underwent digestion with various concentrations of subtilisin, relative to the total amount of protein per sample, for 30 min at room temperature. Digestion was stopped by adding sample loading buffer and boiling immediately. Each sample was then loaded onto 10% SDS/PAGE gels and stained with Brilliant Blue G-Colloidal.

The next step was to verify if the enzyme activity was somehow altered by the presence of oridonin. Hence, we incubated Bovin Serum Albumin (BSA) in presence or in absence of oridonin and the resulting proteolytic pattern was then studied, to investigate if the presence of oridonin protected BSA by subtilisin digestion (Figure10).

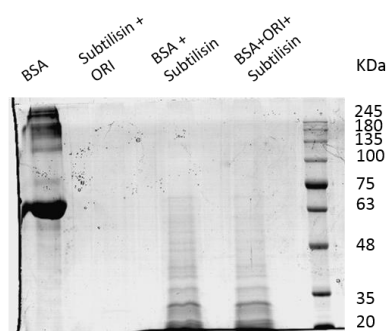


Fig.10: Subtilisin activity is unaffected by oridonin under identical experimental conditions except with BSA as a non-binder control.

The obtained results showed that oridonin did not interfere with the proteolytic activity of the enzyme.

3.6 Identification of molecular targets for oridonin using DARTS

We used DARTS to discover new possible oridonin targets and to validate those previously identified. Jurkat cells were used to perform all the experiments, since oridonin/HSP70 complex formation was previously demonstrated in this leukemia-derived cell line (Dal Piaz F. *et al.* 2013). Thus, whole cell lysates from Jurkat cells were exposed to 20 μ M oridonin for 1 h at R.T. and then digested with subtilisin. We decided to use a dose higher than IC_{50} (reported before) to enhance the possibility to detect oridonin-complexes: generally, any small molecule believed to bind proteins should be suitable for DARTS, but the concentration ranges of small molecule to use is also an important variable. Given that the targets of most small molecules usually are

unknown also the binding affinities will be unknown. Therefore, a high concentration than IC_{50} of oridonin to ensure saturation of the protein targets to obtain the oridonin putative targets was used. For this experiment, three different samples were analyzed: 1) the whole lysate without digestion 2) the digested lysate incubated with oridonin 3) and the digested lysate without oridonin; this last control was a negative control required to discriminate between proteins specifically interacting with the diterpene and unspecific background. Examination and comparison of the lanes in DARTS experiment revealed three protected bands at high molecular weight (Figure 11).

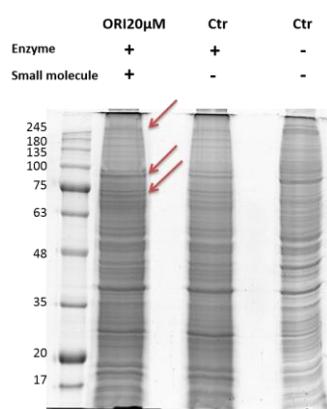


Fig.11: DARTS using whole Jurkat cell-lysate: lane1) lysate treated with Oridonin 20 μ M and then digested for 30 min with subtilisin; lane2) lysate treated with DMSO and then digested with subtilisin; lane3) whole Jurkat cell lysate as control. Note the presence of three protected bands in oridonin treated sample than digested control

These bands and the corresponding gel regions of the control lane were subjected to a classical in situ gel-digestion, followed by mass spectrometry analysis; this procedure allowed us to identify different proteins enhanced in the oridonin-treated sample. DARTS experiments were performed in triplicate the list of proteins identified using this approach is summarized in Table 1.

Table 1: Mass spectrometry identified proteins of DARTS experiment on whole cell-lysate

Swiss Prot Code	Identified protein	Mr	Matches Unique*	Mascot Score*
TLN1_HUMAN	Talin-1 OS=Homo sapiens GN=TLN1 PE=1 SV=3	271766	17	297
SF3B3_HUMAN	Splicing factor 3B subunit 3 OS=Homo sapiens GN=SF3B3 PE=1 SV=4	136575	11	175
IMB1_HUMAN	Importin subunit beta-1 OS=Homo sapiens GN=KPNB1 PE=1 SV=2	98420	10	338
ILF3_HUMAN	Interleukin enhancer-binding factor 3 OS=Homo sapiens GN=ILF3 PE=1 SV=3	95678	11	145
NUP93_HUMAN	Nuclear pore complex protein Nup93 OS=Homo sapiens GN=NUP93 PE=1 SV=2	93943	5	93
ENPL_HUMAN	Endoplasmic reticulum protein OS=Homo sapiens GN=HSP90B1 PE=1 SV=1	92696	12	197
HS90B_HUMAN	Heat shock protein HSP 90-beta OS=Homo sapiens GN=HSP90AB1 PE=1 SV=4	83554	36	2633
NUCL_HUMAN	Nucleolin OS=Homo sapiens GN=NCL PE=1 SV=3	76625	18	1977
HSP7C_HUMAN	Heat shock cognate 71 kDa protein OS=Homo sapiens GN=HSPA8 PE=1 SV=1	71082	21	2005
GRP75_HUMAN	Stress-70 protein, mitochondrial OS=Homo sapiens GN=HSPA9 PE=1 SV=2	73920	6	144
XRCC6_HUMAN	Non-homologous end joining protein 6 OS=Homo sapiens GN=XRCC6 PE=1 SV=1	70084	17	664
CALX_HUMAN	Calnexin OS=Homo sapiens GN=CANX PE=1 SV=2	67982	16	358

* values represent the mean of three independent results

This study led to the identification of several putative oridonin targets; in particular, once again, we found HSP70 as target of oridonin, thus confirming the efficacy of DARTS approach for our purpose.

The next step was to study the targets identified on the lysate into the cell. The lysate is a good starting point to define the interactome of a small molecule but is a very simple model that differs from the real condition in cell; performing a study on live cells also the effects of active metabolism and the cellular compartmentalization are taken into account. Therefore, Jurkat cells were treated with two different concentrations of oridonin (10 μ M and 20 μ M) for 2 hours. The incubation time of our in cells experiment was selected on the basis of results obtained previously. Cells were lysate and their extracts were subjected to subtilisin digestion; a comparison between electrophoretic analysis of digestion mixture from lysates of treated and untreated cells revealed, the presence of a protected band (Figure 12). MS-spectrometer analysis of mixture of peptides of this band confirmed again HSP70, confirming once again that also inside the cells oridonin efficiently interacts with HSP70 and we found other proteins (Table 2)

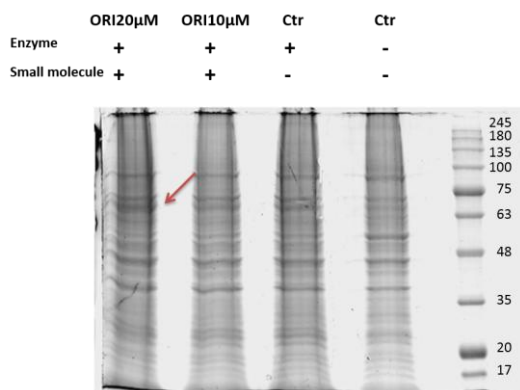


Fig.12: DARTS approach using intact Jurkat cells: lane1) cells treated with Oridonin 20 μ M for 2h of incubation time and then digested; lane2) cells treated with Oridonin 10 μ M for 2h of incubation time and then digested; lane3) cells treated with DMSO for 2h of incubation time and then digested; lane4) whole Jurkat cells as control.

Table 2: Mass spectrometry identified proteins of DARTS experiment on intact Jurkat cell

Swiss Prot Code	Identified protein	Mr	Matches Unique ^a	Mascot Score ^a
HS90B_HUMAN	Heat shock protein HSP 90-beta OS=Homo sapiens GN=HSP90AB1 PE=1 SV=4	83554	6	201
NUCL_HUMAN	Nucleolin OS=Homo sapiens GN=NCL PE=1 SV=3	76625	9	459
HSP7C_HUMAN	Heat shock cognate 71 kDa protein OS=Homo sapiens GN=HSPA8 PE=1 SV=1	71082	11	560
TCPG_HUMAN	T-complex protein 1 subunit gamma OS=Homo sapiens GN=CCT3 PE=1 SV=4	61066	13	350
CH60_HUMAN	60 kDa heat shock protein, mitochondrial OS=Homo sapiens GN=HSPD1 PE=1 SV=2	61187	2	58
TCPA_HUMAN	T-complex protein 1 subunit alpha OS=Homo sapiens GN=TCP1 PE=1 SV=1	60819	4	72
HNRPK_HUMAN	Heterogeneous nuclear ribonucleoprotein K OS=Homo sapiens GN=HNRNPK PE=1 SV=1	51230	4	142

^a values represent the mean of three independent results

3.6.1 Validation of selectivity of oridonin towards identified molecular targets using DARTS approach

The specificity of the putative oridonin targets was tested performing the same DARTS approach using another diterpene, nervosanin B, as possible negative control. This molecule was selected since its structure is very close to that of oridonin (Figure 13) (Wenjing Z. *et al.* 2010) but it shows none or weak cytotoxicity against several cancer cell lines (IC₅₀ on Jurkat cells after 24h was more than 50 μ M). Besides, nervosanin B is a well-known *Isodon rubescence* kaurane diterpene present in our laboratory library. Thus, DARTS procedure was applied on Jurkat lysate using nervosanin B at 20 μ M. The obtained results

showed a different gel profile than DARTS performed using oridonin (Figure 13).

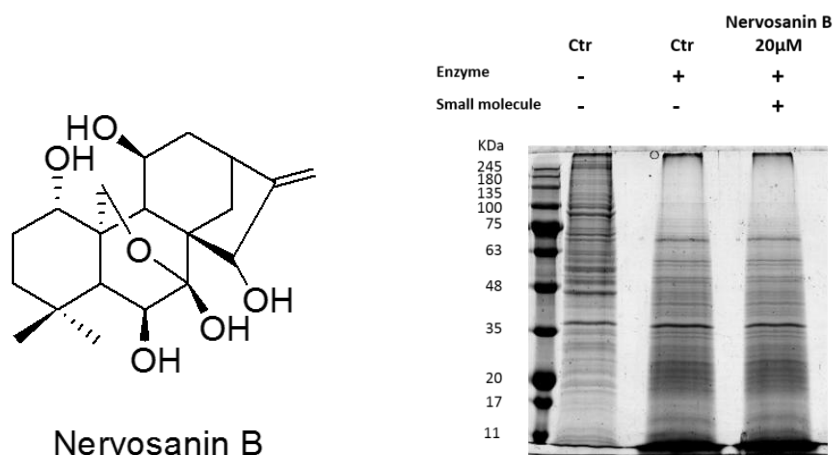


Fig.13: A) Structure of Nervosanin B; B) DARTS approaches on Jurkat lysate: lane 1) Jurkat lysate as control; lane2) Jurkat lysate incubated with DMSO for 1h and then digested with subtilisin; lane3) Jurkat lysate following 1h of incubation time with nervosanin B at 20µM and then digested with subtilisin.

3.6.2 Western Blot analysis to validate some of the molecular targets of oridonin

To confirm the results achieved by DARTS MS-based approaches, we performed DARTS on Jurkat lysates using western blot analysis. In particular, we focused our attention on proteins previously identified by the MS-based approach, whose activity could be related to the oridonin treatment effects.

Therefore, the investigated proteins were: NCL (Nucleolin), HSP70, PPAR γ (Peroxisome proliferator-activated receptor gamma), HSP90 (Heat shock protein HSP 90), Trx (Thioredoxin), TrxR (Thioredoxin Reductase) and finally GAPDH (Glyceraldehyde-3- phosphate dehydrogenase); this last protein was selected as loading indicator, since it is reported to be more resistant to enzymatic activity in this experimental condition (Lomenick B. *et al.* 2009).

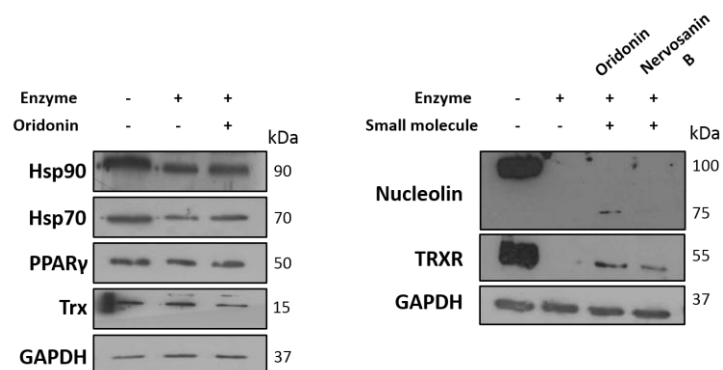


Fig.14: Validation by western blotting of LC-MS identified proteins from DARTS experiments. Protein lysate from untreated Jurkat cells and protein lysates from Jurkat cells digested with subtilisin in presence and in absence of oridonin and nervosamin B were separated on SDS-PAGE and followed by immunoblotting with antibodies against GAPDH, HSP90, HSP70, TRX, TRXR, NCL, PPAR γ .

As we expected, the proteins that specifically interacted with oridonin were protected from digestion with subtilisin and in the resulting blotting more marked bands corresponding to them were observed (Figure 14).

3.7 “Complementary” chemical proteomic approach: affinity purification and mass spectrometry analysis of oridonin partners

With the aim of expanding and validate the knowledges about target(s) of oridonin, an additional orthogonal chemical proteomics approach was applied. In literature is largely reported that α - β unsaturated carbonyl group is responsible for oridonin and related compounds biological activity and targets interactions, herein we decided to also study the contribution of A-B-C rings substitutions on the oridonin bioactivity. In fact, it is well known that in order to stabilized interaction and molecular recognition of a small molecule and the physiological ligand, the main pharmacophore is not the only active part of the molecule important for it, but it's very important also the whole skeleton of the molecule for the interaction stabilization. Given the highly functionalized chemical structure of this molecule, we tried to define also, the possible protein partners of this part of the molecule. In particular, using this approach

we tried to emphasize non covalent binders of oridonin. Therefore, a direct chemical proteomic approach was carried out using the α - β unsaturated carbonyl group as point of attachment on a solid support (making it not available for possible interaction with targets). The experimental procedure we used was based on compound immobilized affinity chromatography and consisted in several steps (Figure 15). First, oridonin was anchored onto a solid support taking advantage of its electrophilic functional group, the α , β -unsaturated carbonyl group. The chemical immobilization of a small molecule ligand is usually achieved through suitable functional group and we used this functionality to achieve this purpose. In particular, a Tentagel resin was used as solid support and we evaluated reaction and the yield of the immobilization by HPLC. The functionalized resin was then incubated with Jurkat lysate. Cell extracts were also incubated with a free matrix, as a control experiment, to distinguish between specifically bound components and background contaminants. Finally, all the tightly bind proteins were eluted and the proteins from the negative control and from oridonin modified resin were identified by mass spectrometer analysis.

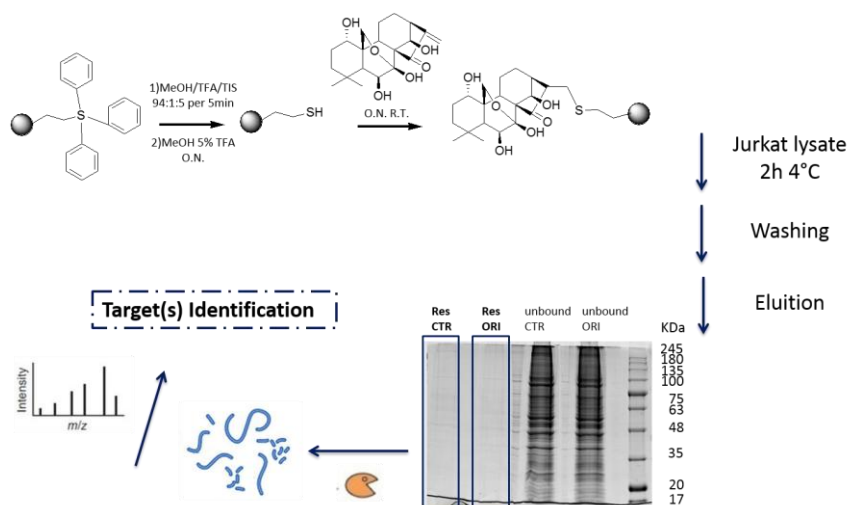


Fig.15: Workflow of “complementary chemical proteomic” on Jurkat lysate using oridonin: oridonin was conjugated to a specific solid support and the incubated with Jurkat cell lysate. Eluted proteins were resolved by SDS-PAGE experiment and after enzymatic digestion proteins were identified by LC-MS/MS

The outcome of the Mascot database search (experiment was performed in triplicate) revealed the whole interactome of this immobilized oridonin. A list of identified proteins, from both gel lanes (control and matrix bearing oridonin), was obtained and compared to establish which proteins were specifically captured by oridonin. (Table 3). In this case, HSP70 was not found as a putative target; this result was not surprising since in this experiment the α , β -unsaturated carbonyl group of oridonin was masked and our previous studies demonstrated that this group was critical for the interaction between oridonin and HSP70 (Dal Piaz F. *et al.* 2013)

Table 3: Mass spectrometry identified proteins of complementary chemical proteomic experiment

Swiss Prot Code	Identified protein	Mr	Matches Unique*	Mascot Score*
NUCL_HUMAN	Nucleolin OS=Homo sapiens GN=NCL PE=1 SV=3	76625	11	130
GRP78_HUMAN	78 kDa glucose-regulated protein OS=Homo sapiens GN=HSPA5 PE=1 SV=2	72333	4	81
PABP1_HUMAN	Polyadenylate-binding protein 1 OS=Homo sapiens GN=PABPC1 PE=1 SV=2	70671	2	52
G6PI_HUMAN	Glucose-6-phosphate isomerase OS=Homo sapiens GN=GPI PE=1 SV=4	63147	2	58
TCPA_HUMAN	T-complex protein 1 subunit alpha OS=Homo sapiens GN=TCP1 PE=1 SV=1	60344	2	54
TCPH1_HUMAN	T-complex protein 1 subunit eta OS=Homo sapiens GN=CTT7 PE=1 SV=2	59367	2	51
KPYM_HUMAN	Pyruvate kinase PKM OS=Homo sapiens GN=PKM PE=1 SV=4	58494	16	200
TCPD_HUMAN	T-complex protein 1 subunit delta OS=Homo sapiens GN=CTT4 PE=1 SV=4	57924	2	51
ATPB_HUMAN	ATP synthase subunit beta, mitochondrial OS=Homo sapiens GN=ATP5B PE=1 SV=3	56561	12	198
COR1A_HUMAN	Coronin-1A OS=Homo sapiens GN=CORO1A PE=1 SV=4	51026	8	87
EF1G_HUMAN	Elongation factor 1-gamma OS=Homo sapiens GN=EEF1G PE=1 SV=3	50119	4	77
HNRH1_HUMAN	Heterogeneous nuclear ribonucleoprotein H OS=Homo sapiens GN=HNRNPH1 PE=1 SV=4	49229	9	155
HNRPF_HUMAN	Heterogeneous nuclear ribonucleoprotein F OS=Homo sapiens GN=HNRNPF PE=1 SV=3	45672	12	145
PGK1_HUMAN	Phosphoglycerate kinase 1 OS=Homo sapiens GN=PGK1 PE=1 SV=3	44615	19	330
HNRPD_HUMAN	Heterogeneous nuclear ribonucleoprotein D0 OS=Homo sapiens GN=HNRNPD PE=1 SV=1	38434	10	89
MDHM_HUMAN	Malate dehydrogenase, mitochondrial OS=Homo sapiens GN=MDH2 PE=1 SV=3	35503	13	132
RLA0_HUMAN	60S acidic ribosomal protein P0 OS=Homo sapiens GN=RPLP0 PE=1 SV=1	34274	4	60
RA1L2_HUMAN	Heterogeneous nuclear ribonucleoprotein A1-like 2 OS=Homo sapiens GN=HNRNPA1L2 PE=2 SV=2	34225	7	89
RSSA_HUMAN	40S ribosomal protein SA OS=Homo sapiens GN=RPSA PE=1 SV=4	32854	6	72
1433E_HUMAN	14-3-3 protein epsilon OS=Homo sapiens GN=YWHAE PE=1 SV=1	29174	6	59
1433G_HUMAN	14-3-3 protein gamma OS=Homo sapiens GN=YWHAG PE=1 SV=2	28303	3	70
1433Z_HUMAN	14-3-3 protein zeta/delta OS=Homo sapiens GN=YWHAZ PE=1 SV=1	27745	13	169
PSB1_HUMAN	Proteasome subunit beta type-1 OS=Homo sapiens GN=PSMB1 PE=1 SV=2	26489	2	53
PSA5_HUMAN	Proteasome subunit alpha type-5 OS=Homo sapiens GN=PSMA5 PE=1 SV=3	26411	2	55
EF1B_HUMAN	Elongation factor 1-beta OS=Homo sapiens GN=EEF1B2 PE=1 SV=3	24764	2	54
RAN_HUMAN	GTP-binding nuclear protein Ran OS=Homo sapiens GN=RAN PE=1 SV=3	24423	4	59
RS8_HUMAN	40S ribosomal protein S8 OS=Homo sapiens GN=RPS8 PE=1 SV=2	24205	2	54
GSTP1_HUMAN	Glutathione S-transferase P OS=Homo sapiens GN=GSTP1 PE=1 SV=2	23356	11	178
RANG_HUMAN	Ran-specific GTPase-activating protein OS=Homo sapiens GN=RANBP1 PE=1 SV=1	23316	2	50
RL18_HUMAN	60S ribosomal protein L18 OS=Homo sapiens GN=RPL18 PE=1 SV=2	21634	6	85
RAC2_HUMAN	Ras-related C3 botulinum toxin substrate 2 OS=Homo sapiens GN=RAC2 PE=1 SV=1	21429	4	70
HBG2_HUMAN	Hemoglobin subunit gamma-2 OS=Homo sapiens GN=HBG2 PE=1 SV=2	16126	2	62

* values represent the mean of three independent results

The results achieved using the three chemical proteomics approaches (DARTS on cell lysates, DARTS on live cells and affinity-based chemical proteomics) were compared, leading to the Venn diagram reported in Figure 16. Interestingly, the only protein emerging in all the experiment as a possible oridonin target was nucleolin (NCL).

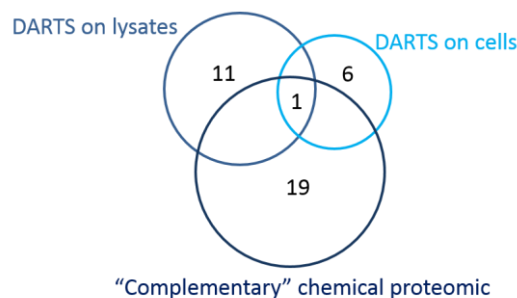


Fig.16: Venn diagram of all experiments performed (DARTS on cell lysates, DARTS on live cells and chemical proteomics)

Recently, NCL has attracted the attention of many researchers as druggable molecule for many reasons. First of all, it's a multifunctional protein present in many different cellular compartments and involved in many functions within the cells and each cellular pool of NCL can play a different role in cancer development (Berger C.M. *et al.* 2015). Moreover, the inhibition of this protein could explain better the complex biological activities of oridonin. Therefore, even if none of the proteins identified in our studies can be excluded a priori as a possible oridonin target, we performed an in-depth investigation on the biological role of oridonin in the interaction with nucleolin, through *in vitro* and in living cells assays.

3.8 Characterization of physical interactions between oridonin and nucleolin

The affinity of oridonin to nucleolin was evaluated by a Surface Plasmon Resonance (SPR)-based binding assay. SPR is an optical technique, based on the evanescent wave phenomenon, able to measure changes in refractive index onto a sensor surface, and it is suitable for characterizing macromolecular interactions. The binding between a compound in solution and its ligand immobilized on the sensor surface results in a change of the refractive index, that could be monitored in real time allowing the measurement of association and dissociation rates (Casper D. *et al.* 2004).

The interaction is monitored in real time, and the amount of bound ligand and the rates of association and dissociation can be measured. Thus, NCL was immobilized on a CM5 sensor chip and oridonin was injected over at concentrations ranging from 0.001 to 0.5 μM . In Figure 17, the sensograms (association and dissociation SPR curves) obtained from the binding of oridonin to nucleolin are shown.

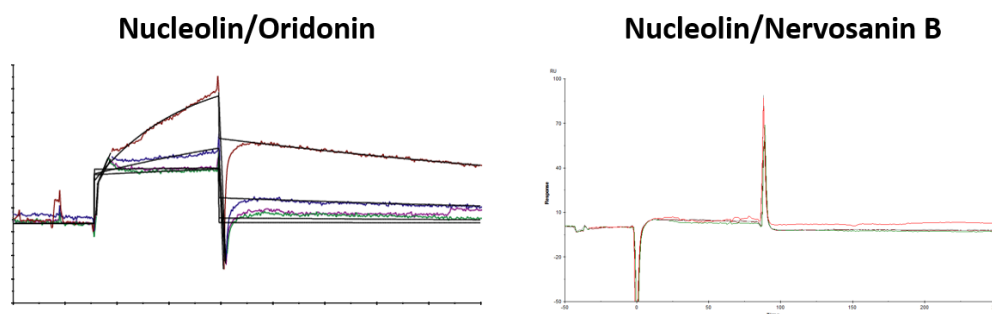


Fig.17: Sensograms obtained from the binding of oridonin to nucleolin and nervosanin B and nucleolin at different concentrations (range of concentrations used from 0.001 to 0.5 μ M for each small molecule)

As expected, the increase of response units (RU) in the association phase and the slope of the dissociation phase of the complex are clearly dependent on the analyte concentration. With the aid of a software (Biaevaluation software 3.0) it was possible measurement the dissociation constant of the complex and it was $K_{D \text{ NCL/oridonin}} = 3.82 \pm 1.2 \text{ nM}$. Moreover, we decided to check also the affinity of nervosanin B to NCL, as reported in Figure 17 there was no binding.

3.9 Monitoring of nucleolin engagement by oridonin in live cells using CETSA assay

In order to get more detailed information and evaluate oridonin and nucleolin interaction inside the cells we optimized and used Cellular Thermal Shift Assay (CETSA) experiment. CETSA, a recently published technique, allows to monitor and quantify the extent to which a drug candidate reaches and directly binds to a protein target of interest within a cell (Jafari R. *et al.* 2014). In particular, this approach offers the possibility to firmly link the observed phenotypic response to a compound with a particular target engagement. CETSA, provided by Molina and coworkers in 2013, relies on the principle of thermodynamic stabilization inferred to the protein as a result of ligand

binding, which can be used for the estimation of binding free energies as well other thermodynamic properties, for isolated systems at equilibrium (Jafari R. *et al.* 2014). Practically, the shift in thermal stability is estimated by measuring the amount of remaining soluble target protein at different temperatures for ligand treated and control samples. Briefly, CESTA protocol starts with the treatment of cells with either molecule of interest and vehicle as control, followed by heating of cells to denature and precipitate the protein of interest, cell lysis, removal of cell debris and aggregates through centrifugation, and finally detection of the remaining thermostabilized target protein by, e.g., denaturing gel electrophoresis and western blot detection using target-specific antibody (Figure 18). The apparent aggregation temperatures (T_{agg}) observed in the presence or in the absence of the drugs can be compared; the detection of substantial shifts as an effect of the presence of the drug demonstrate an effective ligand stabilization on the target protein. Therefore, a typical output form CESTA experiment is a comparison between apparent melting curves (or, more accurately, temperature-induced aggregation curves), in which the protein in the presence and absence of ligand is subjected to a panel of temperatures such that a potential thermal stabilization can be assessed.

Alternatively, an isothermal dose-response fingerprints ($ITDRF_{CESTA}$) is generated, in which the stabilization of the protein can be followed as a function of increasing ligand concentration. The latter requires knowledge of the temperature at which the unliganded protein denatures and precipitates.

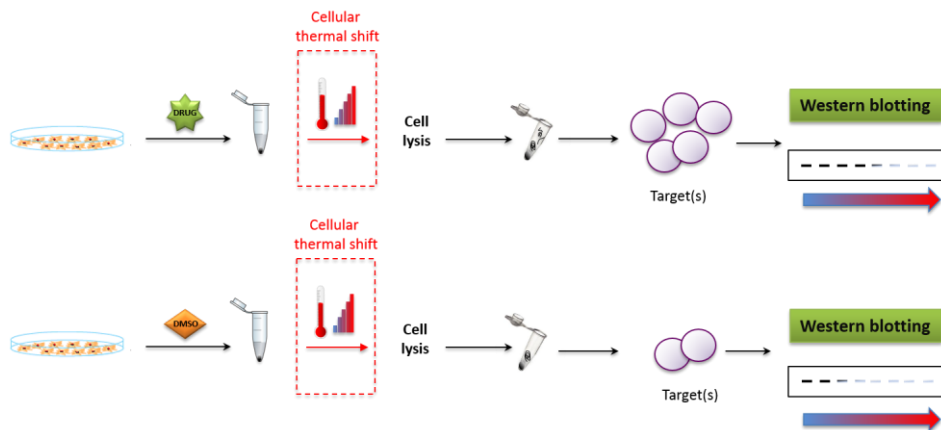


Fig.18: Schematic illustration of CETSA approach

Adopted from Bradley W.D. *et al.*, 2014

In order to obtain information about the best T_{agg} to use for next experiments, Jurkat cells were treated with 20 μ M oridonin for 2h and treated and control cells were exposed to varying temperature. After cooling, the samples were centrifuged to separate soluble fractions from precipitated proteins. We then quantified the presence of nucleolin in the soluble fractions by western blotting (Figure 19).

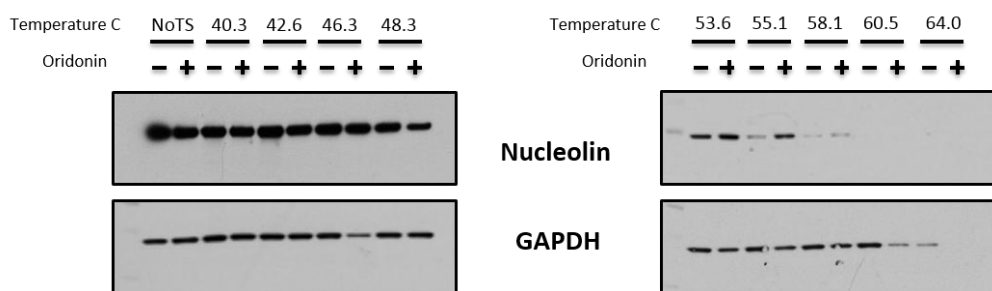


Fig.19: CETSA was employed to monitor oridonin cellular target engagement and to define the best T_{agg} . Therefore, treated and untreated Jurkat cells were heated and then was evaluated the soluble amount of NCL by western blotting

In our experiments, 55.1 °C was the obtained temperature to appreciate thermal stabilization of NCL: the amount of soluble protein at this temperature in the oridonin-treated cells was about 2 or 3 times higher than that observed in the control experiments (Figure 20).

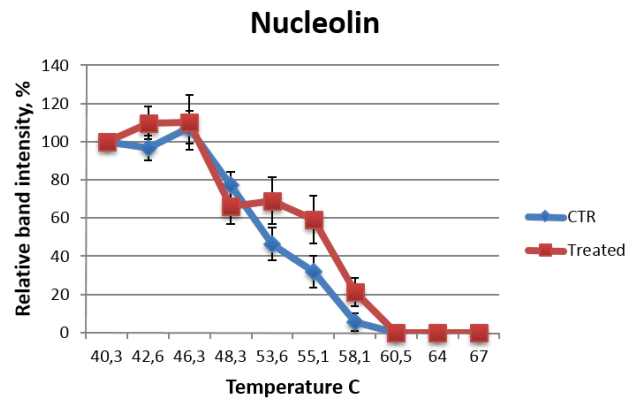


Fig.20: Apparent melting curves of NCL in cell. Densitometry-based quantification of western blot signals was graphed (NCL intensities normalized to GAPDH intensities for each data point). Shown are the mean of three biological replicates.

In order to investigate the kinetic profile of the engagement of NCL in cell, Jurkat cells were treated with oridonin (20 μ M) up to 4h of incubation time and the engagement profile was evaluated (Figure 21).

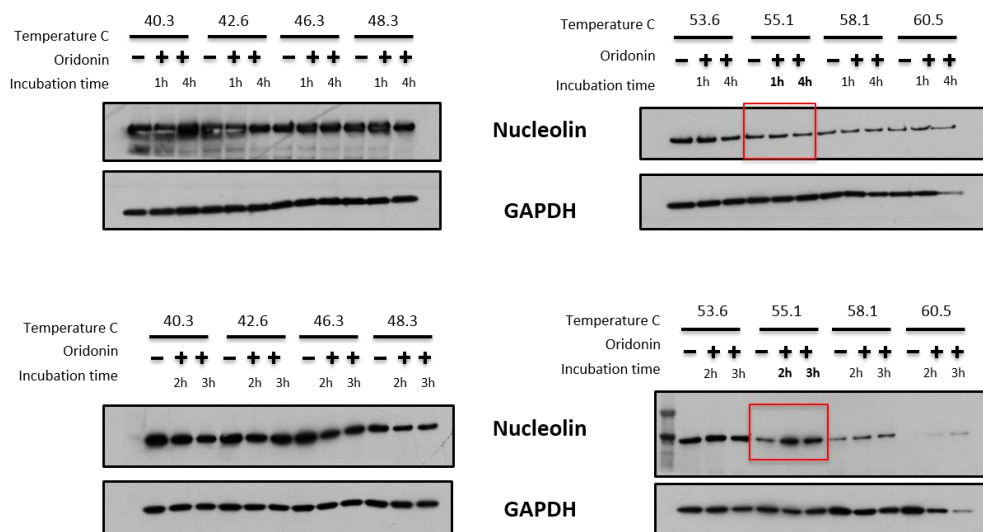


Fig.21: Kinetic profile of the engagement of nucleolin by oridonin in cells using CETSA. Jurkat cells were treated with oridonin 20 μ M for 1h up to 4h. Each samples was heated and then the soluble amount of NCL was evaluated by western blotting analysis

As reported in Figure 21, the time-course experiment revealed that the maximum binding was observed after 2 h of incubation with oridonin; after that the difference between treated and control samples start decreasing, and it became negligible after 4 h of incubation . It has to be underlined that this result is in agreement with that achieved using the fluorescence microscopy (see 3.4), suggesting that oridonin uptake into the Jurkat cells and oridonin interaction with NCL into the same cells have a comparable kinetics.

Taking advantage of defined T_{agg} , we carried out an ITDF_{CETSA} experiment to establish the half-maximal effective dose (EC_{50}) of oridonin towards NCL. Therefore, Jurkat cells were treated with a wide range of concentrations of oridonin up to 20 μ M (Figure 22) while incubation time and temperature were kept constant.

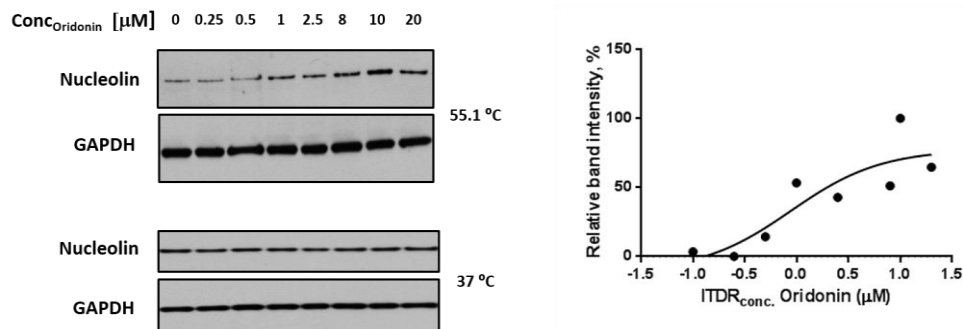


Fig.22: CESTA in Jurkat cells in presence of DMSO or various oridonin concentration (from 0 to 20μM) at 55.1°C and 37°C, and densitometry-based quantification of western blot signals

Increased NCL stabilization was observed at 55.1 °C, but not at 37°C in a oridonin dose-dependent manner. The obtained EC₅₀ was (0.8 μM) was in agreement with previous obtained data.

3.10 Oridonin/HSP70 interaction validation in cell system using CESTA

Since oridonin is able to bind also HSP70, as mentioned before, we decided to evaluate the EC₅₀ and the kinetic profile of this complex by CETSA approach. The first step was to define the T_{agg} of HSP 70 since this temperature is cell model and protein specific. Therefore, Jurkat cells were treated with oridonin 20μM for 2h and 3h of incubation time. The same experimental protocol (see 3.9) was followed but in this case we used a specific antibody to detect the soluble amount of HSP70 in our samples.

In this case the stabilization of HSP70 by its binding with oridonin was not observed. The possibility to establish a CETSA melting curve for a protein with bound ligand is dependent on whether the binding of a ligand and induces a stabilization of the target protein. Large proteins, including protein complexes, are more likely to give weaker or no ligand-induced response in thermal shift assays, although the limitations of assay in this respect have not yet established (Jafari R. *at al.* 2014). Moreover, we supposed that being HSP70 a heat shock protein, the heating of intact cells was not enough to

appreciate its thermal stabilization. In fact, this protein can act to protect cells from thermal or oxidative stress and prevents partially denatured proteins from aggregating, and allows them to refold. Moreover, the melting point of archaeal Hsp70 (DnaK) is around 60-70°C (Popp S.L. & Reinstein J. 2009). Therefore, CETSA assay could not be useful to study HSP70 and similar proteins.

3.11 In vitro imaging of nucleolin colocalization with oridoninBODIPY FL2

One of the most used approaches to confirm molecular interactions inside the cells is the co-localization analysis performed by microscopy analysis. Furthermore, we carried out a fluorescence microscopy analysis aimed to confirm the oridonin/NCL interaction. Based on the results previously obtained by the chemical proteomic approach (see **3.7**), we supposed that the α,β -unsaturated carbonyl group of the diterpene was not crucial for its interaction with NCL, whereas it was essential for the oridonin/HSP70 complex formation.

Thus, the first step was to synthesize the fluorescent modified version of oridonin conjugating the dye to oridonin from its α,β -unsaturated group. In particular, also in this case we used BODIPY FL as dye, for the same reasons mentioned before. The synthetic scheme used (Figure 23) provided the final molecule in two step. In particular, first we conjugated oridonin to a specific linker via Michael addition and then to the selected BODIPY. All steps were monitored and characterized by HPLC and LC-MS/MS.

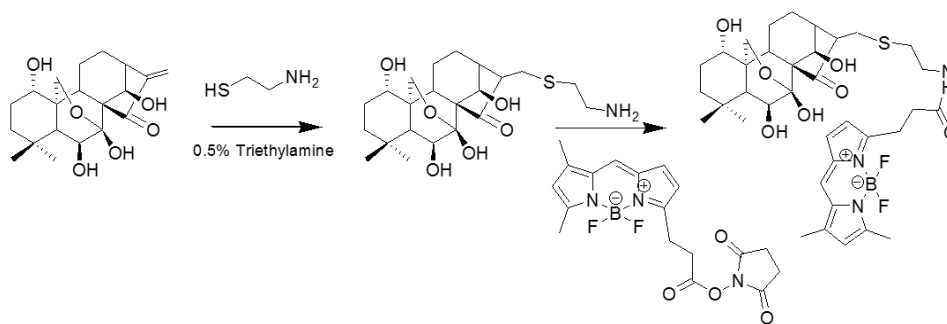


Fig.23: Synthetic scheme to obtain the fluorescence modified version of oridonin BODIPY FL2

Successively, Jurkat cells were treated with the new CID of oridonin at $20\mu\text{M}$ for 2h. Cells were then fixed and stained with nucleolin antibody and microscopy analysis were performed.

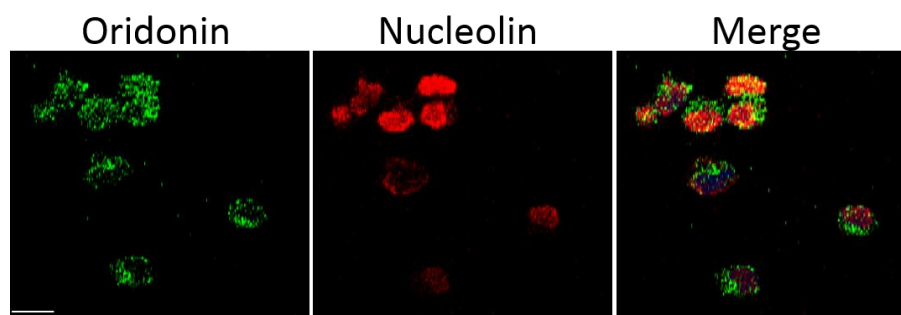


Fig.24: Fluorescence analysis to detect oridonin (green) and nucleolin (red). Nuclei were stained with DAPI. The merged image shows overlapping localization of oridonin with the protein

As depicted in Figure 24, following 2h of incubation of the Jurkat cells with the fluorescent oridonin a significant co localization of oridonin with nucleolin within cells was observed, as demonstrated by the presence of several yellow spots in the “merge” panel. Interestingly, this co-localization seemed to occur both in the cytosol and into the nucleus.

3.12 Oridonin biological effect on nucleolin into the cell

The evidence that NCL binds oridonin opened the way to further investigation on the role of oridonin in the modulation of nucleolin-mediated processes, inside a cell system. Thus, we were intrigued by a new potential application of this molecule in modulating biological processes in which NCL is involved. On this basis, we decided to verify first, the biological relevance of the binding of oridonin to NCL.

3.12.1 Levels and post translational modifications of nucleolin

NCL, a ubiquitously expressed phosphoprotein constitutes almost 10% of total nucleolar proteins and it was first described in 1973 (Srivastava M. & Pollard H.B. 1999). NCL possesses three structural domains: the N-terminal domain contains acidic regions (rich in glutamic acid and aspartic acid) separated by basic stretches, the central domain contains four RNA binding domains (RBDs) and the C-terminal domain is rich in glycine, arginine and phenylalanine residues (Ginisty H *et al.* 1999). NCL protein has multiple sub-cellular locations that are directly implicated in its pleotropic physiological functions. In the nucleolus, it is directly involved in cellular processes e.g. chromatin remodeling (Angelov D. *et al.* 2006), transcriptional regulation (Abdelmohsen K. & Gorospe M. 2012) ribosome biogenesis (Cong R. *et al.* 2012) and telomerase activity (Lee J.H. *et al.* 2014). In the nucleoplasm, it interacts with several proteins and is involved in regulation of the cellular response to stress (Daniely Y. *et al.* 2002; Yang C. *et al.* 2002; Kim K. *et al.* 2005; Saxena A. *et al.* 2006; Bhatt P. *et al.* 2012; Kobayashi J. *et al.* 2012). NCL constantly shuttles between the nucleus and cytoplasm where it is involved in many non-nucleolar functions e.g. centrosome duplication (Ugrinova I. *et al.* 2007) as well as post transcriptional and translational regulation of various mRNAs (Otake Y. *et al.* 2007; Ishimaru D. *et al.* 2010; Abdelmohsen K. *et al.* 2011) including p53 (Takagi M. *et al.* 2005). On the

cell surface NCL serves as a receptor, binds to several ligands to either mediate tumorigenesis or to relay anti-carcinogenic effects (Fujiki H. *et al.* 2014).

An altered expression and function of NCL has been correlated with many cancer types. Presently, there are no known mutations or splicing variants of NCL associated with a disease. Instead, a deregulated accumulation of the NCL mRNA or/and the protein is observed in different cancer cell types (Berger C.M. *et al.* 2015). It is well established that NCL promotes cell proliferation and survival linked to disease processes like carcinogenesis, but the mechanisms that control nucleolin abundance are not well understood.

Differential NCL localization is due to changes in its isoelectric point and/or post-translational modifications. There is evidence that the multiple activities of NCL may be regulated by covalent modifications, most notably phosphorylation (Caizergues-Ferrer M. *et al.* 1989; Peter M. *et al.* 1990; Schneider H.R. *et al.* 1986), proteolysis (Bouche G. *et al.* 1984; Bourbon H.M. *et al.* 1983), autodegradation (Chen C.M. *et al.* 1991; Fang S.H. & Yeh N.H. 1993), and ADP-ribosylation (Leitinger N. & Wesierska-Gadek J. 1993). For example, the aminoterminal domain contains sites for modification by phosphorylation and proteolysis, whereas the carboxyl-terminal domain has sites for methylation and proteolysis. All of these modifications are important for the regulation of NCL functions.

Therefore, as a first step in the study of the effects of oridonin treatment on NCL, we evaluated the levels of this protein and its fragmentation within the cells following their incubation with oridonin. Jurkat cells were then treated with oridonin for 1h up to 4h and then underwent protein extraction procedure. Resulting lysates were resolved by SDS PAGE and the levels of NCL were evaluated using nucleolin antibody. In our experimental conditions, as reported in Figure 25, the levels and the specific pattern of nucleolin remained substantially comparable to control suggesting that oridonin doesn't change

cellular NCL levels. Moreover, also the fragmentation pattern of the protein was not affected by the treatment. Similar results were obtained when nervosanin B was used as negative control.

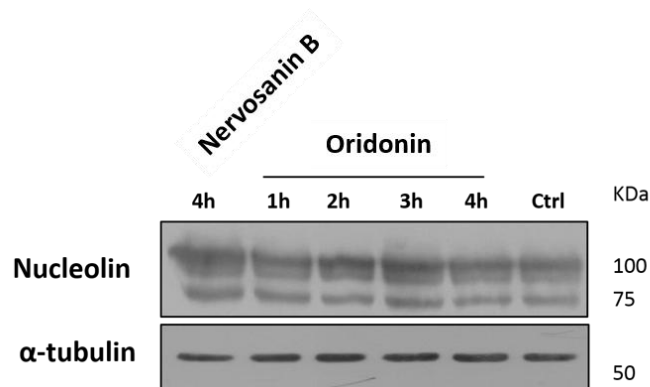


Fig.25: Treatment of Jurkat cells with oridonin and nervosanin B (20 μ M) up to 4h and evaluation of proteolytic fragments of nucleolin in cell

A similar experiment was performed to monitor the NCL phosphorylation following the oridonin treatment. NCL is highly phosphorylated and its phosphorylation is strictly regulated during the cell cycle (Peter M. *et al.* 1990; Morimoto H. *et al.* 2005). Extensive phosphorylation by casein kinase 2 (CK2) occurs at interphase and by CDC2 during mitosis and this regulated phosphorylation of nucleolin probably regulates nucleolin functions during the cell cycle (Ginisty H. *et al.* 1999; Peter M. *et al.* 1990). In addition, massive phosphorylation by CDC2 or CK2 kinases localizes nucleolin to the cytoplasm, and nuclear translocation of NCL accompanies dephosphorylation (Schwab M.S. & Dreyer C. 1997). Moreover, phosphorylation of nucleolin by CKII and CDC2 kinase has been shown to regulate its helicase activity (Tuteja N. *et al.* 1995), and phosphorylation by CK2, CDC2 kinase, PKC-j, cyclic AMP-dependent protein kinase, and ecto-protein kinase may regulate nucleolin's functional abilities in chromatin organization, rRNA packaging, rDNA transcription, or ribosome assembly.

Hence, Jurkat cells were incubated with oridonin and evaluated the phosphorylation of this protein for several time points. After the last experimental point, 24h, oridonin treated and control (DMSO) cells were lysed and samples were analyzed by western blotting using phosphonucleolin antibody.

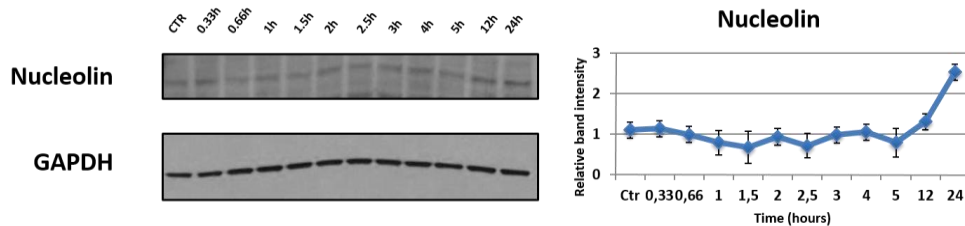


Fig.26: Effect of oridonin on phosphorylation of nucleolin in cells and densitometry-based quantification of western blot signals. Jurkat cells were treated with oridonin 20 μ M at indicated incubation times and followed by western blotting analysis using the phosphorylated NCL antibody

The immunoblot profile (Figure 26) demonstrated a relevant degree of phosphorylation only after 12h in the cells treated with oridonin. A major effect was evident in the case of 24 h. This result suggests that oridonin induced, directly or indirectly, a late phosphorylation of this protein. Moreover, in order to get more information about this post translational modification, we performed CETSA experiments. In this case we used the phosphonucleolin as antibody to better understand if oridonin was able to bind the phosphorylated nucleolin within cell. Therefore, Jurkat cells were treated with oridonin 20 μ M up to 12h and then we evaluated the engagement profile using 55.1 $^{\circ}$ C as T_{agg} (Figure 27).

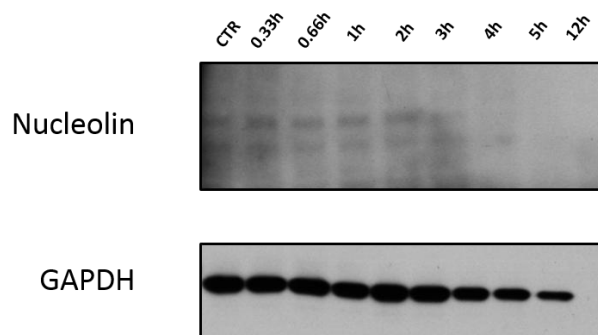


Fig.27: Kinetic profile of the engagement of phosphonucleolin by oridonin in cells by CETSA. Jurkat cells were treated with oridonin 20 μ M for 30min up to 12h. Each samples was heated and then the soluble amount of phosphoNCL was evaluated by western blotting analysis

The profile revealed that oridonin was no able to bind the phosphorylated nucleolin. Therefore, all these results indicate that oridonin binds NCL and it did not induce any post translational modification investigated, at least for the first 4 hours of incubation time.

3.12.2 Regulation and influence of target mRNAs of nucleolin by oridonin

NCL is highly expressed in proliferating cells, including stem cells and cancer cells. The oncogenic effect this appears to be multifactorial, in keeping with the many functions of this protein. Cells acquire a number of features in order to become malignant, including the abilities to grow and proliferate, overcome senescence, evade apoptosis and the immune system, invade and metastasize other tissues and promote angiogenesis (Hanahan D. & Weinberg R.A. 2011; Dunn G.P. *et al.* 2004). NCL through its RNA binding activity conferred by its four RNA binding domains could affect these traits. Toward implementing an anti-apoptotic phenotype, NCL modulates the expression of several proteins that influence the survival of malignant cells during cell damage. In fact, NCL affects mRNA turnover, both increasing and decreasing mRNA half-life, by interacting with the 3'-untranslated region of several target mRNAs. In particular, NCL binds to *BCL2* mRNA and promotes the expression of proto-

oncogene Bcl-2 which blocks apoptosis in cancer cells (Yang J. *et al.* 1997), and it binds to *AKT1* mRNA and enhances translation of Akt1, another potent pro-survival protein (Hers I. *et al.* 2011). On this basis, we decided to verify oridonin effects on the levels of these specific mRNAs. Hence, Jurkat cells were treated with 20 μ M oridonin for 3h and 6h and the stabilization of Bcl2 and AKt1 mRNAs by Real-Time Quantitative Polymerase Chain Reaction (rtq-PCR) was evaluated. As reported in Figure 28 the levels of these mRNAs decrease in a time-dependent manner.

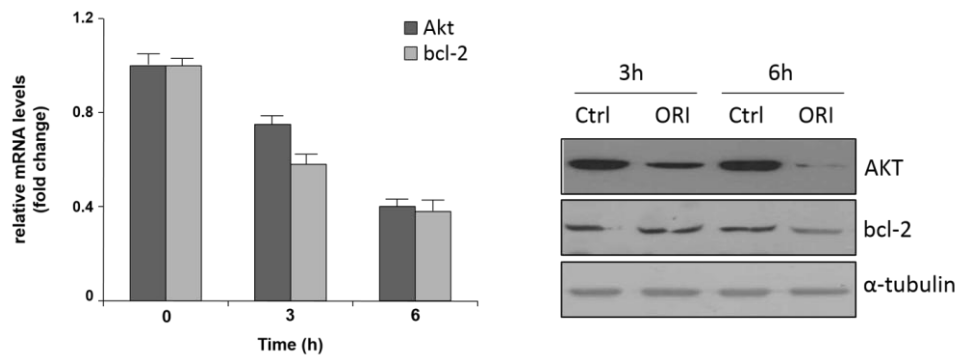


Fig.28: rtq-PCR of AKT1 and BCL2 mRNAs and western blot analysis of these proteins. Jurkat cells were treated with oridonin 20 μ M for 3 and 6 h and either AKT1 and BCL2 mRNAs and levels of these proteins were analyzed

Moreover, all of these results were confirmed by western blotting analysis as reported in the same Figure 28. In fact, we estimated also the amount of these two proteins by western blotting.

3.12.3 Inhibition of protein synthesis by oridonin

Ribosome biogenesis involves rRNA synthesis, maturation, and assembly of rRNA and ribosomal proteins into the large and small ribosome subunits. This process is regulated throughout the cell cycle, primarily at the level of rRNA synthesis (Hannan K.M. *et al.* 1998). rDNA transcription peaks during the S and G2 phases, stops as cells enter mitosis and then reactivates as cells exit from mitosis. Many factors have been shown to participate in various steps of

the processing. These extensive modifications generate 18S, 5.8S, and 28S rRNA. The mature rRNAs are subsequently assembled with ribosomal proteins into preribosomal particles in the nucleolus (Grummt I. 1999).

NCL plays important roles in various steps of ribosomal synthesis, such as the transcription of rDNA repeats, the modification and processing of pre-rRNA, the assembly of pre-ribosomal particles and nuclear-cytoplasmic transport of ribosomal proteins and subunits. In particular, nucleolin involvement in rDNA transcription, pre-RNA processing, ribosome assembly, and maturation mediated through the interaction of nucleolin with rDNA (nontranscribed spacer, 59 and 39-external nontranscribed spacer, internal transcribed spacer, nascent 45S pre-RNAs, RNA polymerase 1, 18S, 28S rRNAs) and ribosomal proteins could be an efficient way for the cell to regulate the production of large amount of ribosomes needed throughout its life (Ginisty H. *et al.* 1999; Tuteja R. & Tuteja N. 1998; Srivastava M. & Pollard H.B. 1999).

Ribosomes are the sites in a cell in which protein synthesis takes place and this process is crucial to cell growth, proliferation, and adaptation to changing environment. Since the main role of NCL about ribosome biogenesis, the effects of oridonin treatment on protein synthesis in different experimental conditions were investigated. Therefore, in a first step of the protein synthesis assay, different samples of Jurkat cells were analyzed: cells incubated with oridonin 20 μ M for 1h, cells with oridonin 20 μ M for 2h, cells with nervosanin B 20 μ M for 2h, with cycloheximide (a well-known inhibitor of the protein synthesis) and with DMSO (as negative control). After the incubation, the samples were treated with Click-iT[®] OPP (O-Propargyl-Puromycin). This reagent is a puromycin analog containing an alkyne moiety. When added to culture media, OPP is readily taken up by actively growing cells. OPP inhibits protein synthesis by disrupting peptide transfer on ribosomes causing premature chain termination during translation. Addition of the 5 FAM azide and the click reaction reagents led to a chemoselective ligation or “click”

reaction between the azide dye and the alkyne OPP, allowing the modified proteins to be detected. Finally, all the samples were analyzed by flow cytometry.

As depicted in Figure 29, the shift in the maximum fluorescence intensity is clearly due to the OPP alone without any inhibitor. Lower fluorescence intensity gave cycloheximide, as expected, since it's able to block this process. Oridonin gave a decreasing of the signal in time-dependent manner, and after 2h gave the same % of inhibition as cycloheximide suggesting a strong inhibition of the protein synthesis process. Nervosanin B gave no inhibition of the protein synthesis, as expected, since we used it as negative control for our experiments.

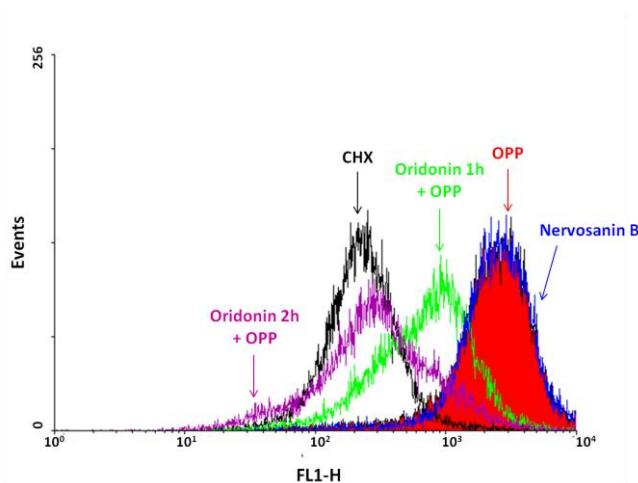


Fig.29: FACS analysis of Jurkat cells to evaluate the inhibition of the protein synthesis: Blue signal: Jurkat cells were treated with nervosanin B 20 μ M for 2h; Red signal: Jurkat cells were treated with OPP; Green signal: Jurkat cells were treated with oridonin 20 μ M for 1h; Purple signal: Jurkat cells were treated with oridonin 20 μ M for 2h; Black signal: Jurkat cells were treated with cycloheximide

All these data clearly demonstrated the ability of oridonin to inhibit the protein synthesis process in a time-dependent manner.

Since is reported that oridonin is able to arrest cell cycle in S-G2/M phase (Dal Piaz F. *et al.* 2013), we verified if in our experimental condition there was

already the block of the cell cycle and consequently the inhibition of the protein synthesis. With this purpose, Jurkat cells were treated with oridonin 20 μ M, nervosanin B 20 μ M, and vehicle for 2h and stained with propidium iodide. Samples were then analyzed by FACS to evaluate cell viability and DNA content for the cell cycle analysis.

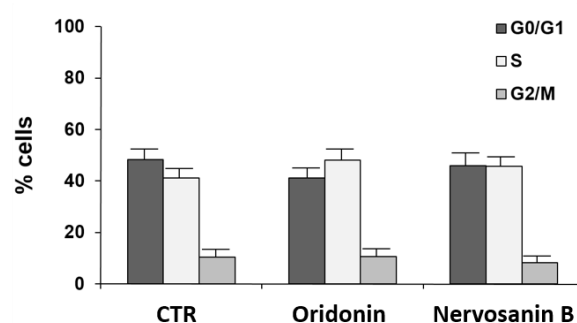


Fig.30: Cell cycle analysis of Jurkat cells after treatment with oridonin and nervosanin B 20 μ M for 2h

Indeed, as reported in Figure 30, oridonin did not produce significant cytotoxic effects on Jurkat cells and changes in cell cycle *vs* control even at 20 μ M for a short incubation time (2h). These results confirmed the influence of oridonin on protein synthesis and its ability to bind NCL and to affect its biological activity in cell.

3.13 Screening in vitro of new potential nucleolin inhibitors using CETSA approach

The results obtained on oridonin strongly suggests this diterpene as an effective modulator of NCL. Presently, in literature there are two reported inhibitors of NCL: the first is AS1411 that is a 26-base G-rich DNA oligonucleotide that functions as a nucleolin-binding aptamer and has antiproliferative activity against a wide range of cancer cells, but little or no effect on nonmalignant cells (Wu D.M. *et al.* 2014). The second is HB 19, a

synthetic multimeric pseudopeptide, that binds cell surface expressed nucleolin and inhibits both tumor growth and angiogenesis (Birmpas C. *et al.* 2009). Therefore, considering the new interest and potential of NCL as druggable protein, could be very advantageous to discover new small molecule as potential inhibitors. Thus, we attempted to identify new compounds able to bind nucleolin in cell, starting from oridonin analogous. Therefore, we developed a highly sensitive CETSA approach for the screening of natural compounds. This target-based technique is very useful since can give critical target engagement informations for a range of different drugs target directly in cell. In particular, this approach can address the fundamental question of whether the drug candidates actually engage their intended targets in a biological relevant settings and at what concentration regimes they exert their effects and it could serve to identify starting points for medicinal chemistry programs. As many target classes offer a broad range of screen assay alternatives, this approach may be of particular interest for targets that are difficult to express and purify in a biologically active and relevant form or for which other assay formats are difficult to establish for technical reasons. Moreover, CETSA approach, rarely gives false positive ligand-binding data, in contrast to many activity-based assay (Jafari R. *et al.* 2014).

Our program started with a screening of ent-kaurane diterpenes, using oridonin as positive control. Experimental conditions were set as reported for oridonin (see **3.9**). A small number of diterpenes were selected on the basis of their structural homology to oridonin, from the wide collection of natural compounds isolated and fully characterized by our research group (Figure 31).

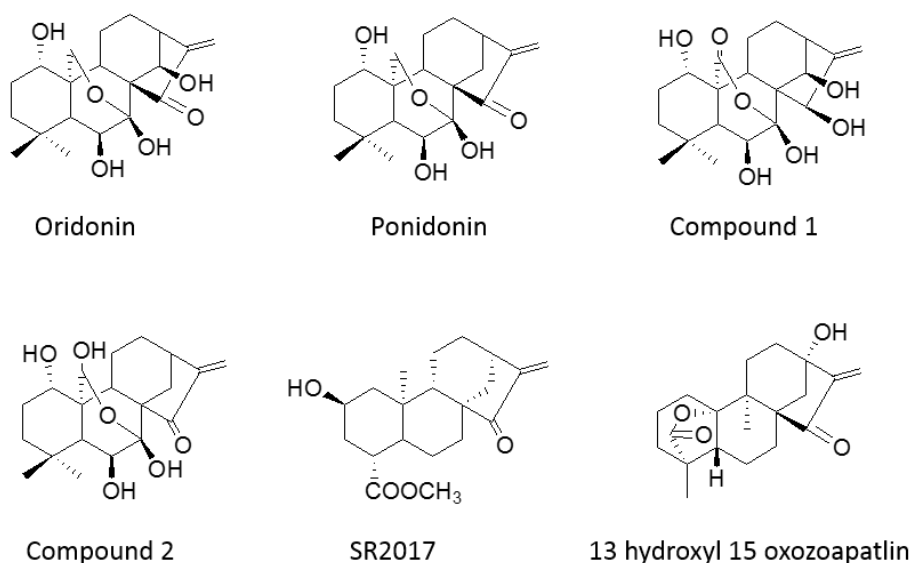


Fig.31: Chemical structure of tested molecule by CETSA

Experimentally, Jurkat cells were treated with selected compounds at 20 μ M for 2h of incubation time (Figure 32). Next, we heated samples at the defined T_{agg} for nucleolin in this cell model and we kept constant all parameters for each samples. Finally, we used nucleolin antibody to detect the soluble amount of this protein in our samples. The achieved results were used to establish new small molecules able to bind NCL in cell and to set further studies.

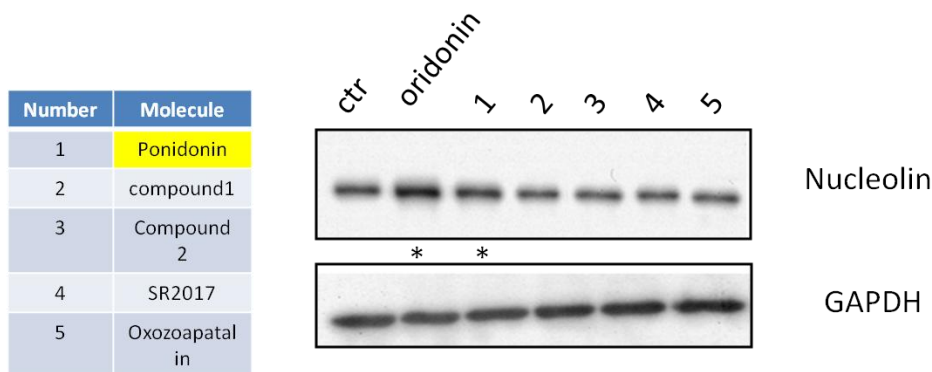


Fig.32: CETSA approach to establish new potential tools for the interaction with nucleolin. Jurkat cells were treated with DMSO or with a small molecule at 20 μ M for 2h of incubation time, followed by heating of each samples at 55.1 $^{\circ}$ C. Western blotting using NCL antibody was performed

Only ponidonin, a compound having close similitude to oridonin both under structural and biological point of view, showed an affinity towards NCL comparable to that of oridonin. Moreover, looking the investigated structures and obtained results suggested that α,β -unsaturated carbonyl group of oridonin structure it did not play a crucial role for the interaction with NCL. Finally, these preliminary data could represent a good starting point for a target oriented study.

3.14 Discussion

In the present research, the mechanism of action of oridonin was investigated by adopting a multidisciplinary approach. Oridonin, the main bioactive diterpenoid isolated from the well known plant *Isodon rubescens*, has been shown to have multiple biological activities. Among them, the anticancer activities have been repeatedly reported by many research groups (Sun H.D. *et al.* 2006; Sartippour M.R. *et al.* 2005; Tan W. *et al.* 2011; Li C.Y. *et al.* 2011). The chemopreventive and antitumor effects of oridonin have been related to its ability to interfere with several pathways involved in cell proliferation, cell cycle arrest, apoptosis and/or autophagy (Zhang T.M. 1982).

This diterpene had already aroused interest in our research group. Using an unbiased chemical proteomic approach we defined the possible protein target of the ent-kaurane diterpene oridonin. In particular, HSP 70 was found out as main target of this molecule. Although many of the activities of this protein could explain the mechanism of action of this molecule, the complex mechanism of action of oridonin was not entirely clear. Moreover, the technique used for the identification of the target is one of the most effective to define the interactome of a bioactive compound, but it faces some limitations (Rix U. & Superti-Furga G. 2009).

Therefore, with the aim to expand our knowledge about this molecule, we carried out a study based on the use of several techniques complementary and orthogonal each other. The first step was to synthesize the fluorescence modified oridonin version to better understand the uptake and the kinetic profile of this molecule in our cell model. Once we established the complete kinetic profile of this molecule for the first 4h of treatment, we carried out an indirect unbiased proteomic study to define protein targets of our diterpene. We used DARTS approach which allowed us first to validate the interaction with HSP70 but also to define a new list of interactors within cells. The study of small molecules/protein interactions using DARTS approach has the advantages of use the molecule without chemical modifications. Thereafter, we conducted a chemical proteomic study. In particular, the aim has been to enhance and then evaluate possible noncovalent interactors of oridonin. In fact, although oridonin has the α,β -unsaturated carbonyl group in the structure as pharmacophore, in order to make a very stable interaction with a target it's important also the interactions of the carbon skeleton of the same molecule with it. Also this study allowed us to define a possible list of putative target of oridonin within cell.

Crossing all the obtained results we focused our studies on nucleolin. This is a ubiquitous phosphoprotein and a multifunctional phosphoprotein, over

expressed in cancer cells (Derenzini M. *et al.* 1995; Srivastava M. & Pollard H.B. 1999) where it can influence cancer development. We confirmed the ability of oridonin to interact with NCL and evaluated the effects of this interaction on NCL activity. Firstly, we defined the thermodynamic parameters of the NCL/oridonin complex formation *in vitro* using SPR analysis, demonstrating that oridonin has a high affinity towards this protein. Subsequently, we evaluated if the treatment of the cells with oridonin can affect the levels and the post translational modifications of this protein. Our data indicate that oridonin does not affect some of these parameters and, above all it selectively binds the unmodified full length protein. Finally, in order to understand the consequences of the NCL-oridonin interaction on protein activity, we deeply investigate how oridonin influence several specific pathways in which NCL plays a fundamental role. Therefore, specific mRNAs stability and protein synthesis were evaluated. Last step was to support all the data obtained before. Therefore, by microscopy analysis it was possible to prove, once again, the possible interaction within cell between oridonin and nucleolin.

The identification of HSP70 and nucleolin as oridonin molecular targets in Jurkat cells suggested a mechanism of action of oridonin consistent with the multiple biological activities described for this diterpene. Specifically, achieved results suggest that although oridonin is able to bind different partners inside the cell, it mainly affects a specific pathway. Several evidences have been reported indicating that HSP70 promote cell protection from external injuries also by enhancing the stability and the activity of NCL (Xu J. *et al.* 2010); the contemporaneous inhibition of HSP70 and NCL could therefore produce significant effects on cell viability and proliferation (Xu Z. *et al.* 2012). Moreover, HSP70 activity is needed to allow the translocation of NCL to the cancer cell membranes, where it plays a pivotal role in the angiogenic induction (Ding Y. *et al.* 2012); thus oridonin could strongly affect

neovascularization of cancer tissues. These findings, shedding light on the molecular basis of the biological activity of oridonin, may therefore be extremely relevant for possible therapeutic applications of oridonin, opening the way to the design of new therapeutic approaches. Some compounds inhibiting HSP70 underwent preclinical and clinical studies exploring the effect of a combination of HSP inhibitors with other anticancer agents in cancer therapy, demonstrating that in most cases they produce additive or synergic effects (Mosser D.D. & Morimoto R.I. 2004; Brodsky J.L. & Chiosis G. 2006; Yerlikaya A. *et al.* 2010). In addition, several molecules have been developed to block the action of NCL, but only the aptamer AS1411 is still continuing its stages as NCL-inhibitory molecule in clinical trials. However, oridonin could be the first example of a small molecule affecting the activities of both these proteins. Thus, this diterpene could be the ideal starting point to design optimized multi-target inhibitors, but it also represents a useful tool to better understand the structural and functional features of HSP70 and NCL. In addition, this research demonstrates the effectiveness of a multidisciplinary approach in drug discovery studies and in orphan drug molecular target identification.

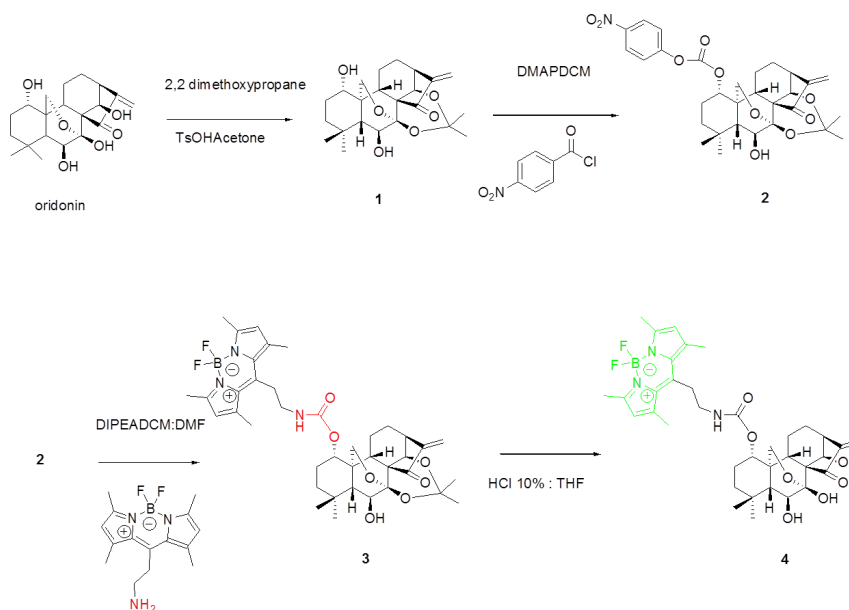
Materials and methods

3.15 Synthesis and Characterization of Oridonin-BODIPY FL

Materials

All reagents were obtained from commercial sources and used without further purification. Dry THF, DCM, and DMF were obtained from Sigma Aldrich (St. Louis, MO, USA).

^1H and ^{13}C NMR spectra were recorded at 23 °C on Bruker 400MHz spectrometer. LC-ESI-MS analysis and HPLC purifications were performed on a Waters (Milford, MA, USA) LC-MS system.



3.15.1 Synthesis and characterization of *ent*-1a,6b-Dihydroxy-7,14-isopropylidene ketal-15-oxo-7,20-epoxy-16-kaurene (compound 1)

Briefly as reported by Wang L. *et al.* 2012: Oridonin (100 mg, 0.27 mmol) was dissolved in acetone (10 ml). TsOH (5 mg) and 2,2-dimethoxypropane (1 ml) were added to this solution. The mixture was stirred at R.T. for 15 min,

and diluted with water and extracted with dichloromethane for 3 times. The extract was washed with saturated NaHCO₃ solution and brine, dried over anhydrous Na₂SO₄, filtered, and evaporated to afford compound 1 (94 mg, 85%) as a white powder. LRMS (ESI) *m/z* calcd for C₂₃H₃₂O₆= 404.22

3.15.2 Synthesis of compound 2

Compound 1 (32mg mmol0.0792) was dissolved in dry DCM (700μl). This solution was purged with nitrogen for 10 min. DMAP (38.7 mg 0.316mmol) and 4Nitrophenyl Chloroformate (32 mg 0.158mmol) were added. The mixture was stirred at R.T. for 1h. After reaction completion, the mixture was dried and then purified with silica gel column chromatography (Ethyl Acetate : Hexane 0:100 to Ethyl Acetate only) to give compound 2 (13 mg, 40%) as a white powder. LRMS (ESI) *m/z* calcd for C₃₀H₃₅NO₁₀ =569.23

3.15.3 Synthesis of compound 3

A solution of compound 2 (10mg 0.024mmol), DIPEA (7ul 0.05 mmol) was added. After 5 min, BODIPY ammine (26mg 0.05mmol) in DCM: DMF 50:50 (900μl) was added. The mixture was stirred at R.T. for 1h. After reaction completion, the mixture was dried and then purified with a C18 reverse phase column (Water : ACN w/0.1% Formic acid = 95:5 to 0: 100) to give compound 3 (14mg, 81%). LRMS (ESI) *m/z* calcd for C₃₉H₅₀BF₂N₃O₇=721.37

3.15.4 Synthesis of compound 4

In order to get the final compound, compound 3 (10mg 0.014 mmol) was dissolved in THF: HCl 10% (2ml) and stirred the solution at R..T. After 1h the mixture was dried and then purified with a C18 reverse phase column (Water : ACN w/0.1% Formic acid = 95:5 to 0: 100) to give compound 4 (6.8mg, 70%). LRMS (ESI) *m/z* calcd for C₃₆H₄₆BF₂N₃O₇=681.34

3.15.5 Stability assay

In order to get information about stability of oridonin BODIPY FL in our experimental conditions, 300µg of this compound was dissolved in different buffers (1ml each): PBS, Sodium Carbonate Bicarbonate 0.5 M pH=10 buffer, 0.1M MES buffer pH=5 and complete growth buffer (RPMI 1640 medium supplemented with 10% (v/v) FBS). After different time points (from T0 to T24h), 100µl of each solution was analyzed by LC-MS.

3.16 Biological characterization of oridonin BODIPY FL

Materials

Fetal Bovine Serum (FBS) was from GIBCO (Life Technologies, Grand Island, NY, USA) and all the other reagents were from Sigma-Aldrich (St. Louis, MO, USA).

3.16.1 Cell Viability Assay

Jurkat cells, obtained from American Type Culture Collection (ATCC) (Manassas, VA, USA), were maintained in RPMI 1640 medium supplemented with 10% (v/v) FBS, 2 mM L-glutamine and antibiotics at 37 °C in humidified atmosphere with 5% CO₂. To ensure logarithmic growth, cells were sub-cultured every 2 days. Under given experimental conditions, untreated Jurkat cells were able to double in number in 24 h. All experiments were performed using cells seeded at 2x10⁵ cells/ml.

The number of viable cells was quantified by MTT ([3-(4,5-dimethylthiazol-2-yl)-2,5-diphenyl tetrazolium bromide]) assay. Absorption at 550 nm was assessed using a microplate reader (LabSystems, Vienna, VA, USA). In some experiments cell viability was also checked by Trypan Blue exclusion assay using a Bürker counting chamber.

More in details, cells were seeded in 96-well microtiter plates in 100 μ l of growth medium. After 24 h and 48h of incubation at 37 °C, cells were exposed to different concentration of oridonin and oridonin BODIPY FL, ranging from 0.01 μ M to 40 μ M, containing as final concentration of DMSO 0.1%. The same amount the of DMSO has been applied as control and the incubation was carried out for the same incubation times. The mitochondrial-dependent reduction of MTT to formazan was used to assess the possible cytotoxic effect of these compounds. The experiment was carried out in triplicate and all the values were normalized to control.

3.16.2 Covalent binding Oridonin BODIPY FL/ HSP70

The ability of oridonin BODIPY FL to stabilize HSP70 with covalent binding mode was investigated. Dal Piaz F. *et al.* 2013 provided the high stability and the covalent binding of oridonin/HSP70 in vitro. Therefore, in order to get a full characterization of the modified version of oridonin was repeated the same experiment in the same conditions. More in details, 0.5 μ g (per data point) of human recombinant HSP70 (GenBank No. NM_005345, Tebu-Bio, Milano, Italy) was incubated with different fold molar excess (starting from 0.01 up to 10 molar folds more) of oridonin BODIPY FL in PBS at 25 °C under stirring for 15 min. Each sample was loaded on a mono-dimensional 12% SDS-PAGE and stained with Brilliant Blue G-Colloidal. Moreover, using Typhoon scanner FLA 7000 (GE Healthcare Life Sciences) was possible to detect the fluorescence intensity of oridonin BODIPY FL into the gel (ex: AlexaFluor 488nm, em: 512nm)

3.17 Live cell fluorescence microscopy in cell of oridonin BODIPY FL

Jurkat cells were seeded into a 96-well plate at 5000 cells per well and incubated for 24h. Cells were incubated in growth media containing 5 μ M of oridonin BODIPY FL 0.1% DMSO for 1h up to 4h. When the incubation time

was done, Hoechst 33342 (ThermoFisher scientific) was added to each sample for 30 min. Live cells were subsequently imaged on a Delta Vision imaging system (Applied Precision, GE Healthcare). Images were processed using Fiji software, an open-source version of ImageJ.

Next experiment was to repeat the same kind of analysis mentioned before but the cells were washed before the microscope analysis. Jurkat cells were treated with oridonin BODIPY FL for 2h and then replaced with growth medium supplemented with FBS 10% (v/v) for 1h, 2h and 3h. Live cells were then imaged.

3.18 Target identification approaches

Materials

Bredford and Brilliant Blue G-Colloidal were from BioRad, 1,4 Dithiothreitol and iodoacetamide were from AppliChem. All the other reagents were from Sigma-Aldrich (St. Louis, MO, USA).

Antibodies: anti-HSP-70 (mouse monoclonal, sc-32239), anti-Trx (rabbit polyclonal sc-20146), anti-GAPDH (rabbit polyclonal, sc-25778) and anti-HSP-90 α/β (rabbit polyclonal, sc-7947), were obtained from Santa Cruz Biotechnology (Santa Cruz, CA, USA); anti-TRXR1 (rabbit polyclonal, 6925) from Cell Signaling Technology (Danvers, MA, USA); anti-PPAR γ (mouse monoclonal, ab-45036) and anti-nucleolin (rabbit polyclonal, ab22758) were from Abcam (Cambridge, CB4 0FL, UK). Peroxidase-conjugated secondary antibodies were from Jackson ImmunoResearch (Baltimore, PA, USA).

3.18.1 Optimization of DARTS protocol

Jurkat lysates (50 μ g) were incubated with DMSO (1% v/v as final concentration) and after 1h of incubation time subtilisin digestion was followed. Different ratio enzyme: lysate (starting from a range of 1:100 up to

1:2500 w/w) for 30 min at R.T. under stirring was added to each samples. Each sample was then boiled for 5min at 100 °C with Laemmli buffer 1X. Finally, proteins were loaded on a mono-dimensional 10% SDS-PAGE and stained with Brilliant Blue G-Colloidal.

3.18.2 Evaluation of oridonin interference with subtilisin using DARTS approach

Recombinant BSA protein (10 µg) was incubated with and without oridonin (20 µM 1%DMSO) in PBS for 1h at R. T. under stirring. Proteolysis of each sample 1:1000 (w:w) subtilisin : BSA for 30 min was followed. Moreover, the same amount of subtilisin was incubated with oridonin 20 µM 1% DMSO for 1h. Peptides were then resolved by mono dimensional 10% SDS-PAGE gel and stained with Brilliant Blue G-Colloidal. Subtilisin digestion of BSA as a nonbinder protein of oridonin was unaffected by oridonin.

3.18.3 DARTS experiment on whole cell lysate

Human Jurkat cells were lysed in RIPA buffer supplemented with protease and phosphatase inhibitors. Protein concentration was determined by Bredford assay using bovine albumin as a standard. Lysates (50 µg) were incubated with 2 µl of PBS 8.5% DMSO, or 2µl of oridonin 170µM 8.5% DMSO in PBS, or 2 µl of Nervosanin B 170µM 8.5% DMSO in PBS to obtain the final concentration of 20 µM 1% DMSO for each small molecule studied. The samples were incubated for 1h at R.T. under stirring. Samples were then underwent proteolysis with Subtilisin (enzyme: lysate 1:1000 w/w) for 30 min and then, 5 µl of Laemmli buffer 4X was added to each sample and incubated at 100 °C for 5 min. All samples were loaded on a 10% mono dimensional SDS-PAGE gel.

3.18.4 DARTS experiment on intact cell

Intact Jurkat cells (2 million of cells per data point) were treated with oridonin to obtain the final concentration of 10 μ M and 20 μ M or 0.1% DMSO control for 2h at 37 °C. Cells were then lysed with RIPA buffer supplemented with protease and phosphatase inhibitors. After centrifugation and determination of protein concentration, the lysates were diluted to the same final volume with PBS. Each sample (50 μ g) was then quickly warmed to room temperature and proteolysed with subtilisin (enzyme: lysate 1:1000 w/w) for 30 min at R.T. Therefore, 5 μ l of Laemmly buffer 4X was added to each sample and incubated at 100°C for 5 min. Mixtures were resolved by 10% mono dimensional SDS-PAGE gel.

3.18.5 “Complementary” chemical proteomic

To perform a proteomic analysis of potential oridonin target protein(s), the first step was to modified the resin with oridonin. Specifically, about 300 μ g Resin TentaGel HL-S-Trityl (FLUKA-Sigma Aldrich) was washed with 100 μ l of MeOH/TFA/TIS (94:1:5 v:v:v) for three times. Subsequently, was added 100 μ l of 5% TFA in MeOH for 20 min at r.t. The activated resin was incubated with 4 μ g Oridonin (equimolar amount 12nmol 1:1 ratio resin : oridonin) and the mixture was maintained under continuous shaking O.N. at R.T.

The amount of immobilized oridonin was calculated integrating the peaks of the free oridonin species after HPLC injections of supernatants at t = 0 h, t= 2h and t=O.N., using an Agilent 1200 Series chromatographer. The HPLC runs were carried out onto a Phenomenex C18 column (250 x 2.0 mm) at a flow rate of 200 μ l/min. The gradient (Solution A: 0.1% F.A., solution B: CAN, 0.1% F.A.) started at 20% and ended at 95% B after 25 min. The residual thiol groups were inactivated with β mercaptoethanol. To obtain the control matrix, activated resin TentaGel was mixed with β mercaptoethanol. The mixture was

maintained under shaking O.N. at R.T. The amount of immobilized oridonin was 71%.

Jurkat cell lysates (400 µg) were incubated with resin modified with oridonin and without for 2h at 4°C undershaking. The beads were washed three times with PBS. Interacting proteins were eluted by 15 µL of Laemmli buffer 4X. Eluted proteins were separated on a mono-dimensional 10% SDS-PAGE and stained with Brilliant Blue G-Colloidal. Each gel line was cut in 10 pieces, and digested as describe below.

3.18.6 Samples preparation for mass spectrometer analysis

In gel digestion by trypsin was performed as previously described (Dal Piaz F. *et al.* 2013). Briefly, the lanes of interest were excised manually and analyzed as follow: gel pieces were discolored and de-hydrated in ACN. Subsequently, samples were subjected to reduction in 10mM 1-4 dithiothreitol (DTT) for 1 hour at 56°C and alkylated in 55mM iodoacetamide (IAA) for 30 min at r.t. in the dark. Samples were washed again, with ACN and Ammonium bicarbonate 100mM and finally digested with 30µl of trypsin, from porcine pancreas (Sigma Aldrich) at a final concentration of 0.013 ng/µl. Supernatans were collected, vacuum dried, dissolved in 15µl of 5% Formic acid for MS analysis. The resulting fragments were extracted and analyzed by LC/MS/MS using a LTQ Orbitrap XL ESI-mass spectrometer (Thermo Fisher Scientific) equipped with a nano-ESI source, coupled with a nano-Aquity capillary UPLC (Waters): peptides separation was performed on a capillary BEH C18 column (0.075 mm × 100 mm, 1.7 µm, Waters) using aqueous 0.1% formic acid (A) and CH₃CN containing 0.1% formic acid (B) as mobile phases. Peptides were eluted by means of a linear gradient from 10 % to 40% of B in 45 min and a 300 nl•min⁻¹ flow rate. Peptide fragmentation was achieved using helium as collision gas and a collision cell energy of 30 eV. Mass spectra were acquired in a *m/z* range from 400 to 1800, and MS/MS spectra in a *m/z* range from 25-

2000. MS and MS/MS data were used by Mascot (Matrix Science) to interrogate the Swiss Prot non-redundant protein database. Settings were as follows: mass accuracy window for parent ion, 10 ppm; mass accuracy window for fragment ions, 50 millimass units; fixed modification, carbamidomethylation of cysteines; variable modifications, oxidation of methionine. Proteins with scores > 65 and identified by at least 2 significant sequences, were considered as reliable proteins.

3.19 SPR analysis of nucleolin complexes

SPR studies on oridonin and on nervosanin B were performed using an optical biosensor BIACORE 3000 (GE Healthcare, Milano, Italy). Briefly, recombinant human nucleolin was immobilized on a CM4 sensor chip using a 5 μ M solution in sodium acetate 50 mM, pH 4.5. The carboxylic groups of the chip were previously activated by EDC 0.2 M and NHS 0.05 M. The exceeding active groups were inactivated with ethanolamine 1 M. To study the interaction of oridonin and nervosanin B with immobilized nucleolin, diterpenes stock solutions (4 mM) in DMSO were diluted 1:1000 in PBS to get a final DMSO concentration of 0.1%. Compound concentration series were prepared as 2-fold dilutions into PBS: for each sample, the complete binding study was performed using a six-point concentration series, typically spanning 0.001 to 0.5 μ M, and triplicate aliquots of each compound concentration were dispensed into single-use vials. Binding experiments were performed at 25 °C, using a flow rate of 50 μ L/min, with 60 s monitoring of association and 200 s monitoring of dissociation, using PBS as running buffer. Simple interactions were adequately fit to a single-site bimolecular interaction model, yielding a single KD. Sensorgram elaborations were performed using the BIAevaluation software provided by GE Healthcare.

3.20 CETSA approach

Materials

Antibodies: anti nucleolin Phosphorylated (Thr76/Thr84) (anti mouse polyclonal 10C7) from BioLegend (San Diego, CA, USA)

3.20.1 Determination of the apparent melting curve of nucleolin by CETSA

Protocol used was adopted from Jafari R. *et al.* 2014 but slightly modified. More in details, approximately 10 million Jurkat cells in a final volume of 10ml of growth media were used for each condition, in a Cell Culture Flasks (T75). A stock solution of oridonin (10µl of 20mM in DMSO) was added to individual flasks to get a final concentration of 20 µM of oridonin (0.1% DMSO); 10µl DMSO was used as control. Cells were gently mixed by pipetting up and down at least 3 times and were incubated for 1h up to 4h in the CO₂ incubator at 37 °C. After, the cell suspensions were collected and transferred to 15-ml conical tubes. Once cells were centrifuged, pellets of cells were washed with PBS and gently resuspended in 1ml of PBS supplemented with protease inhibitors to each respective tube. Each cell suspension was divided into 10 different tubes and the heated using PCR machine (Invitrogen Life Science Technologies) at different temperatures for 3 min.

The temperature used were:

Temperature (°C)	Sample CTR	Sample Treated
40.2	1	11
42.6	2	12
46.3	3	13
48.3	4	14
53.6	5	15
55.1	6	16
58.1	7	17
60.5	8	18
64	9	19
66.6	10	20

Immediately after heating, tubes were kept at room temperature for 3 min. After this 3-min samples were immediately snap-frozen in the liquid nitrogen for 3 times. Therefore, cell lysate-containing tubes were centrifuged at 20,000g for 20 min at 4 °C to pellet cell debris together with precipitated and aggregated proteins. Each supernatant with the soluble protein fraction was transferred to a new tube. Subsequently 10µl of each tubes were loaded on a 10% mono dimensional SDS-PAGE gel and western blotting analysis was performed.

3.20.2 Determination of EC_{50} of complex nucleolin/oridonin by CETSA

To perform the ITDRF_{CETSA} experiments, equal number of Jurkat cells (1 million cells per data points) were seeded in 24 well cell culture plates in 1 ml of growth media and exposed to varying concentration of oridonin for 2h of incubation time in an incubator chamber (range used from 0.25 µM to 20 µM, final concentration of DMSO 0.1%). Following the incubation, the drug-containing media were removed by centrifugation cells were washed with PBS and prepared for CETSA experiment. In this case cells were heated at 55.1 °C for 3min and the protocol used was the same described before. All

immunoblots were processed using Fiji software, an open source version of ImageJ.

3.21 Biological effect of oridonin in cell

Materials

Trizol Reagent, RNase H, SuperScript® II Reverse Transcriptase, random primers, and dNTP mix were purchased from Invitrogen (Life Technologies, Grand Island, NY, USA). SYBR Green I Master Mix and DNase I were from Roche Applied Science (Mannheim, Germany). Primers (custom synthesized) were from Primmbiotech (Milano, Italy) and all the other reagents were from Sigma-Aldrich (St. Louis, MO, USA).

Antibodies: Anti -tubulin (mouse monoclonal, sc-32293), anti-Bcl-2 (C-2, mouse monoclonal, sc-7382), were obtained from Santa Cruz Biotechnology (Santa Cruz, CA, USA); anti-Akt (rabbit polyclonal, 9272) from Cell Signaling Technology (Danvers, MA, USA). Peroxidase-conjugated secondary antibodies were from Jackson ImmunoResearch (Baltimore, PA, USA).

3.21.1 RNA isolation and quantitative real-time RT-PCR (qRT-PCR)

Jurkat cells were treated with oridonin 20 µM 0.1% DMSO as final concentration for 3h and 6h.

Total RNA was isolated using Trizol Reagent according to the manufacturer's instructions and spectrophotometrically quantified. RNA integrity was assessed by agarose gel electrophoresis. RNA (3 µg) was reverse transcribed, and real-time PCR was performed with Light-Cycler® 480 (Roche Diagnostics GmbH, Mannheim, Germany) using SYBR Green detection in a total volume of 20 µl with 1 µl of forward and reverse primers (10 mM) and 10 µl of SYBR Green I Master Mix. Reactions included an initial cycle at 95 °C for 10 min, followed by 40 cycles of denaturation at 95 °C for 10 sec,

annealing at 56°C for 5 sec, extension at 72 °C for 15 sec. The 18S RNA was used as an internal standard. The following primer sets were used for real-time PCR to assay specific mRNAs:

forward AKT 5'-TCT ACA CCC ACA GAT GAC AG-3'

reverse AKT 5'-CTC AAA TGC ACC CGA GAA AT-3'

forward bcl-2 5'-GGA AGT GAA CAT TTC GGT GAC-3'

reverse bcl-2 5'-CTC CAT CAG CTT CCA GAC AT-3'

forward 18S 5'-CGA TGC TCT TAG CTG AGT GT-3'

reverse 18S 5'-GGT CCA AGA ATT TCA CCT CT-3'

3.21.2 Protein Synthesis assay

Jurkat cells were incubated with 20 µM oridonin at different time with nervosanin B 20µM for 2h or with 50 µg/ml cycloheximide (CHX), as positive control, for 30 minutes in a cell culture incubator. Cells were then processed for detection of protein synthesis according to the protocol described in the Protein Synthesis Assay Kit (Cayman Chemical, Michigan, USA).

3.21.3 Cell viability and cell cycle analysis

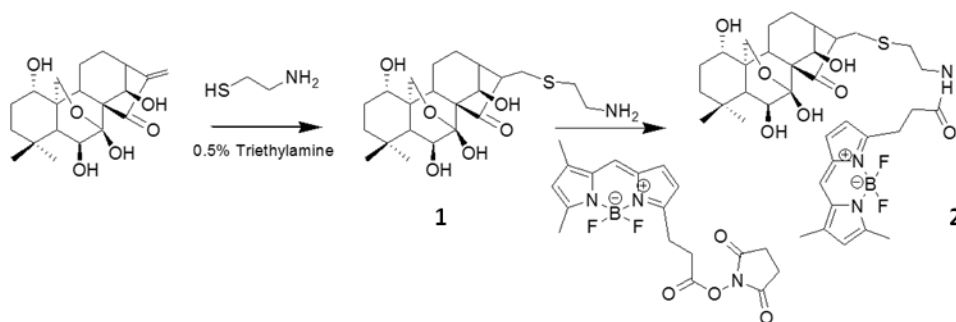
Jurkat cells were treated with oridonin and nervosanin B at final concentration of 20 µM 0.1% DMSO. Cell cycle was evaluated by propidium iodide (PI) staining of permeabilized cells according to the available protocol and flow cytometry (BD FACSCalibur *flow cytometer*, Becton Dickinson, San Jose, CA, USA). Data from 5000 events per sample were collected. The percentages of the elements in G₀/G₁, S and G₂/M phases of the cell cycle were determined using the MODFIT software.

3.22 Synthesis and characterization of oridonin BODIPY FL2

Materials

All reagents were obtained from commercial sources and used without further purification. Dry DMF and all other reagents were obtained from Sigma Aldrich (St. Louis, MO, USA).

^1H and ^{13}C NMR spectra were recorded at 23 °C on Bruker 400MHz spectrometer. LC-ESI-MS analysis and HPLC purifications were performed on a Waters (Milford, MA, USA) LC-MS system.



3.22.1 Synthesis and characterization of compound 1

Oridonin (100 mg, 0.27 mmol) was dissolved in MeOH (1 ml). β -mercaptoethyl-amine (42 mg, 0.54 mmol) in 1ml of MeOH and triethylamine (1% v/v) were added to this solution. The mixture was stirred at R.T. After 30 the mixture was dried and then purified with a C18 reverse phase column (Water : ACN w/0.1% Formic acid = 95:5 to 0: 100) to give compound 1 (102 mg, 90%) as a white powder. LRMS (ESI) m/z calcd for $\text{C}_{22}\text{H}_{35}\text{NO}_6\text{S}$ = 441.22

3.22.2 Synthesis and characterization of compound 2

1 mg of oridonin-mercapto-ethyl-amine (compound 1) has been conjugated with 1.7 mg of BODIPY FL in 1 mL of DMF:PBS buffer (80:20 v/v) for 2h at

37°C under stirring. Compound 2 (1.3 mg, 85%) has been monitored by RP-HPLC-UV. LRMS (ESI) m/z calcd for $C_{36}H_{48}BF_2N_3O_7S=715.66$

3.22.3 Immunofluorescence and co localization of oridonin BODIPY FL2

Control and oridonin-treated Jurkat cells (5 μ M oridonin- BODIPY FL2 for 2h) were fixed in a freshly prepared mixture of 4% paraformaldehyde in PBS for 30 minutes and permeabilized with 0.1% Triton X100 for 10 minutes. After washing with PBS, cells were incubated with primary rabbit anti-Nucleolin (1 μ g) for 2h. Following three further washes in PBS, cells were incubated for 1h with species-specific, fluorescein isothiocyanate (FITC) antibody (Jackson Immunoresearch, UK), at a 1:500 dilution, washed extensively in PBS and finally treated with Hoechst 33342 (10 μ g/ml) for 15 minutes. Confocal images were taken with a Zeiss LSM 510 META confocal microscope with a X63 objective lens.

3.23 Screening of terpenes using CETSA approach

Several terpenes were tested to verify the ability to bind nucleolin in cell using CETSA approach. All molecules were characterized and purified previously from our group of research. More in details, Jurkat cells (1 million of cells per data point) were treated for 2h at 20 μ M 0.1% DMSO with each molecule. The protocol used was the same described before; in this case cells were heated at 55.1 °C followed by western blotting analysis.

3.24 Western blotting analysis

Cell whole lysates for immunoblot analysis were prepared according to the standard protocol. Protein concentration was determined by DC Protein Assay (Bio-Rad, Berkeley, CA, USA), using bovine serum albumin (BSA) as a standard. Proteins were fractionated on SDS-PAGE, transferred into nitrocellulose membranes, and immunoblotted with appropriate primary

antibodies. Signals were visualized with appropriate horseradish peroxidase-conjugated secondary antibodies and enhanced chemiluminescence (Amersham Biosciences-GE Healthcare, NY, USA). Densitometry of bands was performed with ImageJ software (<http://rsbweb.nih.gov/ij/download.html>).

3.25 Statistical analysis

Data reported in each figure are the mean values \pm SD from at least three experiments, performed in duplicate, showing similar results. Differences between treatment groups were analyzed by Student's t-test. Differences were considered significant when $p < 0.05$.

References

- Abdelmohsen K. & Gorospe M., (2012), RNA-binding protein nucleolin in disease., *RNA Biol.*,9(6):799-808.
- Abdelmohsen K., Tominaga K., Lee E.K., Srikantan S., Kang M.J., Kim M.M., Selimyan R., Martindale J.L., Yang X., Carrier F., Zhan M., Becker K.G., Gorospe M., (2011) Enhanced translation by Nucleolin via G-rich elements in coding and noncoding regions of target mRNAs. *Nucleic Acids Res* 39: 8513–8530.
- Angelov D., Bondarenko V.A., Almagro S., Menoni H., Mongélard F., Hans F., Mietton F., Studitsky V.M., Hamiche A., Dimitrov S., Bouvet P., (2006), Nucleolin is a histone chaperone with FACT-like activity and assists remodeling of nucleosomes.,*EMBO J.*, 19;25(8):1669-79.
- Berger C.M., Gaume X., Bouvet P., (2015) The roles of nucleolin subcellular localization in cancer. *Biochimie.*,113:78-85.
- Bhatt P., d'Avout C., Kane N.S., Borowiec J.A., Saxena A., (2012), Specific domains of nucleolin interact with Hdm2 and antagonize Hdm2-mediated p53- ubiquitination., *FEBS J.*, 279: 370–383.
- Birmpas C., Briand J.P., Courty J., Katsoris P., (2012), The pseudopeptide HB-19 binds to cell surface nucleolin and inhibits angiogenesis. *Vasc Cell. Dec* 24;4(1):21.
- Bouche G., Caizergues-Ferrer M., Bugler B., Amalric F., (1984), Interrelations between the maturation of a 100 kDa nucleolar protein and pre rRNA synthesis in CHO cells., *Nuc. Acids Res.*, 12, 3025–3035.
- Bourbon H.M., Bugler B., Caizergues-Ferrer M., Amalric F., (1983), Role of phosphorylation on the maturation pathways of a 100 kDa nucleolar protein., *FEBS Lett.*, 155,218–222.
- Bradley W.D., Arora S., Busby J., Balasubramanian S., Gehling V.S., Nasveschuk C.G., Vaswani R.G., Yuan C.C., Hatton C., Zhao F., Williamson K.E., Iyer P., Méndez J., Campbell R., Cantone N., Garapaty-Rao S., Audia J.E., et al., (2014), EZH2 inhibitor efficacy in non-Hodgkin's lymphoma does not require suppression of H3K27 monomethylation., *Chem Biol.*, 20;21(11):1463-75.
- Brodsky J.L., Chiosis G., (2006), Hsp70 molecular chaperones: emerging roles in human disease and identification of small molecule modulators., *Curr Top Med Chem.*,6:1215–25.
- Caizergues-Ferrer M., Mariottini P., Curie C., Lapeyre B., Ga N., Amalric F., Amaldi F., (1989), Nucleolin from *Xenopus laevis*: cDNA cloning and expression during development., *Genes Dev.* 3, 324–333.
- Casper D., Bukhtiyarova M., Springman E.B., (2004), A Biacore biosensor method for detailed kinetic binding analysis of small molecule inhibitors of p38alpha mitogen-activated protein kinase., *Anal Biochem.*,1;325(1):126-36.

- Chen C.M., Chiang S.Y., Yeh N.H., (1991), Increased stability of nucleolin in proliferating cells by inhibition of its self-cleaving activity., *J. Biol. Chem.* 266, 7754–7758.
- Cong R., Das S., Ugrinova I., Kumar S., Mongelard F., Wong J., Bouvet P., (2012), Interaction of nucleolin with ribosomal RNA genes and its role in RNA polymerase I transcription., *Nucleic Acids Res.*,40(19):9441-54.
- Dal Piaz F., Cotugno R., Lepore L., Vassallo A., Malafrente N., Lauro G., Bifulco G., Belisario M.A., De Tommasi N., (2013), Chemical proteomics reveals HSP70 1A as a target for the anticancer diterpene oridonin in Jurkat cells., *J Proteomics.*, 26;82:14-26.
- Daniely Y., Dimitrova D.D., Borowiec JA., (2002), Stress-dependent nucleolin mobilization mediated by p53-nucleolin complex formation., *Mol Cell Biol.*,22(16):6014-22.
- Derenzini M., Sirri V., Trerè D., Ochs R.L., (1995), The quantity of nucleolar proteins nucleolin and protein B23 is related to cell doubling time in human cancer cells, *Lab. Invest.* 73 (4) 497-502.
- Ding Y., Song N., Liu C., He T., Zhuo W., He X., Chen Y., Song X., Fu Y., Luo Y., (2012), Heat shock cognate 70 regulates the translocation and angiogenic function of nucleolin., *Arterioscler Thromb Vasc Biol.*, 32(9):e126-34.
- Dubach J.M. & Vinegoni C., (2014), Steady state anisotropy two-photon microscopy resolves multiple, spectrally similar fluorophores, enabling in vivo multilabel imaging., *Opt Lett.* 1;39(15):4482-5.
- Dunn G.P., Old L.J., Schreiber R.D., (2004), The immunobiology of cancer immunosurveillance and immunoediting., *Immunity.*, 21(2)137-48.
- Fang S.H. & Yeh N.H., (1993), The self-cleaving activity of nucleolin determines its molecular dynamics in relation to cell proliferation. ,*Exp. Cell Res.*, 208, 48–53.
- Fujiki H., Watanabe T., Suganuma M., (2014), Cell-surface nucleolin acts as a central mediator for carcinogenic, anti-carcinogenic, and disease-related ligands. *J Cancer Res Clin Oncol.*, 140(5):689-99.
- Fujita E., Katayama H., Shibuya M., (1967), Oridonin, a new diterpenoid from isodon. *Species.*,*Chem Commun.*, 252-254.
- Fujita E., Nagao Y., Kohno T., Matsuda M., Ozaki M., (1981). Antitumor activity of acylated oridonin., *Chem Pharm Bull (Tokyo)*, 29(11):3208–3213.
- Fujita E., Nagao Y., Node M., Kaneko K., Nakazawa S., Kuroda H., (1976), Antitumor activity of the isodon diterpenoids: structural requirements for the activity., *Experientia.*, 32(2):203-6.
- Fujita T., Takao S., Fujita E., (1973), Biosynthesis of the diterpenes enmein and oridonin from ent-16-kaurene. *J Chem Soc Chem Commun* 1973:434–5.

- Gao F.H., Guo Z.Y., Xu M.H., Wang S.T., (2010) Oridonin induces apoptosis and senescence of colorectal cancer SW1116 cells in vitro and in vivo. *J Shanghai Jiaotong Univ (Med Sci)* 2010:30.
- Ginisty H., Sicard H., Roger B., Bouvet P., (1999), Structure and functions of nucleolin, *J Cell Sci.*, 112 (Pt 6):761-72.
- Grummt I., (1999), Regulation of mammalian ribosomal gene transcription by RNA polymerase I., *Prog Nucleic Acid Res Mol Biol.*, 62:109-54.
- Hanahan D. & Weinberg R.A., (2011), Hallmarks of cancer: the next generation., *Cell*; 144(5):646-74.
- Hannan K.M., Hannan R.D., Rothblum L.I., *Front Biosci.*, (1998), Transcription by RNA polymerase I. d376-98.
- Hers I., Vincent E.E., Tavaré J.M., (2011), Akt signalling in health and disease., *Cell Signal.*,23(10):1515-27.
- Ikezoe T., Chen S. S., Tong X J., Heber D., Taguchi H., Koeffler H P., (2003). Oridonin induces growth inhibition and apoptosis of a variety of human cancer cells., *Int J Oncol.*, 23(4): 1187–1193.
- Ishimaru D., Zuraw L., Ramalingam S., Sengupta TK., Bandyopadhyay S., Reuben A., Fernandes DJ, Spicer EK., (2010), Mechanism of regulation of bcl-2 mRNA by nucleolin and A+U-rich element-binding factor 1 (AUF1)., *J Biol Chem* 285: 27182–27191.
- Jafari R., Almqvist H., Axelsson H., Ignatushchenko M., Lundbäck T., Nordlund P., Martinez Molina D., (2014), The cellular thermal shift assay for evaluating drug target interactions in cells. *Nat Protoc.*, 9(9):2100-22.
- Kim K., Dimitrova D.D., Carta K.M., Saxena A., Daras M., Borowiec J.A., (2005) Novel checkpoint response to genotoxic stress mediated by nucleolin-replication protein a complex formation. *Mol Cell Biol.*, 25: 2463–2474.
- Kobayashi J., Fujimoto H., Sato J., Hayashi I., Burma S., Matsuura S., Chen D.J., Komatsu K., (2012), Nucleolin participates in DNA double-strand break-induced damage response through MDC1-dependent pathway., *PLoS One.*, 7: e49245.
- Lee J.H., Lee Y.S., Jeong S.A., Khadka P., Roth J., (2014), Catalytically active telomerase holoenzyme is assembled in the dense fibrillar component of the nucleolus during S phase., *Histochem Cell Biol* ,141: 137–152.
- Leitinger N. & Wesierska-Gadek J., (1993), ADP-ribosylation of nucleolar proteins in HeLa tumor cells., *J.Cell. Biochem.*, 52,153–158.
- Li C.Y., Wang E.Q., Cheng Y., Bao J.K.,(2011), Oridonin: an active diterpenoid targeting cell cycle arrest, apoptotic and autophagic pathways for cancer therapeutics., *Int J Biochem Cell.*;43:701–4.

- Liu Y.Q., Mu Z.Q., You S., Tashiro S., Onodera S., Ikejima T., (2006), Fas/FasL signaling allows extracellular-signal regulated kinase to regulate cytochrome c release in oridonin-induced apoptotic U937 cells., *Biol Pharm.*,29:1873–9.
- Lomenick B., Hao R., Jonai N., Chin R.M., Aghajan M., Warburton S., Wang J., Wu R.P., Gomez F., Loo J.A., Wohlschlegel J.A., Vondriska T.M., Pelletier J., Herschman H.R., Clardy J., Clarke C.F., Huang J.,(2009), Target identification using drug affinity responsive target stability (DARTS)., *Proc Natl Acad Sci U S A.*, 106(51):21984-9.
- Mei Y., Xu J., Zhao J., Feng N., Liu Y, Wei L.,(2008), An HPLC method for determination of oridonin in rabbits using isoporsalen as an internal standard and its application to pharmacokinetic studies for oridonin-loaded nanoparticles., *J Chromatogr B Analyt Technol Biomed Life Sci.*, 869(1-2):138-41.
- Morimoto H., Ozaki A., Okamura H., Yoshida K., Amorim B.R., Tanaka H., Kitamura S., Haneji T., (2005) Differential expression of protein phosphatase type 1 isotypes and nucleolin during cell cycle arrest., *Cell Biochem Funct.* ; 25(4):369- 75.
- Mosser D.D & Morimoto R.I., (2004), Molecular chaperones and the stress of oncogenesis. *Oncogene.*, 12;23(16):2907-18.
- Node M., Sai M., Fuji K., Fujita E., Takeda S., Unemi N., (1983). Antitumor activity of diterpenoids, trichorabdals A, B, and C, and the related compounds: synergism of two active sites., *Chem Pharm Bull (Tokyo)*, 31(4): 1433–1436.
- Otake Y., Soundararajan S., Sengupta T.K., Kio E.A., Smith J.C., Pineda-Roman M., Stuart R.K., Spicer E.K., Fernandes D.J., (2007) ,Overexpression of nucleolin in chronic lymphocytic leukemia cells induces stabilization of bcl2 mRNA., *Blood* 109: 3069–3075.
- Peter M., Nakagawa J., Doree M., Labbe J C., Nigg E.A., (1990), Identification of major nucleolar proteins as candidate mitotic substrates of cdc2 kinase., *Cell* 60, 791–801.
- Popp S.L. & Reinstejn J., (2009), Functional characterization of the DnaK chaperone system from the archaeon *Methanothermobacter thermautotrophicus* DeltaH. *FEBS Lett.* Feb 4;583(3):573-8.
- Rix U. & Superti-Furga G., (2009), Target profiling of small molecules by chemical proteomics. *Nat Chem Biol.*,5(9):616–24.
- Sartippour M.R., Seeram N.P., Heber D., Hardy M., Norris A., Lu Q., (2005), *Rabdosia rubescens* inhibits breast cancer growth and angiogenesis. *Int J Oncol.* 26(1):121-7.
- Sartippour M.R., Seeram N.P., Heber D., Hardy M., Norris A., Lu Q., Zhang L, Lu M, Rao JY, Brooks M.N., (2005), *Rabdosia rubescens* inhibits breast cancer growth and angiogenesis., *Int J Oncol.*,26(1)121–7.
- Saxena A., Rorie C.J., Dimitrova D., Daniely Y., Borowiec J.A., (2006) Nucleolin inhibits Hdm2 by multiple pathways leading to p53 stabilization. *Oncogene* 25: 7274–7288.

- Schneider H.R., Reichert G.U., Issinger O.G., (1986), Enhanced casein kinase II activity during mouse embryogenesis. *Eur. J. Biochem.*, 161, 733–738.
- Schwab M.S. & Dreyer C., (1997) Protein phosphorylation sites regulate the function of the bipartite NLS of nucleolin., *Eur. J. Cell Biol.*, 73, 287–297.
- Srivastava M. & Pollard H.B., (1999), Molecular dissection of nucleolin's role in growth and cell proliferation: new insights., *FASEB J.*, 13 (14):1911–1922.
- Sun H.D., Huang S.X., Han Q.B., (2006), Diterpenoids from *Isodon* species and their biological activities. *Nat Prod Rep*, 23(5)673–98.
- Takagi M., Absalon M.J., McLure K.G., Kastan MB., (2005), Regulation of p53 Translation and Induction after DNA Damage by Ribosomal Protein L26 and Nucleolin., *Cell* 123: 49–63.
- Tan W., Lu J., Huang M., Li Y., Chen M., Wu G., Gong J, Zhong Z, Xu Z, Dang Y, Guo J, Chen X, Wang Y., (2011), Anti-cancer natural products isolated from Chinese medicinal herbs., *Chin Med* 6:27–41.
- Tuteja N., Huang N.W., Skopac D., Tuteja R., Hrvatic S., Zhang J., Pongor S., Joseph G., Faucher C., Amalric F., Falaschi A., (1995), Human DNA helicase IV is nucleolin, an RNA helicase modulated by phosphorylation., *Gene.*, 160 (2), 143-148.
- Tuteja R. & Tuteja N., (1998), Nucleolin: A multifunctional major nucleolar Phosphoprotein. *Crit Rev Biochem Mol Biol.*, 33(6):407- 36.
- Ugrinova I., Monier K., Ivaldi C., Thiry M., Storck S., Mongelard F., Bouvet P., (2007), Inactivation of nucleolin leads to nucleolar disruption, cell cycle arrest and defects in centrosome duplication. *BMC Mol Biol* 10,8: 66.
- Wenjing Z., Qilai H., Zi-Chun H., (2010), Oridonin: a promising anticancer drug from China, *Biol.* 2010, 5(6): 540–545.
- Wu D.M., Zhang P., Liu R.Y., Sang Y.X., Zhou C., Xu G.C., Yang J.L., Tong A.P., Wang C.T., (2014), Phosphorylation and changes in the distribution of nucleolin promote tumor metastasis via the PI3K/Akt pathway in colorectal carcinoma., *FEBS Lett.*, 588(10):1921-9.
- Xu J., Wang K., Zhang X., Qiu Y., Huang D., Li W., Xiao X., Tian Y., (2010), HSP70: a promising target for laryngeal carcinoma radiotherapy by inhibiting cleavage and degradation of nucleolin., *J Exp Clin Cancer Res.*, 6;29:106.
- Xu J., Yang J., Ran Q., Wang L., Liu J., Wang Z., Wu X., Hua W., Yuan S., Zhang L., Shen M., Ding Y (2008), Synthesis and biological evaluation of novel 1-O- and 14-O-derivatives of oridonin as potential anticancer drug candidates., *Bioorg Med Chem Lett.*, 18 (16): 4741–4744.
- Xu Z., Joshi N., Agarwal A., Dahiya S., Bittner P., Smith E., Taylor S., Piwnicka-Worms., D, Weber J., Leonard J.R., (2012), Knocking down nucleolin expression in gliomas inhibits tumor growth and induces cell cycle arrest., *J Neurooncol.*;108(1):59-67.

- Yang C., Maiguel D.A., Carrier F., (2002), Identification of nucleolin and nucleophosmin as genotoxic stress-responsive RNA-binding proteins., *Nucl Acids Res* 30: 2251–2260.
- Yang J., Liu X., Bhalla K., Kim CN., Ibrado AM., Cai J., Peng TI., Jones DP., Wang X., (1997) Prevention of apoptosis by Bcl-2: release of cytochrome c from mitochondria blocked., *275:1129-32.*
- Yerlikaya A., Okur E., Eker S., Erin N., (2010), Combined effects of the proteasome inhibitor bortezomib and Hsp70 inhibitors on the B16F10 melanoma cell line., *Mol Med Rep.*,3:333–9.
- Zhang C., Wu L., Tashiro S., Onodera S., Ikejima T., (2004), Oridonin induces apoptosis of HeLa cells via altering expression of Bcl-2/Bax and activating caspase-3/ICAD pathway. *Acta Pharmacol Sin.*,25(5):691–8.
- Zhang T.M. Recent studies on the antitumor activity of *Rabdosia rubescences*. *Chin J Oncol* 1982;4:322–3.
- Zhou G.B., Chen S.J., Wang Z.Y., Chen Z., (2007a), Back to the future of oridonin: again, compound from medicinal herb shows potent antileukemia efficacies in vitro and in vivo., *Cell Res.*,17:274–6.
- Zhou G.B., Kang H., Wang L., Gao L., Liu P., Xie J., Zhang F.X., Weng X.Q., Shen Z.X., Chen J., Gu L.J., Yan M., Zhang D.E., Chen S.J., Wang Z.Y., Chen Z., (2007b), Oridonin, a diterpenoid extracted from medicinal herbs, targets AML1-ETO fusion protein and shows potent antitumor activity with low adverse effects on t(8;21) leukemia in vitro and in vivo., *Blood.*,109(8)3441–50.
- Zhu Y., Xie L.P., Chen G., Wang Z., Zhang R.Q., (2007),. Effects of oridonin proliferation of HT 29 human colon carcinoma cell lines both in vitro and in vivo in mice., *Pharmazie.*,62:439–44.

- Chapter 4 -

Introduction

4.1 Background and aims of the projects

Small-molecule therapeutic drugs typically exert their effects binding to one or a few protein targets. This critical interaction—a prerequisite of therapeutic drug efficacy—is often poorly understood; it can generally not be visualized in live cells or in entire organisms due to the lack of methods to directly measure drug–target engagement in a biological setting (Martinez Molina D. *et al.* 2013; Adibekian A., *et al.* 2012). Traditional pharmacokinetics relies heavily on measurements of plasma concentration and is commonly described by the processes of Absorption, Distribution, Metabolism and Excretion (ADME). Unfortunately, compartmental analyses do not consider the high heterogeneity of drug distribution in cell. As a result, most of our knowledge is incomplete, as it relies on target extraction assay systems or on indirect measurements, where critical spatiotemporal information is lost; thus drug development and optimization is severely complicated. The use of invitral microscopy using fluorescence tool can help to overcome these problems (Vinegoni C *et al.* 2015).

Invitral microscopy approach can, indeed, offer several advantages. Recently, studies based on the applications of fluorescent drugs provided direct *in vivo* evidences of the presence of drug heterogeneity at tissutal (Thurber G.M. *et al.* 2013), cellular (Laughney A.M. *et al.* 2014) and subcellular levels (Thurber G.M. *et al.* 2014) and highlighting several routes of drug failure and potential solutions. Additionally, cellular resolution imaging of pharmacokinetics enables differentiation of cell type within tissue increasing specificity of delivery to organs or tumors promising to decrease systemic toxicity of therapeutic treatment. Finally, microscopy analysis imaging can provide quantitative measurements with spatial and temporal information (Vinegoni C *et al.* 2015). Therefore, in order to improve and learn different techniques to

study the mechanism of action of small molecules, I spent a period of research activity at MGH (Massachusetts General Hospital) in Boston (MA, USA) under the supervision of Prof. Vinegoni Claudio. During this period, I contributed to study new methods, complementary to proteomics, allowing to describe the molecular mechanism of action of small molecules. In fact, the research group of the MGH laboratories set up the experimental conditions to use high-resolution intravital microscopy imaging for drug pharmacology, through the development of companion imaging drugs, fast imaging platforms, methods for automated processing, data analysis and machine learning.

My specific aims consisted in 1) to synthesize new fluorescent drugs that could provide spatially and temporally resolved mapping, enabling live cell imaging of target engagement of small-molecule drugs; 2) to use chemical biology and bioorthogonal chemistries to develop a new method based on CETSA approach. Recent advances in chemical techniques have allowed the creation of fluorescent drugs, prodrugs and activity-based probes to interrogate target engagement.

4.2 Fluorescence polarization applied to invitral microscopy analysis

Firstly, I paid my attention on the use of fluorescence anisotropy based on fluorescence polarization (FP) coupled with invitral microscopy analysis. FP could be used to accurately measure drug binding *in vitro* and *in vivo* through multiphoton microscopy and it has many advantages. FP has been extensively used for different measurement in non-imaging, plate reader and kinetic *in vitro* assays to study fluorescent molecules and drug interactions (Jameson D.M. & Ross J.A., 2010; Weber G. 1952). The application of FP to optical microscopy imaging modalities could provide high resolved maps, enabling live cell imaging of target engagement by small-molecule drugs. However, this technique (Bigelow C.E *et al.* 2013) was used for different applications such as the study of membrane dynamics (Varma R. & Mayor S. 1998;

Sharma P. *et al.* 2004; Weber P. *et al.* 2010), the study of structures in biological systems (Vrabioiu A.M. & Mitchison T.J. 2006; Kampmann M. *et al.* 2011) and endogenous small molecules (Yu Q. & Heikal A.A. 2009) or labelled protein interactions (Gough A.H. & Taylor D.L. 1993).

FP considers the photoselection under polarized excitation of all excited fluorophores aligned with the same emission dipole orientation: due to the presence of rotational Brownian motion, fluorophores rotate with a correlation time (τ_θ) dependent on different parameters (viscosity, molecule size and temperature (Lakowicz, J.R. 2006)). If the excited fluorophore is free to rapidly rotate on a timescale that is shorter than its fluorescence lifetime ($\tau_\theta \ll \tau$), emission will be isotropic (depolarized). However, when rotating slowly, the rotational correlation time will increase ($\tau_\theta \gg \tau$) and emission will be preferentially aligned along one axis (Figure 1). This happens, for example, when a dye is bound to a macromolecule, or to something that slows down its rotation.

To characterize the extent of linearly polarized emission, fluorescence anisotropy (FA), a dimensionless parameter similar to FP and independent of excitation intensity, can be calculated. Thus, the measurements of anisotropy provide insight into the rotational diffusion rate of molecules, which can be used in term to directly determine drug engagement with the target.

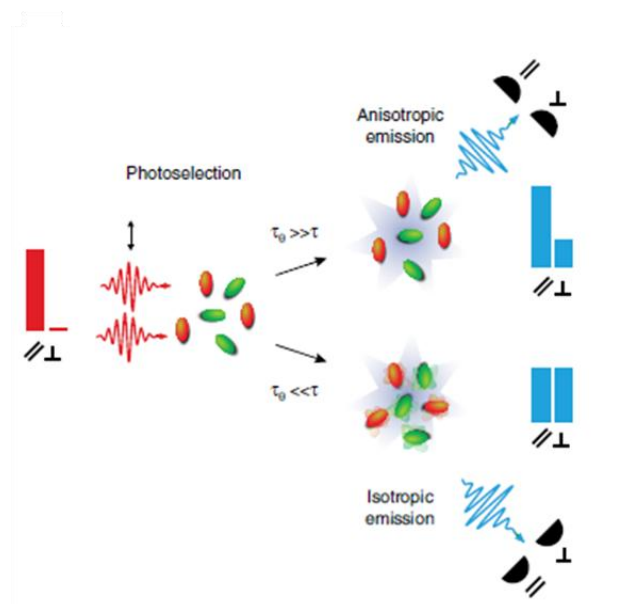


Fig.1: Schematic representation of the two-photon photoselection. Blue bars indicate the distribution of emission along the two orthogonal linear polarization components as measured at the two detectors, for the two cases. Orange particles represent excited molecules.

Adopted from Dubach J.M. *et al.* 2014

I applied this methodology on the study of a new class of drugs: ADCs (Antibody Drug Conjugates). ADCs are formed by a highly potent cytotoxic drug, a linker, and an antibody and their aim is to take advantage of the specificity of monoclonal antibodies (mAbs) to deliver potent cytotoxic drugs selectively to antigen-expressing tumor cells. My aim was to study two different ADCs, using *in vitro* microscopy analysis and the ADCs fluorescence version, to get information about their mechanism of action *in vitro* and *in vivo*; indeed, their pharmacodynamics and kinetics parameters were still not fully described.

The two molecules studied were trastuzumab emtansine (Figure 2A) (T-DM1, Kadcyla™) and milatuzumab-doxorubicin (Immu-110). The first ADC is composed of trastuzumab, a nonreducible thioether linker (4-[N-maleimidomethyl]-cyclohexane-1-carbonyl [MCC]) (Lewis Phillips *et al.*, 2008), and the cytotoxic agent DM1 (N2'-deacetyl-N2'-(3-mercapto-1-oxopropyl) maytansine) (Cassady J.M. *et al.* 2004). DM1 is derived from the

highly potent antitumor agent maytansine and inhibits microtubule polymerization (Cabanillas F *et al.* 1978; Chabner B.A. *et al.* 1978).

The second ADC studied is a humanized monoclonal antibody targeting tumors that express the CD74 antigen, a cleavable linker, and doxorubicin as cytotoxic agent (Figure 2B).

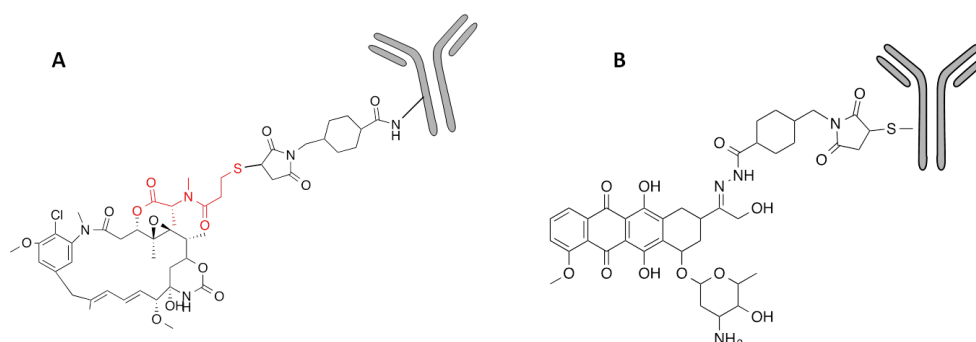


Fig.2: A) Chemical structure of Trastuzumab emtansine; B) Chemical structure of Milatuzumab-doxorubicin

The first step of this study was to optimize the synthetic scheme to get the fluorescence versions of both drugs. Unfortunately, the expected results were not reached.

Therefore, I decided to focus on the study of pharmacodynamics and kinetics of doxorubicin using invitral microscopy on live cells, taking advantage of its intrinsic fluorescence. In particular, HT1080 (Human fibrosarcoma) cells were treated with 10 μ M doxorubicin and different incubation times were evaluated (Figure 3).

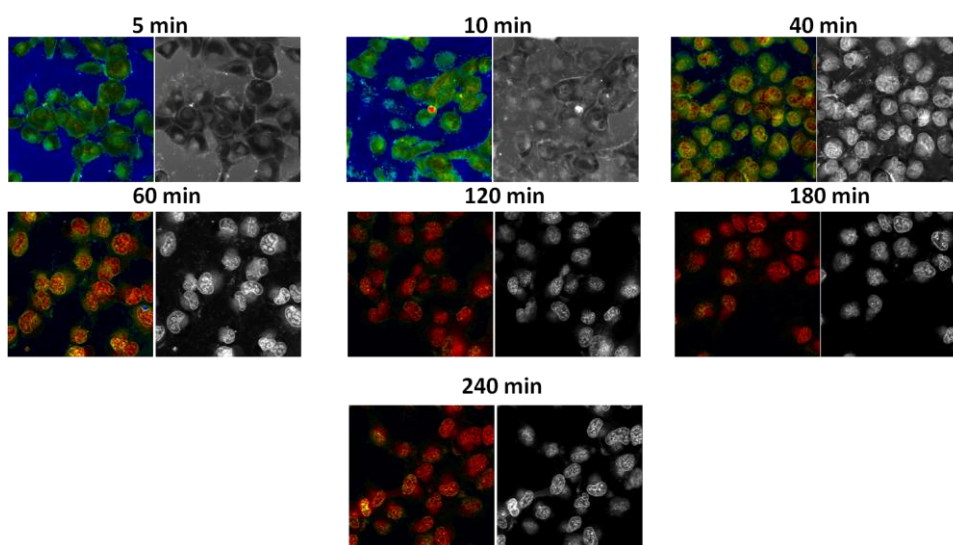


Fig.3: Real time imaging of HT1080 cells following different incubation times with doxorubicin 10 μ M. Anisotropy (green/red scale) and corresponding fluorescence intensity (gray scale) images of doxorubicin at different representative time points during drug loading. Scale bar: 20 μ m

As reported in Figure 3, real-time *in vitro* measurements showed that the amount of doxorubicin within the cells reached its maximum after 2h of incubation (red scale represent maximum anisotropy reached) and after 3h it started decreasing. The drug accumulated mainly in the nucleus of the treated cells, as expected since its mechanism of action.

All these preliminary results represent a good starting point for further investigations and studies *in vitro* and *in vivo*.

4.3 A new method based on CESTA approach

Furthermore, during my last period there, we tried to develop a new method based on CESTA approach. The specific aim was to develop a new technique based on the combination of CETSA assay and the monitoring of specific fluorescence parameters (fluorescence intensity and fluorescence anisotropy) in order to obtain an analytical method suitable for drugs highthroughput screening.

The CETSA approach provided by Molina and coworkers (Martinez Molina D. *et al.* 2013) is based on the detection of the soluble amount of the protein target thermally stabilized by its small molecule through western blotting analysis. This kind of detection (immunoblot) has several disadvantages: first it is time-consuming compared to other techniques; second it has a high demand in terms of experience of the experimenter; finally it requires a deep optimization of the experimental conditions (i.e. protein isolation, buffers, type of separation, gel concentration, etc.). Therefore, with the aim to obtain a new technique faster, less expensive and thus useful for highthroughput screening of drugs, we decided to base this technique on fluorescence parameters. This implementation of CETSA approach could provide higher sensitivity, reproducibility and accuracy.

The experimental design was optimized separately for two different classes of drugs: for drugs that covalently bind to their target, we focused on the use of the fluorescence version of the studied molecule; for drugs non-covalently interacting with their targets, we planned to use specific antibodies conjugated to fluorescent dyes (Figure 4).

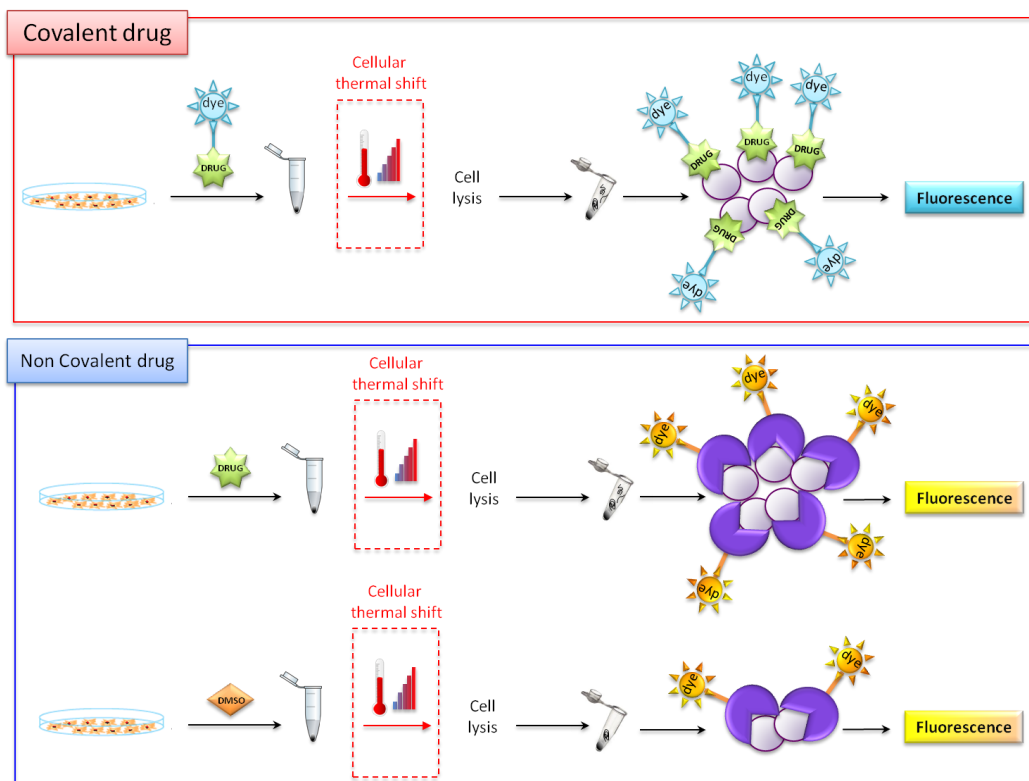


Fig.4: Schematic representation of new method based on CETSA approach

In my period at MHG, my attention was paid on the first case, and Ibrutinib (Figure 5) was chosen as model drug for our study; it is a well-known covalent inhibitor of Bruton's tyrosine kinase (Btk) and its fluorescent version of this drug (Ibrutinib SirCOOH) was already well characterized *in vitro* and *in vivo* (Kim E. *et al.* 2015).

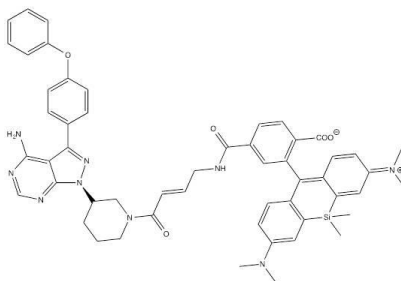


Fig.5: Chemical structure of Ibrutinib SirCOOH

Therefore, HT1080 cells were treated with Ibrutinib SirCOOH at 5 μ M for 2,5h of incubation time to reach the maximum equilibrium with Btk (Kim E. *et al.* 2015). Next, we heated samples in order to define the T_{agg} for Btk in this cell model. Finally, we used Btk antibody to detect the soluble amount of this protein in our samples. Simultaneously, the intensity of fluorescence emission and the fluorescence anisotropy were measured (Figure 6).

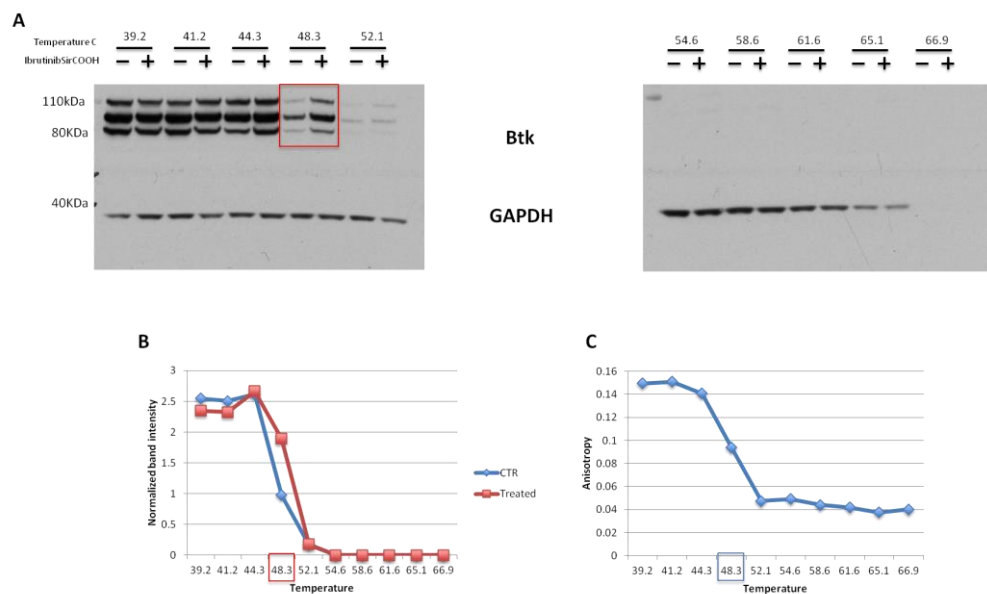


Fig.6: A) CETSA was employed to monitor Ibrutinib SirCOOH cellular target engagement and to define the best T_{agg}. Therefore, treated and untreated HT1080 cells were heated and then was evaluated the soluble amount of NCL by western blotting; B) Apparent melting curves of Btk in cell. Densitometry-based quantification of western blot signals was graphed Bk intensities normalized to GAPDH intensities for each data point. Shown are the mean of three biological replicates. C) Anisotropy-based quantification of Ibrutinib SirCOOH after CETSA approach was graphed.

As reported in Figure 6, the fluorescence curve and the quantitative analysis of the immunoblots gave the same result. In our experiments, 48.2 °C was the best temperature to appreciate thermal stabilization of BTK.

Next, EC₅₀ of the Ibrutinib SirCOOH/Btk complex into the cell was evaluated, using the fluorescence intensity of Ibrutinib SirCOOH. Therefore, HT1080

cells were treated with a wide range of concentrations of Ibrutinib SirCOOH up to 5 μ M while incubation time and temperature were kept constant. Analysis of obtained results (Figure 7) gave an EC₅₀ of 0.208 μ M, very close to the value reported in literature (Kim E. *et al.* 2015).

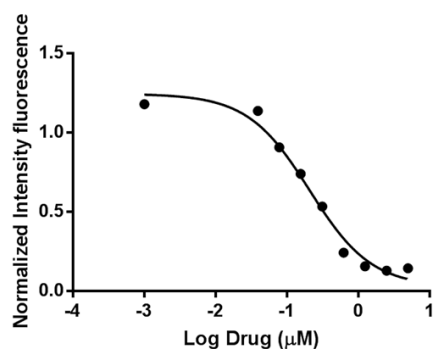


Fig.7: Intensity-based quantification of Ibrutinib SirCOOH after CETSA approach to define EC₅₀ was graphed. Fluorescence intensities of Ibrutinib SirCOOH was normalized to total intensities for each data point

All these promising data represent preliminary results which will be further investigated and validated for following studies.

In conclusion, thanks to this period of research at MGH, I expanded my knowledge and learn new techniques useful for the study of the mechanism of action of small molecules. Therefore, the skills I have acquired have been extremely rewarding in helping me to broaden my prospective about the importance and the development of techniques useful for the study of small molecules.

Materials and methods

Materials

Fetal Bovine Serum (FBS) was from GIBCO (Life Technologies, Grand Island, NY, USA) and Ibrutinib SirCOOH was obtained from Ralph Weissleder's laboratory. All the other reagents were from Sigma-Aldrich (St. Louis, MO, USA).

4.4 Live cell fluorescence microscopy in cell of doxorubicin

HT1080 (Human fibrosarcoma cell line) were seeded into a 96-well plate at 5000 cells per well and incubated for 24h. Cells were incubated in growth media containing 10 μ M of doxorubicin 0.1% DMSO for 30min up 4h. When the incubation time was done, live cells were subsequently imaged on a Delta Vision imaging system (Applied Precision, GE Healthcare). Images were processed using Fiji software, an open-source version of ImageJ.

4.5 CETSA approach

Materials

Antibodies: anti-Btk (anti rabbit monoclonal Y440) from Abcam (Cambridge, CB4 0FL, UK)

4.5.1 Determination of the apparent melting curve of Btk by CETSA

Protocol used was adopted from Jafari R. *et al.* 2014 but slightly modified. More in details, approximately 10 million HT1080 in a final volume of 10ml of growth media were used for each condition, in a Cell Culture Flasks (T75). A stock solution of Ibrutinib-SirCOOH (10 μ l of 5mM in DMSO) was added to individual flasks to get a final concentration of 5 μ M of Ibrutinib-SirCOOH (0.1%DMSO); 10 μ l DMSO was used as control. Cells were gently mixed by

pipetting up and down at least 3 times and were incubated for 2.5h in the CO₂ incubator at 37 °C. After, cells were trypsinized and cell suspensions were collected and transferred to 15-ml conical tubes. Once cells were centrifuged, pellets of cells were washed with PBS and gently resuspended in 1ml of PBS supplemented with protease inhibitors to each respective tube. Each cell suspension was divided into 10 different tubes and the heated using PCR machine (Invitrogen Life Science Technologies) at different temperatures for 3 min.

The temperature used were:

Temperature (°C)	Sample CTR	Sample Treated
39.2	1	11
41.2	2	12
44.3	3	13
48.3	4	14
52.1	5	15
54.6	6	16
58.6	7	17
61.6	8	18
65.1	9	19
66.9	10	20

Immediately after heating, tubes were kept at room temperature for 3 min. After this 3-min samples were immediately snap-frozen in the liquid nitrogen for 3 times. Therefore, cell lysate-containing tubes were centrifuged at 20,000g for 20 min at 4°C to pellet cell debris together with precipitated and aggregated proteins. Each supernatant with the soluble protein fraction was transferred to a new tube. Subsequently 10µl of each tubes were loaded on a 10% mono dimensional SDS-PAGE gel and western blotting analysis was performed.

In order to obtain fluorescence intensity and fluorescence anisotropy, 50µl of each supernatants were analyzed by Tecan Infinite[®] M1000 PRO - Life Sciences.

4.5.2 Determination of EC₅₀ of Btk/IbrutinibSirCOOH complex by CETSA

To perform the ITDRF_{CETSA} experiments, equal number of HT1080 (1 million cells per data points) were seeded in 24 well cell culture plates in 1 ml of growth media and exposed to varying concentration of Ibrutinib SirCOOH for 2.5h of incubation time in an incubator chamber (range used from 0.005µM to 5µM, final concentration of DMSO 0.1%). Following the incubation the drug-containing media were removed by centrifugation cells were washed with PBS and prepared for CETSA experiment. In this case cells were heated at 55.1°C for 3 min and the protocol used was the same described before. All immunoblots were processed using Fiji software, an open source version of ImageJ.

4.6 Western Blot analysis

Cell whole lysates for immunoblot analysis were prepared according to the standard protocol. Protein concentration was determined by DC Protein Assay (Bio-Rad, Berkeley, CA, USA), using bovine serum albumin (BSA) as a standard. Proteins were fractionated on SDS-PAGE, transferred into nitrocellulose membranes, and immunoblotted with appropriate primary antibodies. Signals were visualized with appropriate horseradish peroxidase-conjugated secondary antibodies and enhanced chemiluminescence (Amersham Biosciences-GE Healthcare, NY, USA). Densitometry of bands was performed with ImageJ software (<http://rsbweb.nih.gov/ij/download.html>).

4.7 Statistical analysis

Data reported in each figure are the mean values \pm SD from at least three experiments, performed in duplicate, showing similar results. Differences between treatment groups were analyzed by Student's t-test. Differences were considered significant when $p < 0.05$.

References

- Adibekian A., Martin B.R., Chang J.W., Hsu K.L., Tsuboi K., Bachovchin D.A., Speers A.E., Brown S.J., Spicer T., Fernandez-Vega V., Ferguson J., Hodder P.S., Rosen H., Cravatt B.F., (2012), Confirming target engagement for reversible inhibitors in vivo by kinetically tuned activity-based probes., *J Am Chem Soc.*;134(25):10345-8.
- Bigelow C.E., Conover, D.L., Foster T.H., (2003), Confocal fluorescence spectroscopy and anisotropy imaging system. *Opt. Lett.* 28, 695–697.
- Cabanillas F., Rodriguez V., Hall S.W., Burgess M.A., Bodey G.P., Freireich E.J., (1978), Phase I study of maytansine using a 3-day schedule, *Cancer Treat Rep*;62(3):425-8.
- Cassady J.M., Chan K.K., Floss H.G., Leistner E., (2004), Recent developments in the maytansinoid antitumor agents., *Chem Pharm Bull*;52(1):1-26.
- Chabner B.A., Levine A.S., Johnson B.L., Young R.C., (1978), Initial clinical trials of maytansine, an antitumor plant alkaloid, *Cancer Treat Rep*;62(3):429-33.
- Dubach J.M., Vinegoni C., Mazitschek R., Fumene Feruglio P., Cameron L.A., Weissleder R., (2014), In vivo imaging of specific drug-target binding at subcellular resolution., *Nat Commun.* 2014 May 28;5:3946.
- Gough A.H. & Taylor D.L., (1993), Fluorescence anisotropy imaging microscopy maps calmodulin binding during cellular contraction and locomotion. *J. Cell Biol.* 121, 1095–1107.
- Jameson D.M. & Ross J.A., (2010), Fluorescence polarization/anisotropy in diagnostics and imaging., *Chem. Rev.*; 110, 2685–2708.
- Kampmann M., Atkinson C.E., Mattheyses A.L., Simon S.M., (2011), Mapping the orientation of nuclear pore proteins in living cells with polarized fluorescence microscopy. *Nat. Struct. Mol. Biol.* 18, 643–649.
- Kim E., Yang K.S., Kohler R.H., Dubach J.M., Mikula H., Weissleder R., (2015), Optimized Near-IR Fluorescent Agents for in Vivo Imaging of Btk Expression., *Bioconjug Chem.* 19;26(8):1513-8.
- Lakowicz, J.R., (2006). *Principles of Fluorescence Spectroscopy* 3rd edn., Springer.
- Laughney A.M., Kim E., Sprachman M.M., Miller M.A., Kohler R.H., Yang K.S., Orth J.D., Mitchison T.J., Weissleder R., (2014), Single-cell pharmacokinetic imaging reveals a therapeutic strategy to overcome drug resistance to the microtubule inhibitor eribulin., *Sci Transl Med.*;5;6(261):261ra152.
- Martinez Molina D., Jafari R., Ignatushchenko M., Seki T., Larsson E.A., Dan C., Sreekumar L., Cao Y., Nordlund P., (2013), Monitoring drug target engagement in cells and tissues using the cellular thermal shift assay. *Science.*, 5;341(6141):84-7.

- Sharma P., Varma R., Sarasij R.C., Ira Gousset K., Krishnamoorthy G., Rao M., Mayor S., (2004), Nanoscale organization of multiple GPI-anchored proteins in living cell membranes, *Cell.*;116(4):577-89.
- Thurber G.M., Reiner T., Yang K.S., Kohler R.H., Weissleder R., (2014), Effect of small-molecule modification on single-cell pharmacokinetics of PARP inhibitors., *Mol Cancer Ther.*;13(4):986-95.
- Thurber G.M., Yang K.S., Reiner T., Kohler R.H., Sorger P., Mitchison T., Weissleder R., (2013), Single-cell and subcellular pharmacokinetic imaging allows insight into drug action in vivo., *Nat Commun.*;4:1504.
- Varma R. & Mayor S.,(1998), GPI-anchored proteins are organized in submicron domains at the cell surface. *Nature* 394, 798–801.
- Vinegoni C., Dubach J.M., Thurber G.M., Miller M.A., Mazitschek R., Weissleder R., (2015), Advances in measuring single-cell pharmacology in vivo., *Drug Discov Today.*;20(9):1087-92.
- Vrabioiu A.M. & Mitchison T.J., (2006), Structural insights into yeast septin organization from polarized fluorescence microscopy. *Nature* 443, 466–469.
- Weber G., (1952), Polarization of the fluorescence of macromolecules. I. Theory and experimental method. *Biochem. J.* 51, 145–155.
- Weber P., Wagner M., Schneckenburger H., (2010), Fluorescence imaging of membrane dynamics in living cells. *J. Biomed. Opt.* 15, 046017.
- Yu Q. & Heikal A.A. (2009), Two-photon autofluorescence dynamics imaging reveals sensitivity of intracellular NADH concentration and conformation to cell physiology at the single-cell level. *J. Photochem. Photobiol. B* 95, 46–57.